

Title of Thesis : Studies in Cosmic Rays

Name of candidate : Dinesh Patel

Thesis advisor : Prof. Vikram Sarabhai
Physical Research Laboratory
Ahmedabad.

Submitted to : Gujarat University
for the degree of
Doctor of Philosophy.

043



B3894

August 1970

Physical Research Laboratory
Ahmedabad.

S T A T E M E N T

Triple coincidence Geiger counter directional telescopes inclined at an angle of 45° with respect to vertical and pointing in east and west directions, have been operated by the author at Ahmedabad (23°N , 72.61°E) during May 1963 to April 1965. Telescopes of different semi-angles of opening were simultaneously operated. Transistorized circuits were fabricated for the operation of the E-W telescopes. Fast switching action of quenching and coincidence circuits was ensured by selection of appropriate transistors. The characteristics of the solar daily variation, the influence of the angle of opening of telescopes in the east-west plane and the long term changes of daily variation of cosmic ray intensity for east and west directions have been studied.

The daily variation of intensity of galactic cosmic rays measured by an instrument fixed to the spinning earth has in general two principal harmonic components, diurnal and semi-diurnal. In the present work we have studied the anisotropy of galactic cosmic rays through the diurnal and semi-diurnal components of the cosmic ray variations. The daily variation measured with a net work of high counting rate monitors ($> 5 \times 10^5$ counts/hr) is used to derive with precision, the spectrum of the variation, the amplitude

and the principal directions of maximum and minimum intensity of the anisotropy in interplanetary space on each day during 1964-65.

To deduce the characteristics of the anisotropy from the observed variations, correction is required for geomagnetic field effects because of the fact that cosmic rays suffer considerable deflection in the geomagnetic field. Following the method of variational coefficients (McCracken et al. 1962) we have evaluated for a set of stations used in the analysis, the relative amplitude and the correction for the geomagnetic bending for each combination of exponent and the lower limit of the energy of the spectrum of variation. The exponent of the spectrum of variation ranges from +1.0 to -1.2 and the lower limits of the energy are 2, 4, 6, 8 25 GeV while the upper limit of the energy E_{\max} was kept constant at 250 GeV.

We derive an energy spectrum of variation of the anisotropy specified by the exponent X , and limiting energies E_{\min} and E_{\max} in the relation,

$$\begin{aligned} \frac{\delta D(E)}{D(E)} &= a E^X \quad \text{for } E_{\min} \leq E \leq E_{\max} \\ &= 0 \quad \text{for } E < E_{\min} \text{ or } E > E_{\max} \end{aligned}$$

where $D(E)$ is the differential energy spectrum of primary cosmic ray particles of energy E and $\delta D(E)$ is the energy

spectrum of variational part. 36 different combinations of exponents (X) and energies (E_{\min}) have been considered to describe the energy dependence of the anisotropy. Applying the method of best fit, the energy spectrum of variation has been determined separately for the diurnal and the semi-diurnal components of the variation.

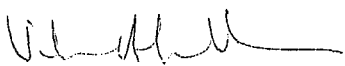
Once the optimum spectrum is determined, the optimum values of the diurnal and the semi-diurnal components in space are obtained. We derive the direction in space of maximum intensity T_{\max} and of minimum intensity T_{\min} . The magnitude of the anisotropy in space defined in terms of a percent change in the 24 hourly mean intensity of galactic cosmic rays, has been obtained. The characteristics of the anisotropy during the solar maximum (58-60), during the years of declining activity (61-63) and during the solar minimum (64-65) are studied. The experimental results are compared with the predictions of the characteristics arising from the four processes which appear capable of contributing to the creation of an anisotropy of galactic cosmic rays in interplanetary space. They are (1) Azimuthal streaming (Parker, 1964; Axford, 1965; Krymskiy, 1964) (2) Streaming due to nonuniform diffusion in a longitudinal sector structure of interplanetary magnetic fields, (Parker, 1964), (3) Scattering at irregularities along the interplanetary magnetic

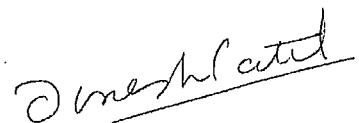
field short circuiting latitudinal gradients (Sarabhai and Subramanian, 1966) and (4) Latitudinal gradients in a relatively smooth magnetic field (Subramanian and Sarabhai, 1967; Lietti and Quenby, 1968).

The observational implications of the azimuthal drift process on the low energy limit of modulation through E_{\min} and at high energy end through E_{\max} are examined by calculating the expected diurnal amplitudes for the neutron monitors at Deep River and Huancayo for various values of E_{\min} and E_{\max} .

It is demonstrated that the diurnal and semi-diurnal components of the anisotropy have characteristically different energy spectra of variation. The predominant process responsible for the diurnal component is the azimuthal streaming while the semi-diurnal component appears to be due to scattering at magnetic field irregularities and latitudinal gradients.

Knowing the energy spectrum of the variation of the anisotropy of galactic cosmic rays during 1966, an attempt has been made to derive the variation in meson component due to atmospheric temperature changes by comparing the solar daily variation observed by crossed telescopes at Bologna (46.95°N , 7.43°E) with expected variation due to the primary anisotropy and barometric pressure changes.


(VIKRAM SARABHAI)


(DINESH PATEL)

22 - 8 - 1970

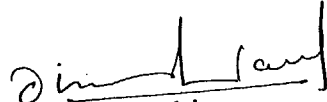
A C K N O W L E D G E M E N T S

I am sincerely grateful and express my deepest appreciation to Prof. Vikram Sarabhai for giving the guidance and encouragement throughout the course of the work, presented in this thesis.

I would like to thank Dr. G. Subramanian, Dr. P. N. Pathak and Mr. L. V. Kargathra for their helpful suggestions and criticism.

I am thankful to Mr. S. R. Thakore, Chief of the Computing Centre, Physical Research Laboratory, for giving the computer facilities. Thanks are also due to Mr. K. C. Patel for his help in processing data. The neat typing by Mr. R. R. Nair is greatly acknowledged.

The author is thankful to the Department of Atomic Energy, Government of India, for financial assistance.


(DINESH PATEL)

C O N T E N T S

CHAPTER I INTRODUCTION

1.1	Galactic cosmic rays		
1.2	Time variation of cosmic ray intensity	..	4
1.3	Terrestrial Atmospheric effect	..	5
	a. Barometric effect		
	b. Temperature effect		
1.4	(a) The earth's magnetic field and cut-off rigidity	12
	(b) Asymptotic direction		
	(c) Asymptotic cone of acceptance		
1.5	Relation of secondary time variation to primaries	18
1.6	Modulation of cosmic ray intensity	..	23
	a. The interplanetary magnetic field		
	b. 11-year modulation		
	c. Different models of 11-year modulation mechanism		
	d. Diffusion-Convection model		
	e. Forbush Decreases		
	f. 27 day variation		
	g. Daily variation		
1.7	A study of the cosmic ray daily variation.		55

CHAPTER II DIRECTIONAL MEASUREMENTS OF THE COSMIC RAY
DAILY VARIATION AT AHMEDABAD.

2.1	Introduction	57
2.2	The apparatus	59
2.3	The Geiger Muller counter	61
2.4	Electronic Units	62
	a. Quenching unit				
	b. Emitter follower				
	c. Coincidence circuit				
	d. Scaler				
	e. Recording unit				
	f. Photographic unit				
	g. Power supplies				
	h. Low voltage power supply				
2.5	a. Processing of data	73
	b. Method of moving average				
	c. Harmonic analysis				
2.6	Cosmic-ray daily variations recorded by the inclined telescopes at Ahmedabad	77
2.7	Daily variation of cosmic ray intensity for east and west during solar maximum and solar minimum.	82

CHAPTER III CHARACTERISTICS OF THE ANISOTROPIES OF GALACTIC COSMIC RAYS

3.1	Introduction	88
3.2	Variational coefficients	90
3.3	Methods of analysis	95
3.4	Day-to-day changes of anisotropy	101
3.5	Characteristics of process of producing anisotropies in interplanetary space	106
3.6	Identification of anisotropies	111
3.7	Orientation of the diurnal and semi-diurnal components with respect to the interplanetary magnetic field.	113
3.8	Amplitudes in space for the different processes of the modulation	116
3.9	Variation in anisotropy associated with sector structure of the interplanetary field	116
3.10	Estimation of the limiting energies E_{\max} and E_{\min} for the process of azimuthal streaming	120
3.11	Anisotropy of galactic cosmic rays during the solar cycle	126
3.12	Variations in upper atmospheric temperature estimated from the daily variation of cosmic rays	131

CHAPTER IV SUMMARY AND CONCLUSIONS OF THE WORLDWIDE
STUDY OF DAILY VARIATION

4.1	Study of anisotropies of galactic cosmic rays	134
4.2	Estimation of the atmospheric temperature effect	137
4.3	Conclusions	138
/ REFERENCES	 (i) to (xiv)	

CHAPTER - I

INTRODUCTION

1.1 Galactic Cosmic Rays

Galactic cosmic rays may be regarded as probes for understanding the state of interplanetary medium and the source and propagation mechanisms of particles in the solar system. These cosmic ray particles are divided into two groups, the solar cosmic ray particles which originate in the sun and the galactic cosmic ray particles which originate outside the solar system (Cocconi, 1960).

Galactic cosmic rays are incident upon the earth at all times. Their energy extends as high as 10^{20} ev and their intensity is greatest during the periods when the sun is least active. Experiments performed on satellites, balloons and on earth's surface have determined the intensity, the energy spectrum, the isotopic composition, the direction of arrival and the time variations of these particles. The particles are mainly protons. A measurement of primary cosmic radiation made at an energy of 2.4 BeV per nucleon indicates that 94 percent are protons, 5.5 percent are alpha particles, and 0.5 percent are heavier nuclei of atomic number up to 28. The particle flux given in Table-1 refers to sunspot minimum condition.

Table 1*

Nuclear composition of cosmic ray flux

Group of atomic nuclei	Z	I Intensity (m ² .sec sr) ⁻¹	% by number	% by mass
Protons	1	1510 ± 150	94	74
α - particles	2	89 ± 3	5.5	17.4
L (Li, Be, B)	3 - 5	2 ± 0.2		
M (C, N, O, F)	6 - 9	5.6 ± 0.2	0.5	8.6
H (A = 31)	10 - 19	1.9 ± 0.3		
VH (A = 51)	20 - 28	0.7 ± 0.16		

* Waddington (1966).

The abundances of heavy nuclei with respect to protons are much higher in cosmic rays than in the universal scale (Ginzburg and Syrovatskii, 1964). There is an anomalous abundance of the light elements He³, Li, Be and B in cosmic rays. These are accounted for by fragmentation of the heavy nuclei on the inter-stellar hydrogen in their propagation from the source through the interstellar medium to the observer (Ramaty and Lingenfelter, 1969).

In addition to the nucleonic component the electron component of primary cosmic rays which contains electrons

as well as positrons, has been identified in 1961 (Earl, 1961, Meyer and Vogt, 1961). In general the electron flux is approximately 1% of the proton flux for $E \geq 1$ BeV (Agrinier et al, 1964). The electron positron ratio gives information as to whether the electron component arises from the nuclear interactions of the cosmic rays during their passage through the galactic medium, or whether the electrons are coming predominantly from the source regions. An equal abundance of electrons and positrons would favour former; an excess of electrons over positrons would be expected in the latter case. Considerable effort has been made to establish the electron-positron ratio at different energies (Hartman et al, 1965; Bland et al, 1966; Daniel and Stephens, 1966; Hartman, 1967). For energies between .5 and 10 BeV the positron contribution amounts to about 10 percent of the total electron flux (Hartman, 1967, Fanselow et al, 1969).

Apart from nucleonic and electron components Gamma rays have also been observed. A possible source of Gamma rays is from nuclear interactions of cosmic rays with interstellar and intergalactic materials which create π^0 mesons. The flux will depend upon the thickness of matter traversed.

The particles comprising the cosmic radiation have a wide range of energies from 10 MeV up to more than 10^{19} ev,

the flux falling off with increasing energy. It is convenient to divide the cosmic radiation into three energy ranges (Marsden, 1968). These are:

- (i) Low energies, say $E \leq 10^{10}$ ev.
- (ii) Medium energies, $10^{10} \leq E \leq 10^{15}$ ev.
- (iii) Very high energies, $E > 10^{15}$ ev.

In the energy range 10^{10} to 10^{14} ev. the intensity is distributed over the particle energies according to a power law

$$\frac{dJ}{dE} = KE^{-\gamma}$$

where the value of the power law index $\gamma = 2.5$. At greater energies the value of γ increases and approaches ~ 3 at $E \simeq 10^{17}$ ev.

1.2 Time variation of cosmic rays intensity

Measurements of the cosmic ray intensity as a function of time have established the existence of several distinct variations of cosmic ray intensity with time. The study of time variations of the cosmic radiation can lead to a knowledge about the mechanism of production of cosmic rays, about their place of origin, their mode of propagation to the earth and about various influences on them, arising from the electromagnetic conditions of interplanetary space and

of the sun. Variations of cosmic ray intensity can be expressed by the relation (Dorman, 1957)

$$\frac{\delta N_{\lambda}^i}{N_{\lambda}^i} = - \delta E_{\lambda} W_{\lambda}^i(E_{\lambda}^c, h) + \int_{E^c}^{\infty} \frac{\delta m^i(E, h)}{m^i(E, h)} W_{\lambda}^i(E, h) \cdot dE + \int_{E^c}^{\infty} \frac{\delta D(E)}{D(E)} \cdot W_{\lambda}^i(E, h) \cdot dE \quad (1)$$

where N_{λ}^i is the observed intensity at latitude λ and at atmospheric depth h , E_{λ}^c is the cut off energy at a latitude λ , $D(E)$ is the differential energy spectrum, $m^i(E, h)$ is the multiplicity and $w_{\lambda}^i(E, h)$ is the coupling coefficient. In equation -1, the first term of the right hand side represents the variation due to the changes in geomagnetic cut off energy, the second due to changes in the multiplicity as a result of the alternations in the terrestrial atmosphere and the third one due to the variations of the primary energy spectrum.

1.3 Terrestrial Atmospheric effects

When primary cosmic rays impinge on the earth's atmosphere they produce secondary cosmic rays. The secondary particles are subjected to absorption processes and decay processes on their way from this region down to the altitude of the recording instruments. In the case of the stable nucleonic component, the absorption of the particles depends

on the mass of the air between the place of production and the point of recording. As this mass is proportional to the pressure at the altitude of recording, the number of particles recorded per unit time varies with the atmospheric pressure. For the meson component with finite but small life time, apart from the absorption process, the number of recorded particles depends on the temperature distribution in the atmosphere.

1.3 (a) Barometric effect

The counting rate of the detector is subjected to the integrated effect of the density variations in the atmosphere above the detector. Consequently the counting rate will vary with atmospheric pressure and the intensity as a function of atmospheric pressure can be described by an exponential law. It follows that the counting rate N , recorded at a given altitude, can be corrected for variations of pressure by the formula

$$N = N_0 \exp (\alpha_p \cdot \Delta p) \quad \text{-----} (2)$$

where Δp is the deviations from the mean barometric value for the given altitude and α_p is the pressure coefficient. The pressure coefficient depends on the latitude of the recording station and to the detector as the spectral sensitivity of the particles differ.

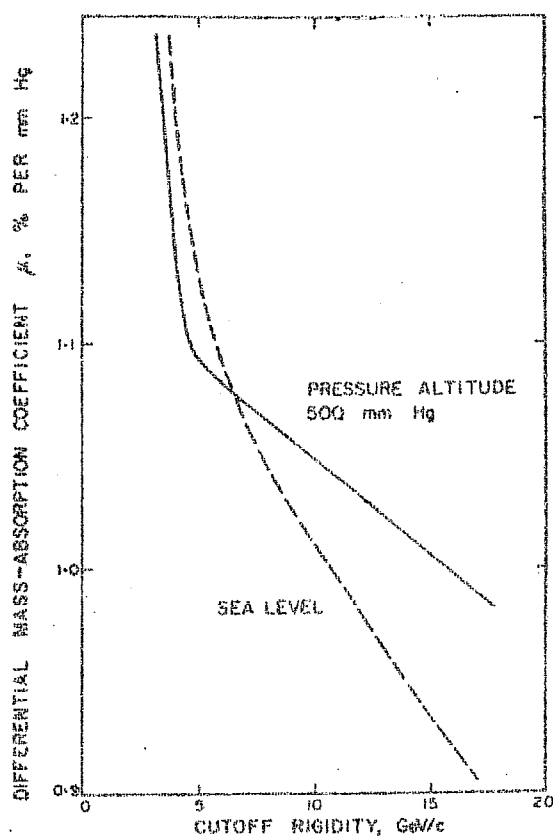
For the meson component, the pressure coefficient is about -0.1 per cent mb^{-1} . Therefore, the series expansion of equation (1), as

$$N = N_0 (1 + \alpha_p \Delta p) \quad (3)$$

is often used to calculate the pressure coefficient. The pressure coefficient of the nucleon component is approximately -0.7 per cent mb^{-1} at sea level, which is a large one, and hence equation (2) has to be employed.

α_p - the pressure coefficient may be determined by a linear regression analysis between the variables, $\ln \left(\frac{N}{N_0} \right)$ and ΔP (Dorman, 1957; McCracken and Jones, 1959; Lapointe and Rose, 1962; Bachelet et al, 1965). A variation in the barometric coefficient during the eleven years solar cycle has been shown by Girffiths et al (1966) for the Leeds IGY neutron monitor and by Lockwood and Kaplan (1967) for the Mt. Washington. The former finds 6% decrease in the barometric coefficient at Leeds, the later finds about 3% change at Mt. Washington between solar minimum (1965) to solar maximum (1958). The change in the barometric coefficient over the solar cycle is due to two effects: modulation of the primary energy spectrum and a change in the relative contribution to the counting rate from nucleon and muon neutron production. A well defined latitude effect of the order of 10% of the barometric coefficient between $P_c = 2$ bV

and $P_c = 15$ bV has been reported by Bachelet et al (1965) and measured by Carmichael et al (1966). Fig.1.1 shows the differential mass absorption coefficient calculated by Forman (1968) for rigidities between 2 and 15 bV for the IGY-type neutron monitors at sealevel and at 500 mm.Hg. pressure altitude.



Differential mass-absorption coefficients for IGY-type neutron monitors at 500 mm.Hg. pressure altitude (full line) and sea level (dashed line) (Forman, 1968).

Fig.1.1

1.3 (b) Temperature effect

Measurements of the cosmic rays intensity using ionization chambers have shown that in addition to the well known barometric effect, there is a correlation between the intensity and the temperature at ground level. Dorman and Feinberg (1955) and Maeda and Wada (1954), have described the effect of temperature on the muon intensity as the weighted mean of temperature change throughout the atmosphere. Thus the fractional change in intensity due to temperature changes in the atmosphere can be written as

$$\frac{\delta N_{\mu}(x_0)}{N_{\mu}(x_0)} = \alpha_p \cdot \delta T(x_0) + \int_0^{x_0} W_T(X) \cdot \delta T(X) dX \quad (4)$$

where $N_{\mu}(x_0)$ is the muon intensity at atmospheric depth x_0 , α_p is the barometer coefficient, $\delta T(X)$ is the temperature change at depth X and $W_T(X)$ is a weighting factor which Dorman has called the "density temperature coefficient". Dorman (1957) has derived $W_T(X)$ from a detailed theoretical treatment of muon production and propagation in the atmosphere. In practice, the integral may be broken up into summation over a series of isobaric levels for each of which the average temperature change δT may be available from Radiosonde data. Maeda (1960) has elaborated the calculation of $W_T(X)$ to include obliquely incident muons, the effects of curvature of the isobaric levels and deflection of the particles in earth's magnetic field.

Using the Cascade theory, Dorman (1957) has calculated the effect of atmosphere temperature changes on counting rate of neutron monitors. The effect of such changes has usually been neglected when correcting neutron monitor data for meteorological effect.

Kaminer et al (1966) have investigated the annual temperature effect by comparing the counting rate of a neutron monitor in the Northern hemisphere (Chicago) with that of a geomagnetically equivalent one in Southern hemisphere (Hobart). They find for 1960-62 period an annual seasonal wave of 1.2%, about 1.8 times the value calculated from Dorman's temperature coefficients. Using Deep River and Inuvik neutron monitor data, Bercovitch (1967) has obtained an average value of $1.93 \pm .09$ for temperature effect. The result agrees well with Harman and Hatton's (1968) value of $1.20 \pm .0.13$. They have also calculated the temperature weight factors, $W_T(X)$ for both IGY and NM64 monitors. Fig.1.2, shows the variation of W_T and h , together with Dorman's original curve.

These results indicate that for IGY monitor the temperature effect should be a factor of 1.2 ± 0.3 larger than Dorman's prediction while for NM64 the factor is

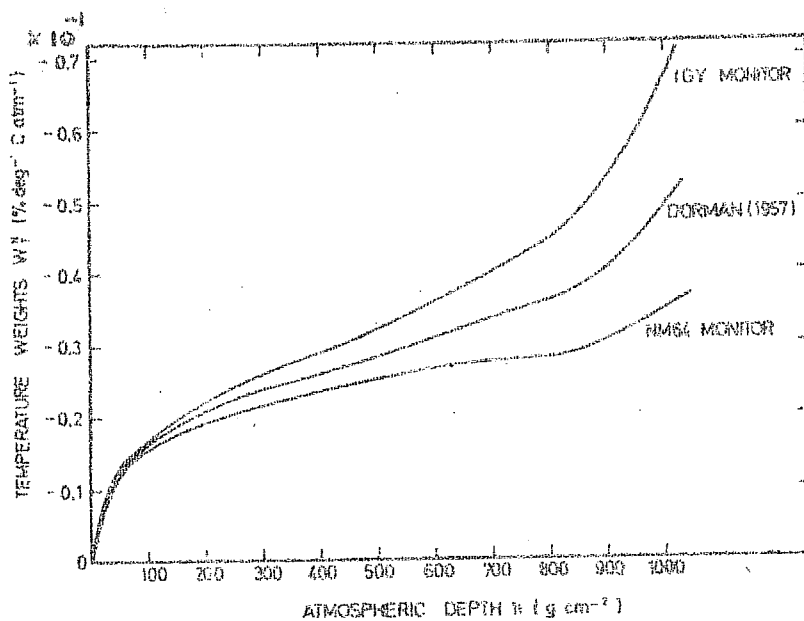


Fig.1.2 The calculated variation of the temperature weights with height for IGY and NM64 monitors compared with Dorman's values.

0.85 ± 0.2 . It is shown that fewer muons are stopped in the NM64 monitor than in the IGY monitor. Comparison of various methods of temperature correction have been published by Bachelet and Conforto (1956), Mathew (1959), Wada (1961), Lindgren and Lindholm (1961) and Carmichael et al (1967).

1.4 (a) The earth's magnetic field and cut off rigidity

During ocean voyages between Java and Holland, Clay (1927) found a consistently lower cosmic ray ionization near the equator and thus made first use of the magnetic field of the earth as a charge spectrometer. The comprehensive studies of the radiation and the magnetic field surrounding the earth have been made during IGY period and more recently with artificial satellites.

The internal or surface magnetic field of the earth may be represented as a spherical harmonic potential expansion,

$$V = a \sum_{n=1}^{\infty} \left(\frac{a}{r}\right)^{n+1} \sum_{m=0}^n (g_n^m \cos m\phi + h_n^m \sin m\phi) P_n^m(\theta) \quad (5)$$

where 'a' is a scale factor generally chosen to be earth's radius, r, θ and ϕ are the geomagnetic co-ordinates and $P_n^m(\theta)$ are the Schmidt normalized spherical functions (Schmidt, 1935). The coefficients g_n^m and h_n^m are generally determined by least square fit to magnetic data. Numerous evaluations of the field have been made for various epochs

with the number of terms ranging up to 512 ($n = 24$, $m = 27$). (Finch and Leaton, 1957, Jensen and Whitaker, 1960, Jensen and Cain, 1962, Cain et al; 1965, Hendricks and Cain, 1966, Hurwitz et al; 1966).

The dominant term in the harmonic expansion of the earth's potential field is that of a dipole which should form the basis of a model of the earth's field to examine the motion of charged particles. Stormer (1930, 1931, 1955), has computed the trajectories of charged particles in a dipole field, following the terrella experiments of Birkeland (1908, 1913) and has obtained a first integral of the equations of motion which together with the kinetic energy integral provided substantial information about the allowed motion of the particles. It was found that the cut-off rigidity P_c , the minimum magnetic rigidity a particle is required to possess in order to reach a specified location in space from infinity with a specific direction of arrival, in a dipole field is given by

$$P_c = \left(\frac{14.9}{r^2} \right) \left\{ \frac{1 \pm \sqrt{1 + \cos w \sin^3 \Theta}}{\cos w \sin \Theta} \right\}^2 \text{ GV} \quad (6)$$

where r is the distance from the origin in earth radii,

Θ is the co-latitude of the observation point and w is the angle that the direction of arrival of particles make with the eastward direction.

It had been evident that the cosmic ray measurements exhibited discrepancies with respect to results to be expected from a dipole representation (Meyer and Simpson, 1957, Koodama and Miyazaki, 1957). Improvements to the calculation of the cutoff rigidities, using non-dipole terms for the field were made by Quenby and Webber (1959). However, even these values proved to be inaccurate as was shown by Freon and McCracken (1965). The advent of high speed digital computers have made possible the determination of the cut-off rigidity by tracing the trajectories of charged-particles as they traverse through a high-degree simulation of the geomagnetic field. (Shea et al, 1965). Shea and Smart (1967) have also calculated the cutoff rigidities, for a grid of locations on the earth spaced at 15° increment of latitude and longitude.

1.4 (b) Asymptotic direction

Brunberg (1953) has introduced the concept of the asymptotic direction which is defined as the direction that a cosmic ray particle has prior to its entry into the domain of the geomagnetic field. The direction of the particle velocity vector in terms of 'asymptotic latitude' λ and 'asymptotic longitude' ψ (Fig.1.3) is given as:

$$\tan \lambda = \frac{-V_\theta \sin \theta + V_r \cos \theta}{(V_\phi^2 + (V_\theta \cos \theta + V_r \sin \theta)^2)^{\frac{1}{2}}} \quad (7)$$

$$\psi = \phi + \arctan \left(\frac{V_{\phi}}{V_{\theta} \cos \theta + V_r \sin \theta} \right) \quad (8)$$

where V_r , V_{θ} , V_{ϕ} are the velocity components in r , θ and ϕ directions.

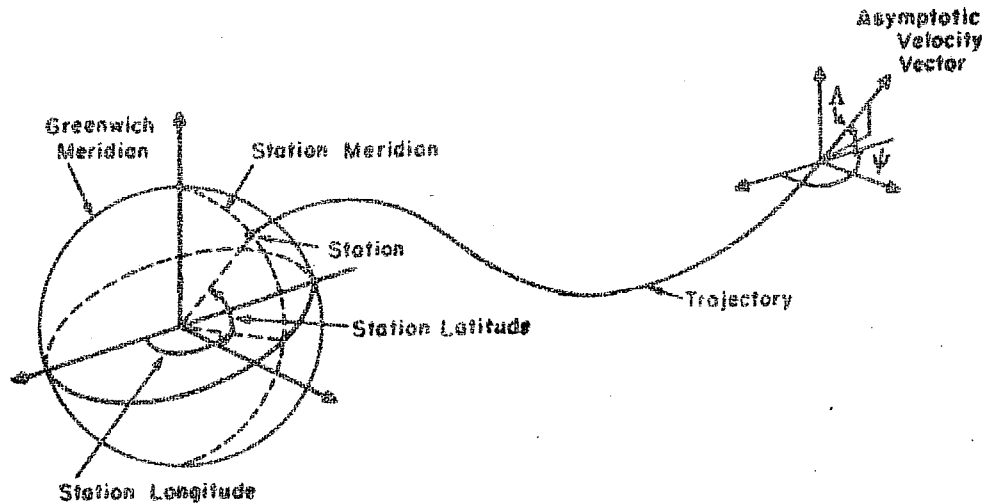


Fig.1.3 The Trajectory of a charged particle through geomagnetic field.

Malmfors (1954), Brunberg (1953), and Brunberg and Dattner (1953) have computed the asymptotic directions considering the model experiments in which a small model of the earth and its field is used to simulate the actual physical situation. These have been also computed by numerical integration of the equation of motion of cosmic ray particle by Stormer, (1955), Jory (1956) and Lust and Simpson (1957). Using high simulation model of internal sources of the field and with a high-speed digital computer McCracken et al.(1962), Hatton and Carswell (1963), Kodama (1964), and Shea et al.(1968) have published tables of asymptotic directions for several directions of incidence for cosmic ray stations. Recently directions have also been computed by Gall et al.(1968) with models that include the external currents in the tail and magnetopause.

1.4 (c) Asymptotic cone of acceptance

McCracken (1958) has introduced the concept of 'asymptotic cone' of acceptance to determine the dependence of the counting rate of the detector on the asymptotic directions. It is defined as the solid angle containing the asymptotic directions of approach that significantly contribute to the counting rate of detector. Rao et al. (1963) have shown how the asymptotic cones of acceptance can differ considerably from station to station.

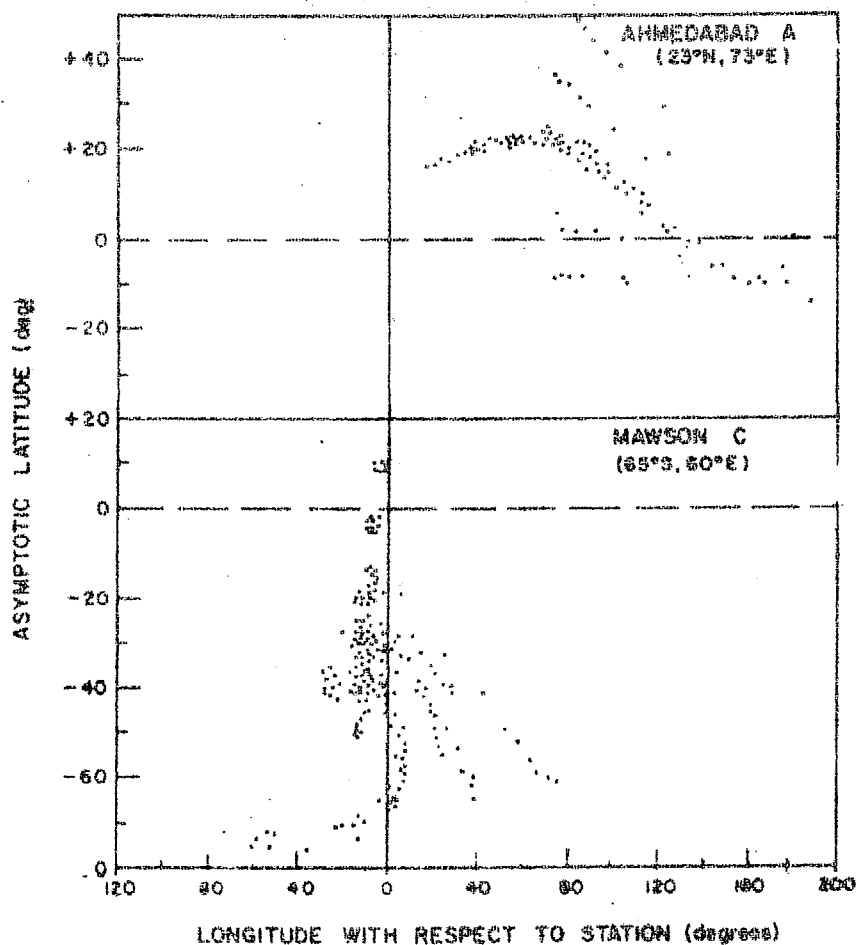


Fig.1.4 The asymptotic directions of approach for particles arriving at two locations.

Fig.1.4 shows the asymptotic cones of acceptance for Ahmedabad (23°N , 73°E) and Mawson (65°S , 60°E) stations. The co-ordinates being the geographic latitude and longitude of the asymptotic directions of approach of particles,

arriving with zenith angles of 0° , 16° and 32° in the N-S and E-W geomagnetic field.

It can be seen that the cone of acceptance of Ahmedabad is wide in longitude while for a high latitude station like Mawson, the cone of acceptance is narrow. An anisotropy of small angular extent will therefore lie within the cone of acceptance of Ahmedabad for many more hours compared to the cone of acceptance of Mawson.

1.5 Relation of secondary time variation to Primaries

Different authors have used different terminologies to express the relationship between primary changes and secondary changes. Treiman (1952) called it a "yield function" as does Fonger (1953). Nagashima (1953) has termed it "multiplicity" and "relative intensity spectrum" and Dorman (1955) defined it as the "coupling coefficients".

Basically all of the above authors use experimental data on the latitude variation of the ionizing or neutron component. Let $N(\lambda, h)$ denote the intensity of the secondary radiation at latitude λ and at atmospheric depth h , and $D(E)$ the primary differential energy spectrum, then the 'multiplicity function' $M(E, h)$ that gives the number of secondary particles produced at altitude h due to a primary particle of energy E incident on top of atmosphere, can be expressed as

$$M(E, h) = -\frac{1}{D(E)} \cdot \frac{dN(\lambda, h)}{d\lambda} \cdot \frac{d\lambda}{dE} \quad (9)$$

The differential contribution to the secondary intensity is given by

$$n(E, \lambda, h) = m(E, h) \cdot D(E)$$

and the total intensity will be

$$N(\lambda, h) = \int_{E_c}^{\infty} n \cdot dE$$

or

$$N(\lambda, h) = \int_{E_c}^{\infty} m(E, h) \cdot D(E) \cdot dE \quad (10)$$

Dorman (1957) has introduced the idea of 'coupling constants' $W(E, h)$ to estimate the contribution of primary of energy E to the secondary component of type i . It is defined as:

$$W(E, h) = \frac{D(E) \cdot M(E, h)}{N_i(\lambda, h)} \quad (11)$$

$W(E, h)$ can be estimated from geomagnetic effect, that relate $N_i(\lambda, h)$ with E . Differentiating equation (10) partially with respect to the lower limit of integration one can obtain.

$$\frac{\delta N_i(\lambda, h)}{\delta E} = -D(E) \cdot M_i(E, h) \quad (12)$$

and combining equation (10) and equation (11)

$$W(E, h) = -\frac{1}{N_i(\lambda, h)} \cdot \frac{\delta N_i(\lambda, h)}{\delta E} \quad (13)$$

The right hand side of equation (12) represents geomagnetic effects that are experimentally known for secondary components. These can be calculated for the energy region 0 to about 15 Gv, which is the maximum cut-off rigidity for vertical intensity at the equator. For higher rigidities the coefficients have been calculated by extrapolation.

Considering quadrupole and higher order terms of the earth's magnetic field, instead of a dipole representation, Quenby and Webber (1959) have calculated the revised values of cut-off rigidities E_c and have derived the coupling coefficients $W(E)$ which are shown in Figure 1.5.

They have assumed the relationship between $\frac{\partial N}{\partial E}$ and E , to be a power law of the form $\frac{\partial N}{\partial E} = KE^{-V}$ for extrapolation beyond the 15 Gv rigidities. V can be obtained from the slope of the differential response curve at 15 Gv for neutrons and 25 Gv for mesons.

The angular dependence of coupling coefficients of the meson components of cosmic rays has been calculated by Krimsky et al. (1966), using the energy spectrum $KE^{-2.5}$ and the multiplicity, calculated by considering Pal and Peters (1963) model of elementary interaction of excited nucleons.

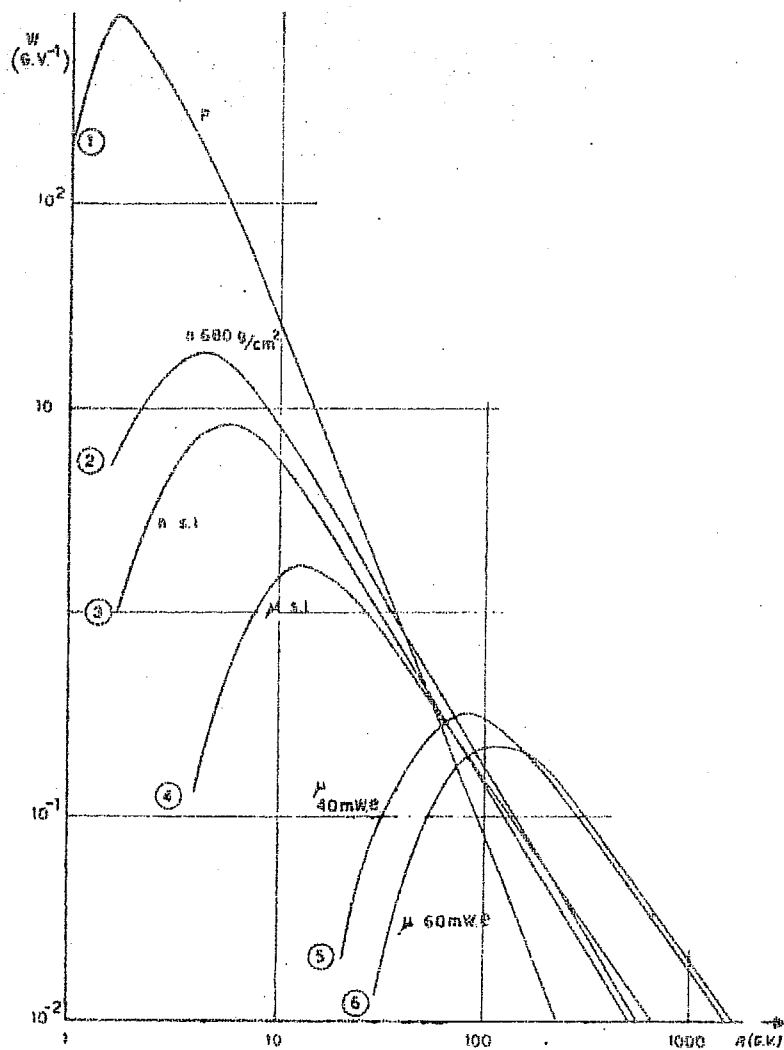


Fig.1.5 Differential response for different secondary components at different depth.

Fig.1.6 shows the estimated differential response functions for the meson intensity observed at different zenith angles $0^\circ, 8^\circ, 16^\circ, 24^\circ, \dots, 64^\circ$.

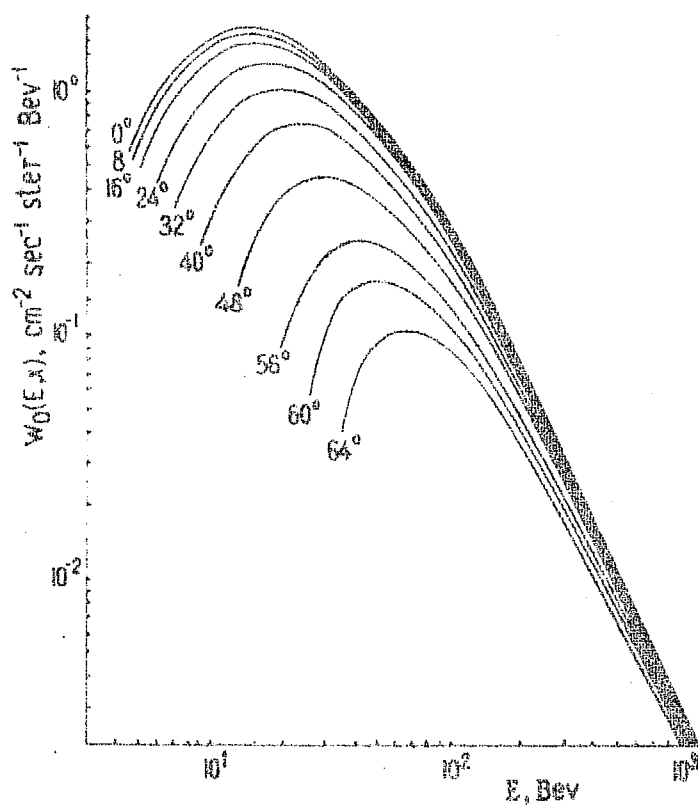


Fig.1.6 Coupling coefficients of the meson component for different zenith angles.

1.6 Modulation of cosmic ray intensity

It is well known that the interplanetary magnetic field controls the propagation of cosmic rays in the solar system. The sun and the interplanetary medium however, exert a profound influence on the cosmic radiation causing them to undergo deviation from isotropy and change of energy spectra as well as of intensity. The intensity of galactic cosmic rays shows several characteristic time variations. They can be divided into the following major categories:

- (a) Long term changes in the galactic cosmic ray intensity which are anticorrelated with the 11 years cycle of solar activity.
- (b) Decreases of the intensity of the galactic cosmic rays associated with magnetic storms called Forbush decreases.
- (c) The variation of the intensity associated with the 27-day period of solar rotation known as 27-day variations.
- (d) Variations with a period of one day, the so called daily variation which is studied as diurnal and semi-diurnal variations of the galactic cosmic rays.
- (e) Short period variations of the order of a few minutes of the cosmic ray intensity.

The various intensity modulations of galactic cosmic rays have been generally accounted for in terms of the dynamics of charged particles moving through solar-controlled magnetic fields. In the following section we describe briefly the interplanetary magnetic field and its observations which are important from the point of view of the theories of modulation of galactic cosmic rays.

1.6 (a) The interplanetary magnetic field

Observations of ionised cometary tails have led Biermann (1951) to the conclusion that solar corpuscular radiation is emitted from the sun. Parker (1958) proposed that this could be accounted for by a simple outward hydrodynamic expansion of the solar corona and named the resulting streaming coronal plasma the 'solar wind'. The wind is composed of coronal gas fully ionized and mainly hydrogen. The velocity of the solar wind was of the order of 350 - 600 Km/sec during the recent solar cycle (Shlovskii et al; 1960, Neugebauer and Snyder, 1963, Bridge et al; 1965). The temperature of the solar wind is observed to fluctuate widely from 10^4 °K upto 10^6 °K during times of solar activity (Neugebauer and Snyder, 1965; Sturrock, 1966).

The solar wind is filled with the magnetic lines of force of the general field (Parker, 1958 b, 1963) which is observed to be of the general order of a few gauss at the

solar photosphere (Babcock, 1959; Bumba and Howard, 1965). The solar wind carries the magnetic field lines out through interplanetary space. Thus, through the hydromagnetic equation the uniform radial wind of velocity v would lead to the field

$$\frac{\partial \vec{B}}{\partial t} = \nabla \times (\vec{V} \times \vec{B}) \quad (14)$$

If Ω is the angular velocity of the sun, r , the distance measured from the sun, θ , the polar angle measured from the axis of rotation of the sun and ϕ is the azimuth measured around the sun, then the lines of force will rotate in interplanetary space in an Archimedes spiral pattern of the form

$$r = \frac{V \phi}{\Omega \sin \theta} \quad (15)$$

The components of the field are given by

$$B_r = B_1 \left(\frac{R_1}{r} \right)^2 \quad (16)$$

$$B_\theta = 0 \quad (17)$$

$$B_\phi = B_1 \frac{R_1^2 \Omega}{V r} \sin \theta \quad (18)$$

where B_1 is the radial component of the magnetic field at $r = R_1$. The angle χ between the normal to spiral field lines and the radial direction is given by

$$\tan \chi = \frac{V}{\Omega r} \quad (19)$$

On this underlying pattern are superposed a variety of both small and large magnetic irregularities caused, by variation of v with θ , ϕ and t ; by variation of $B(\theta, \phi)$ with t and by instabilities in the wind etc. Near the orbit of the earth the average angle between the interplanetary magnetic field and earth-sun direction would be expected to be about 45° . The field strength at the orbit of the earth is about 3×10^{-5} gauss for each gauss at the photosphere. From the observations of the photospheric magnetic field Babcock (1953) and Ahluwalia and Dessler (1962) have pointed out that changes of polarity may be expected in the interplanetary field.

Observations of the interplanetary magnetic field

The analysis of different flare events by McCracken (1962) indicates the preferential guiding of the solar particles to the earth. The cosmic ray flux has been the greatest from a direction 50° to the west with respect to earth-sun line. This suggests the development of the Archimedean spiral structure in the interplanetary field. The first extensive direct measurements of the interplanetary magnetic field were carried out with the Pioneer V (Coleman et al; 1960). The analysis of Pioneer V data by Greenstadt (1965) shows that the fields measured nearly at the plane of the ecliptic are of the order of 5 to 10 gammas.

The observations obtained with IMP-1 satellite confirm that on the average the direction of the field is close to that predicted by the Archimedes spiral model and the field is approximately between $4-7 \times 10^{-5}$ gauss (Ness et al; 1964, Ness and Wilcox, 1964). Ness and Wilcox (1965) have also shown that the interplanetary magnetic field had a sector structure in which the interplanetary field was predominantly away from the sun for several consecutive days and then predominantly towards the sun for the next several days. The sector pattern corotates with the sun such that a particular feature such as sector boundary is observed near the earth approximately once every 27 days. Corotation of the field structure has been also established by examining simultaneous observations from two spacecraft, IMP-3 and Pioneer-VI, which were on opposite side of earth and separated by 1.3×10^6 Km.(Ness, 1966). The sector pattern observed by IMP-1, IMP-2 and Mariner-IV were very similar. Observations from both Pioneer-VI and IMP-3 have indicated that there can exist a small order structure that may take a time of the order of an hour to rotate past the earth, called 'filaments' of the interplanetary magnetic field. Solar cosmic rays produced by flares often appear to be guided by along such filaments (McCracken and Ness, 1966; Bartly et al; 1966).

As the sector pattern rotates past the earth profound changes are observed in geomagnetic activity. The geomagnetic activity tends to be higher near the leading edge of each sector (Ness and Wilcox, 1965). The work of Snyder et al; (1963) shows that geomagnetic activity is strongly correlated with wind velocity. A stronger wind near the leading edge of each sector causes the leading edge to crowd into the trailing edge of sector. Sarabhai (1963) has pointed out that this should lead to turbulence and/or a shock wave toward the leading edge of each sector. Dessler and Fejer (1963) have shown that the leading portions of the sectors may be responsible for the recurring magnetic storms in much the same way that the blast wave from an outburst at the sun produces a magnetic storms.

Measurements of the interplanetary plasma and magnetic field give us a clear understanding of the features of the magnetic fields which are important for the motion of energetic charged particles and for the different theories of the galactic cosmic ray modulation. Following are the important features of the interplanetary field from the point of view of the average features of the modulation of galactic cosmic rays.

- (1) The average character of the field is that of a garden hose spiral resulting from the motion of the

solar plasma in which field is embedded. The diurnal anisotropy and the 27-day recurrent Forbush decreases are prime examples of the co-rotation effect.

- (2) The field is divided into well defined "sectors" in which the field direction is alternately towards or away from the sun. The sector structure plays an important role in manifesting the 27-day cosmic ray periodicity or recurrent Forbush type decreases.
- (3) Superimposed on this large scale field is a continuous distribution of magnetic irregularities. The irregularities that exist in the field cause scattering of the particles and give rise to diffusion-like flux characteristics. The diffusion tensor describing the motion of the charged particles in the interplanetary space has been estimated from the power spectrum of magnetic field fluctuations in interplanetary space (Gloeckler and Jokipii, 1966; Jokipii, 1966, 1967, 1968; Jokipii and Coleman, 1968; Jokipii and Parker, 1969). The cosmic ray diffusion coefficients so obtained agree with cosmic ray observations carried out on the Mariner-IV interplanetary probe in 1965 (O'Gallagher and Simpson, 1967). The diffusion coefficient has been applied

to Parker's (1958) diffusion-convection model of 11-year modulation of galactic cosmic rays.

1.6 (b) 11-year variation

The intensity variation follows inversely the cycle of solar activity has been shown by Forbush (1954, 1958), Simpson (1963), and Katzman and Rose (1962). This inverse correlation suggests that the process is one of exclusion of galactic particles. The 11-year changes in solar modulation of galactic cosmic radiation are produced by changes in the characteristics of the solar wind and the magnetic field which it carries into interplanetary space over 11-year solar cycle.

Experimental observations by Forbush (1958) show that the 11-year variation in cosmic ray intensity are of a world-wide nature and that low energy particles are subjected to greater variation than high energy particles. Simpson (1962), Callender et al; (1965) and Dorman and Dorman (1965) have shown that this modulation is not in phase with 11-year solar activity cycle as measured by sunspot number but lags behind the level of solar activity by 9 to 12 months. It has been found however that the coronal green-line intensity is a better index of solar plasma emission than either sunspot number or K_p (Gnevyshev and Ol', 1966). When the coronal green-line intensity in

the heliographic latitude range $\pm 22\frac{1}{2}^{\circ}$ is compared with the cosmic ray intensity a high degree of anti-correlation is found (Simpson and Wang, 1967; Hatton et al; 1968). Pathak and Sarabhai (1970) however have shown that a good correlation is obtain^{ed} between $\pm 5^{\circ}$ to 10° heliolatitudes. It is clear from cosmic ray data of Neher and Anderson (1965) over three solar cycles that the modulation effects are strongly energy dependent. There are papers supporting the modulation as being energy, velocity or rigidity dependent as well as combination of these quantities (Gloeckler, 1965; Balasubrahmanyam, 1967; Nagashima et al; 1966; Silberberg, 1966; Gloeckler and Jokipii, 1966).

4.6 (c) Different models of 11-year modulation mechanism

The modulation of cosmic rays has been studied extensively for a considerable period of time. Many models and processes have been proposed for the 11-year modulation. They can be grouped into three categories (1) by electric deceleration, (2) by a solar dipole and (3) by solar wind. The first was proposed by Nagashima (1953) using a geocentric model and later used by Ehmert (1960) in a heliocentric model. This theory has subsequently been explored and compared to experimental data by McDoland and Webber (1959), Fitchel (1961), Freier and Waddington (1965) and others. The main objections to the electric deceleration model, in

addition to its failure to give entirely satisfactory agreement with experimental data, are (1) The electrical conductivity in interplanetary space will almost certainly not support the necessary potential. Electron data disagrees with the existence of a large potential (Abraham et al, 1966); (2) The detailed characteristics of the heavy nuclei argue against a large deceleration (Fichtel and Reames, 1966).

The modulation of the cosmic radiation by a solar dipole field was first proposed by Janossy (1937) and extended by Elliot (1960). The principal arguments against this theory are (1) the disagreement between the magnetic field configuration required by the theory and that which is observed and (2) the prediction of the variation in intensity with distance from the sun, i.e., the cosmic ray flux should increase as we go away from the sun. Investigation by the Pioneer V space craft have revealed no significant change in the cosmic ray intensity from 1 - 0.75 A.U. from the sun.

In the solar wind picture the modulation is due to the diffusion and convection of particles in the presence of small-scale irregularities in the magnetic field of the outward-moving interplanetary plasma (Parker, 1963, 1965). From the detailed observations in space of magnetic fields, (Ness et al, 1964; Ness and Wilcox, 1965; Davis et al, 1966;

Coleman et al, 1966 a) and of plasmas (Neugebauer and Snyder 1962, Bridge et al, 1965), one can conclude that the solar wind theory of the modulation of cosmic rays seems to be on firm experimental ground. It is considered to be most satisfactory model to account for the main observational features of the modulation.

1.6 (d) Diffusion-convection model

Parker (1958, 1963, 1966) has treated modulation as both a convective process whereby the scattering centers in the magnetic fields are being strongly affected by solar activity, and in terms of adiabatic deceleration of incoming particles due to the expanding magnetic field in the solar wind. Theoretical treatments of solar modulation have been done by Gleeson and Axford (1968), Jokipii (1967, 1968) and Jokipii and Parker (1967). Parker's model of diffusion-convection predicts that to a first approximation the outward convection of cosmic rays resulting from scattering by magnetic irregularities frozen into the solar wind, in the steady state, be balanced by the particle's diffusion through the modulating region. This is expressed by

$$dJ_e(P, r) = dJ_\infty(r_0, P) \exp \left(- \int_{r_0}^r \frac{w}{K} dr \right) \quad (20)$$

where dJ_e is the differential flux at a radial distance r from the sun, dJ_∞ is the unmodulated flux and w and K are

the solar wind velocity and isotropic diffusion coefficient respectively. r_0 is the boundary of the solar wind and P is the particle's rigidity.

The statistical analysis of scattering from magnetic inhomogeneities by Jokipii (1966) has yielded an expression for the parallel diffusion coefficient in terms of the transverse power spectrum of the magnetic field, measured at frequencies corresponding to fluctuations with scale sizes approximately equal to the gyroradii of the cosmic ray in the average field. If the power spectrum throughout the modulating region can be represented by a power law, $f^{-\alpha}$, Jokipii (1966) finds that

$$K_{11} = 2\alpha (\alpha + 2) \frac{c \beta P^2}{9 w P_{ZZ}(f_0)} \quad (21)$$

where β is the particle's velocity divided by c , and $P_{ZZ}(f_0)$ is the power spectrum of a non-radial component of the magnetic field measured at frequencies $f_0 = \frac{w B}{2\pi P}$. From equation (21), we can express (20) as

$$dJ_e(P, r) = dJ_\infty \exp \left[-\frac{\eta}{B P^{2-\alpha}} \right] \quad (22)$$

where the spatial dependence and various constants are included in the parameter η . Assuming that the galactic cosmic ray flux is constant, and following Nagashima et al. (1966), the fractional modulation, or the logarithm of the ratio of the particle densities observed at times t_1 and t_2 will be given by

$$\ln \frac{dJ(P, t_2)}{dJ(P, t_1)} \sim \frac{1}{\beta P^{2-\alpha}} \quad (23)$$

Power spectra based on Pioneer 6 interplanetary magnetic field data (Sari and Ness, 1969) indicate that α is between $3/2$ and 1 for low frequencies and is 2 for frequencies greater than 2.8×10^{-4} CPS. In an average field of $B = 6\gamma$, and solar wind velocity $w = 400$ Km/sec, this frequency corresponds to cosmic ray rigidities of $P \sim 0.4$ Gv. At rigidities below 0.4 Gv the fractional modulation varies as $1/\beta$ while at higher rigidities the modulation varies between $1/\beta P^{\frac{1}{2}}$ to $\frac{1}{\beta P}$. Ormes and Webber (1968), from a direct analysis of cosmic ray data, find a rigidity independent modulation for rigidities below 0.5 Gv and $1/\beta P^{\frac{1}{2}}$ dependence at greater rigidities.

The diffusion coefficient K_{11} derived from the observed radial gradient of cosmic ray intensity is found to be 3.2×10^{21} cm²/sec for a particle with $P\beta = 1$ Gv. (O'Gallagher, 1967), however calculation based on observed magnetic field power spectra (Jokipii, 1966) gives $K_{11} = 7.6 \times 10^{21}$ cm²/sec which is larger by about a factor of 2 than that derived from the gradient. Jokipii (1967) suggests that the inclusion of the effects of adiabatic deceleration may account for this difference in K .

Analysis of the phase lag between the solar cycle variations of the cosmic ray intensity and appropriate solar

activity indices permits an estimate of the size of the modulating region - the heliocentric distance beyond which turbulence in the wind becomes too weak to exclude cosmic rays effectively. A number of investigators have shown that the modulation is not in phase with the 11-year cycle of solar activity as measured by sunspot number. The amplitude of cosmic ray modulation changes approximately inversely with sunspot number but with a time lag of 9 to 12 months. If the sunspot number is indeed a true measure of the properties of the solar wind that modulate the cosmic ray flux, the delay can be ascribed to the travel time of the solar wind through the modulating region (Simpson and Wang, 1967). If Δt_1 is the observed phase lag and V_s is the solar wind velocity then the modulating region r_0 could be express as

$$r_0 = \Delta t_1 \times V_s$$

For a solar wind velocity $V_s \sim 400$ Km/sec in 1965, a lag in reaching minimum modulation $\Delta t_1 = 6 - 9$ months leads to modulating region $r_0 > 40$ A.U. On the basis of these principles Dorman and Dorman (1967) have developed a mathematical model which yields $r_0 = 80 - 160$ A.U.

These values are an order of magnitude greater than those deduced from gradient and spectral studies for the same period. With measurements from satellites and space probes it has been possible to determine the radial gradient

of the cosmic radiation and its dependence upon particle parameters leading to an upper limit of $\gamma_0 \sim 5$ A.U.

(O'Gallagher and Simpson, 1967) at that particular period of time. The gradient measurements along with the residual modulation calculated by Biswas et al. (1966) from the observed differential spectra of $\text{He}^3/\text{He}^3 + \text{He}^4$, also give $\gamma_0 < 5$ A.U. (O'Gallagher, 1967).

Therefore there lies a discrepancy in the assumption that the changes in the solar wind velocity are in phase with the changes in solar activity deduced from sunspot number. The intensity of the coronal emission line at 5303 \AA° (green) peaks approximately 12 months after sunspot maximum and may be a good indicator of solar wind properties. Simpson and Wang (1967) and Hatton et al. (1969) have shown a close correlation between cosmic ray modulation and the intensity of the green line measured between $\pm 20^\circ$ and 30° of the solar equator, while Pathak and Sarabhai (1970) have shown that a good correlation is obtained between $\pm 5^\circ$ and 10° heliolatitudes. Around the time of minimum cosmic ray modulation the correlation indicates a phase lag of $\Delta t_1 < 1$ to 2 months. This leads to a modulating region ~ 10 A.U. Recently Jokipii and Davis (1969) have predicted that cosmic ray modulation ceases at 3 - 10 A.U. and Jokipii (1969) finds the dimension of the modulating region $\gamma_0 \sim 2.7 \pm 0.4$ A.U.

1.6 (e) Forbush Decreases

An abrupt and short-lived Forbush type galactic cosmic ray decrease generally occurs in coincidence with a geomagnetic storm phenomenon. The onset of a decrease is quite rapid and the intensity may fall as much as 5 percent per hour. Decreases as great as 40 per cent in intensity of sea level neutron monitor have been observed. The recovery to a normal level before the decrease may require many days. It has been demonstrated by the measurements with the space probe Pioneer V (Fan, Meyer and Simpson, 1961; Coleman et al. 1961) that the Forbush decrease phenomenon occurs in the interplanetary medium. Parker (1963) has explained this effect considering the distortion of the basic field pattern by an idealized blast wave which occurs due to a sudden outburst in the solar corona. The blast wave compresses the magnetic field which then becomes a reflector of cosmic rays. The reflectivity tends to isolate the region between the wave and the sun so that individual particles in that region tend to remain there for several hours leading to a reduction of the cosmic ray energy density. Laster et al. (1962) have developed the energy loss model to explain Forbush decreases.

Detailed analysis of several Forbush decreases events has been described by Dorman (1963). The rapid onset and

flat energy spectrum are the characteristics of a Forbush decrease. McCracken and Parson (1958), Lockwood and Razdan (1963) have observed that the onset of the Forbush decrease was always earlier from west of the earth sun line regardless of the location on the sun of the solar flare. They have also observed short and long lived anisotropies in the intensity.

1.6 (f) 27-day variation

Variation of coronal conditions around the sun in interplanetary space leads to different wind and field conditions around the sun. The 27-day recurring cosmic ray decreases result from the enhanced solar wind velocity and increased field disorder associated with active regions on the sun.

Sarabhai (1963) has suggested that the slow wind in particular direction from a cool coronal region will be overtaken by the faster wind in the same direction when a hotter coronal region comes around. This may lead to a relatively thin region of turbulence between the fast and slow wind regions giving rise to geomagnetic activity and reduction in the cosmic ray intensity. After 27 days as the sun completes one rotation, a similar situation arises in interplanetary space resulting in a recurrent decrease.

Considering a similar situation where the fast plasma from the "hot spot" creates a standing shock wave at its interface with the slower plasma from the remainder of the corona, Axford (1965) and McCracken et al. (1966) have also shown that a depression of the cosmic ray intensity would be observed due to enhanced outward convection of the cosmic rays along the lines of force within the shock. Since a shock would remain stationary relative to a point on the rotating sun it would appear to be corotating with the sun for an observer near earth, where the shock would be observed once every 27 days resulting in recurrent decreases in the cosmic ray intensity.

1.6 (g) The daily variation

The daily variation in cosmic ray intensity with the predominant diurnal and semi-diurnal components has been extensively investigated in the past by use of data from ion chambers, neutron monitors and meson monitors. A long term variation of the phase and amplitude of the diurnal variation with a period close to 22 years, has been observed (Sarabhai and Kane, 1953, ; Thambyahpillai and Elliot, 1953; Forbush, 1967; Wada and Kudo, 1968). If days are characterised as D type (having maxima during sunlit hours) and N type (maxima during night), then particularly D type days occur each with a 27 day recurrence tendency (Sarabhai and

Bhavsar, 1958). They have also observed that N type days are associated with decreases of intensity and D types of days with increases of daily mean intensity after the respective epochs. The evidence supports the result of Simpson et al.(1955) who have shown a close association of the central meridian passage of unipolar regions with cosmic ray increases during 1953. A characteristic difference of 6 hour in the diurnal time of maximum for the east and west direction is observed to occur on many days (Rao and Sarabhai, 1961). However there are days on which the daily variation has a maximum near noon for both directions. They have suggested that this may be due to the influence of a local source situated within the influence of the geomagnetic field. McCracken and Rao (1966) have shown that the amplitude of the annual mean diurnal anisotropy remains almost constant between 1957 and 1965 while Duggal et al., (1967) have reported a decrease of 26% in the average magnitude of the diurnal anisotropy between 1958 and 1965 as observed at 15 stations. There are also seasonal changes but these are mostly due to temperature effect. Mathews et al.(1969) have shown that there are sequences of days on which practically no daily variation exists in contrast to others with a pronounced variation.

It is observed that the amplitude of the diurnal variation in free space is about .4% and the time of maximum

at 1800 hour (Bercovitch, 1963; McCracken and Rao, 1966; Faller and Marsden, 1966). The amplitude is independent of rigidity between 2 Gv and the upper cut-off the order of 100 Gv., the latter value being dependent on the phase of the solar cycle (Jacklyn and Humble, 1965). The diurnal amplitude varies as the cosine of the declination (Sandstrom et al. 1962; McCracken and Rao, 1965).

However significant changes in the characteristics of the anisotropy from the average values have been observed when studied on a day-to-day basis. The time of maximum and minimum of the anisotropy are not separated by 12 hours but by 8-10 hours (Rao and Sarabhai, 1964) as shown in Fig.1.7, indicating an additional modulation. This receives further support from Sarabhai et al. (1965) who demonstrate that a deficiency of cosmic rays is often observed along the garden hose direction. The fact that $(T_{\max} - T_{\min})$ is 8 to 10 hours instead of 12 hours, shows that the daily variation is not of a purely diurnal character.

There are various theories to explain the observed diurnal anisotropy (Dattner and Venkatesan, 1958; Ahluwalia and Dessler, 1962; Parker, 1964; Axford 1965; Krymskiy, 1965). It has been interpreted in terms of the corotation of the cosmic rays with spiral field.

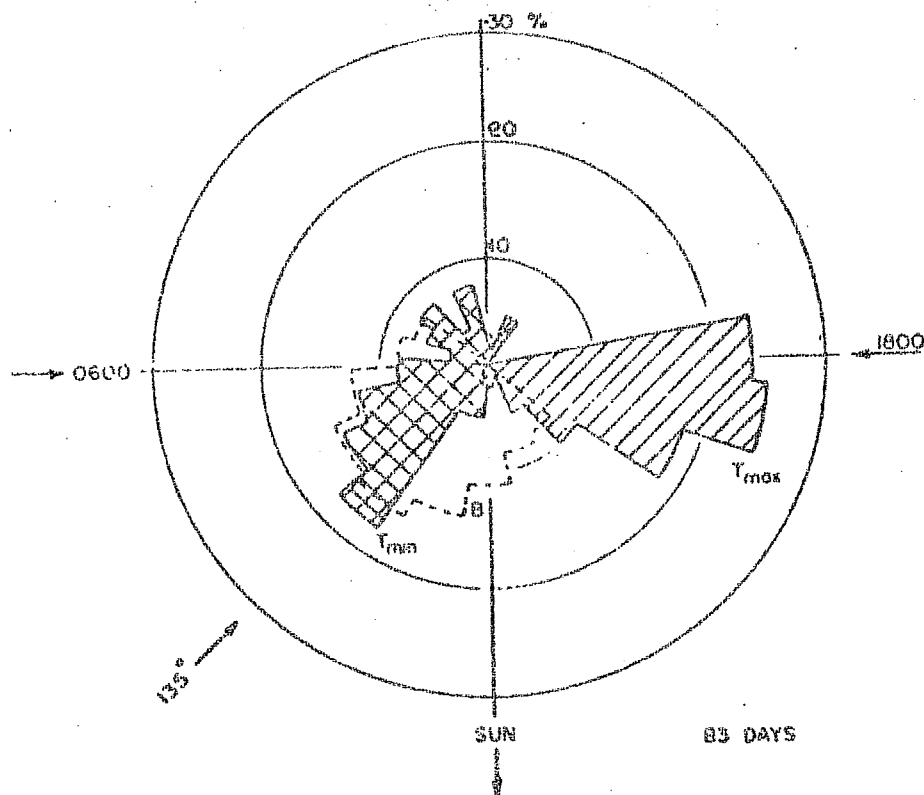


Fig.1.7 Polar histogram showing the measured times of maximum and minimum of the daily variation.

Ahluwalia and Dessler (1962) had attributed the cosmic ray anisotropy to the spirally-shaped magnetic field of the sun which is drawn out by the solar wind and which co-rotates with the sun. If V is the velocity of the solar wind, then the motion of the magnetic field would give rise to an electric field

$$\mathbf{E} = \frac{-\bar{V} \times \bar{B}}{c} \quad (24)$$

in the fixed frame of reference. The guiding centre of a cosmic ray particle would drift under the influence of the electric and magnetic fields with a velocity

$$V_D = C \frac{\bar{E} \times \bar{B}}{B^2} = \omega r \sin \chi \quad (25)$$

where C is the velocity of light, ω the angular velocity of the sun, r the radius vector from the sun, and χ the garden hose angle (Fig.1.8).

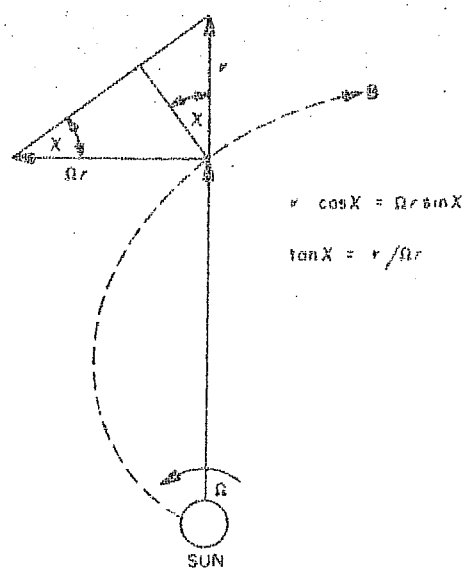


Fig.1.8 "Garden Hose" Angle.

Since cosmic ray particle flux is isotropic in the frame of reference moving with the magnetic field, the relative motion between the guiding centres of the cosmic ray particles and the earth gives rise to an anisotropy of cosmic ray flux as seen from the earth (Compton and Gettling, 1935). The amplitude of the anisotropy being given by

(Compton and Getting, 1935; Gleeson and Axford, 1968a)

$$\alpha = (2 + \gamma) u/c \quad (26)$$

where γ is the exponent of the differential energy spectrum which is assumed to be of the form $D(E) = AE^{-\gamma}$, and u is streaming velocity.

The theory of Ahluwalia and Dessler agrees with experimental results regarding the energy spectrum of variation of the anisotropy and variation with the asymptotic latitude of viewing of the detector, but does not agree with the direction (Bercovitch, 1963) and dependence of amplitude on solar wind velocity (Snyder et al. 1963).

A theoretical objection to this model has been made by Stern (1964) from Liouville's theorem, which tells us that the cosmic ray density in phase space is preserved in any conservative system (i.e. $\bar{\nabla} \times \bar{E} = 0$). Hence, if the cosmic ray intensity is the same in all directions at any given point outside the solar system, it must be the same in all directions at any accessible point inside the solar system. That is to say, no time independent magnetic field system ($\frac{\partial \bar{E}}{\partial t} = 0$) can produce an anisotropy such as the diurnal variation.

Parker (1964) has proposed a model of interplanetary space which consists of two heliocentric and spherically symmetrical regions. The inner region containing the earth

corresponds to the model considered by Ahluwalia and Dessler, where the field pattern is a smooth spiral. The outer region (~ 1.4 A.U.) consists of a large number of magnetic irregularities. The net streaming perpendicular to the magnetic line is due to two competitive processes operating at any time, namely the drift caused by the electric and magnetic fields (equation 25) and the other, cosmic ray pressure gradient normal to the magnetic field. The cosmic ray gradient produced in the incoming particle is (Parker, 1964)

$$\nabla \frac{1}{2} NMW_1^2 + q N \nabla \phi = 0 \quad (27)$$

where ϕ is the electrostatic potential, N is the cosmic ray particle density, M and q are the mass and charge per particle and W_1 particle velocity perpendicular to field \vec{B} . This pressure gradient leads to a streaming (Parker, 1967)

$$\bar{U} = \frac{MC}{B^2 e N} \bar{B} \times \nabla \left(\frac{1}{2} NW_1^2 \right) \quad (28)$$

using equation (27), equation (28) becomes.

$$\bar{U} = -C \left(\frac{\bar{E} \times \bar{B}}{B^2} \right) \quad (29)$$

If \bar{U} is added to the electric drift, given by equation (25) which is a part of the rigid rotation of particles with a spiral pattern, there is no streaming left. Hence there is no anisotropy, in accord with the conclusion from Liouville's theorem.

Therefore, an anisotropy or diurnal variation exists only if the cosmic ray gradient set up by the polarization field is reduced. Parker shows that the large number of inhomogeneities beyond the orbit of the earth reduce the pressure gradient. The cosmic ray particles random walk in the frame of reference moving with the wind. In this frame of reference there is no electric field. Hence the random walk leads to diffusion which progressively reduces the pressure gradient. If there is sufficient diffusion in the small scale irregularities to reduce the initial $\frac{1}{2} N M W_1^2$ to negligible values, then $U = 0$ and there would be the rigid rotation with spiral pattern leading to a diurnal amplitude of about .7% and the direction of the anisotropy will be along 1800 hours. The observed diurnal variation is, on the average, about .4%, indicating that the diffusion wipes out about half the initial pressure gradient. It has been shown (Parker 1967) that the ratio $K_1/K_{11} = 10^{-2}$, of the cosmic ray diffusion coefficients perpendicular and parallel to the spiral interplanetary field, as deduced (Jokipii, 1966, 67) from the observed (Coleman, 1966) small scale fluctuations in the magnetic field, is sufficient to relieve half the gradient across the field.

Axford (1965) has considered an inner region in interplanetary space where the magnetic lines are spiral and contain magnetic irregularities which increase monotonically

with distance from the sun. The inner region is bounded by an outer region (5-40 A.U.) where the solar wind becomes subsonic as it is terminated by interstellar medium (Axford et al, 1963). Cosmic ray propagation throughout the inner region is one of anisotropic diffusion, particles diffusing with comparative ease along the field lines than across. Under the simplifying assumption, Axford obtains a drift velocity in the plane of V and B , when $\nabla \left(\frac{1}{2} N W_1^2 \right) = 0$. In the vicinity of the earth the drift velocity obtained is $V_D = -\Omega r$.

Therefore the results are similar to Parker's model except that a radial cosmic ray density ^{gradient} exists throughout the solar wind cavity. Both require that the pressure gradient perpendicular to the magnetic field vanishes. According to Parker this happens through isotropic scattering at magnetic field irregularities beyond the orbit of the earth (> 1 A.U.), while according to Axford it is not a necessary condition.

In addition to the diurnal component of the cosmic ray intensity a semi-diurnal component has been known to exist and is unlikely to be due to atmospheric effects (Sarabhai et al. 1955; Katzman and Venkatesan, 1960; Rao and Sarabhai, 1964; Hasim et al. 1969). Applying the technique of numerical filtering to the data of neutron

monitors Ables et al. (1966) have concluded that a semi-diurnal anisotropy persists throughout the period 1954-1964. The average magnitude of the anisotropy is about .1% and the direction in space of maximum of the anisotropy is found to be perpendicular to the interplanetary field. Ables et al (1966); Patel et al. (1968); Quenby and Lietti (1968) and Rao and Agarwal (1970) find that the semi-diurnal component is approximately proportional to the first power of rigidity. Using the underground and sea level directional telescope data, Hasim et al. (1969) have shown that an extrapolation of the first power of rigidity dependence found at low rigidities fits the high rigidity data provided a cut-off about 85 Gv is used. The semi-diurnal anisotropy seems to vary as $\cos^2 \lambda$ rather than $\cos \lambda$ as in the case of diurnal component, λ is the mean asymptotic latitude of response (Subramanian and Sarabhai, 1967; Quenby and Lietti, 1968; Rao and Agarwal, 1970).

Subramanian and Sarabhai (1967) and Lietti and Quenby (1968) have suggested that the semi-diurnal component in the cosmic ray intensity is caused by a rising cosmic ray density gradient symmetrical about the solar equatorial plane. Viewing along the interplanetary magnetic field lines of force, a detector on earth measures cosmic ray flux characteristic of the equatorial plane. Viewing in a direction perpendicular to the magnetic field, a detector

samples particles arriving from higher heliolatitudes, the heliolatitudes corresponding to the gyroradius of the particle under consideration. Since a detector on the spinning earth measures cosmic ray intensity twice along the interplanetary magnetic field and twice perpendicular to it in the course of a day, a positive gradient of cosmic ray density with increase in heliolatitude, gives rise to a semi-diurnal component with a maximum perpendicular to the interplanetary magnetic field.

Considering three different types of distributions as shown in Fig.1.9 the existence of latitudinal gradients of cosmic ray intensity due to the dependence of solar activity on heliolatitude has been suggested by Subramanian and Sarabhai (1967). Following an empirical relation they have described the distribution of galactic cosmic ray density, symmetrical about a heliolatitude $\theta_1 (\neq 0)$, (case II in Fig.) as

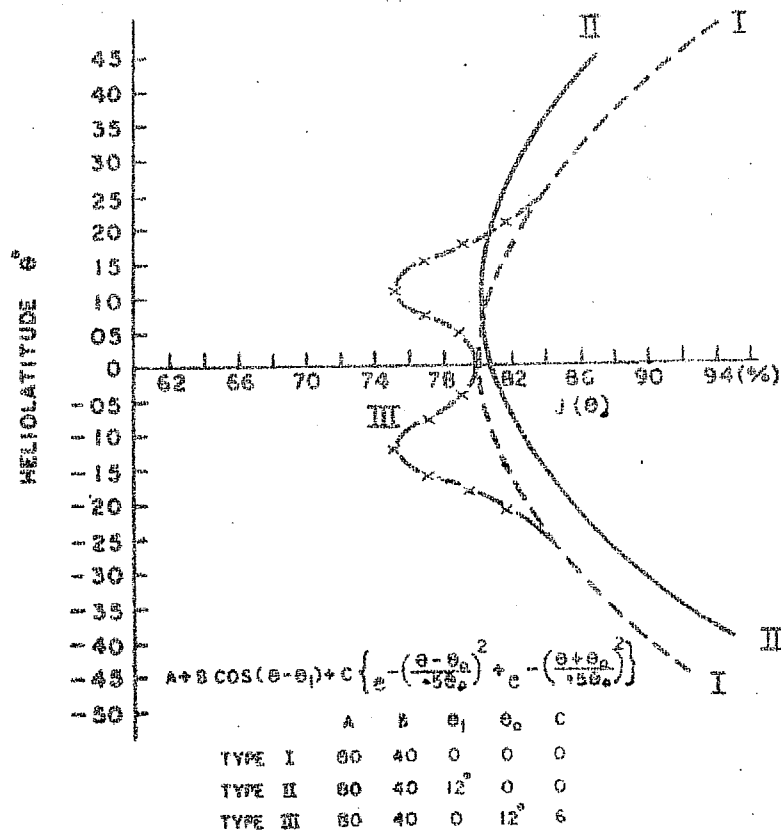


Fig.1.9 Cosmic ray density distribution with Heliolatitude.

$$\frac{N(P, \theta_g)}{N(P, \theta_1)} \cdot dP = \frac{1}{2} INP^{-\beta} \left[\theta_1^2 + \frac{1}{2} \left(\frac{P \cos \lambda}{45H} \right)^2 - \frac{1}{2} \left(\frac{P \cos \lambda}{45H} \right)^2 \cos 2\alpha - 2 \theta_1 \frac{P \cos \lambda}{45H} \sin \alpha \right] \cdot dP \quad (30)$$

where I determines the over all decrease of cosmic ray

intensity between the poles and the equator; n determines the rapidity of decrease of cosmic ray intensity with decreasing heliolatitude. P is the rigidity, H is the interplanetary field, α - an angle subtended by a detector with the magnetic field, λ is a latitude of the celestial sphere, a detector scans and β determines the rigidity dependence of the latitudinal variation of cosmic ray density.

A semi-diurnal component can be represented by the third term of the right hand side of equation(30), as

$$r_2(P).dP = \frac{1}{4} \ln P^{-\beta} \frac{P^2 \cos^2 \lambda}{(45H)^2} . dP \quad (31)$$

and the direction of maximum intensity will be perpendicular to the magnetic field. The energy spectrum of variation of the semi-diurnal component has an exponent $2-\beta$ which could be positive whenever β is less than 2, as in the case during most periods of solar cycle. Its dependence on the asymptotic latitude of viewing of the detector will be $\cos^2 \lambda$.

A diurnal component can be represented by the fourth term of the right side of equation (30), as

$$r_1(P).dP = \frac{1}{2} \ln P^{-\beta} \Theta_1 . \frac{P \cos \lambda}{45H} . dP \quad (32)$$

with a direction of maximum perpendicular to the magnetic field. This diurnal component will reverse its direction

of maximum with reversal of interplanetary field or with a change of sign of θ_1 i.e., with the reversal of the north-south asymmetry of solar activity.

Quenby and Lietti (1968) by considering the interplanetary field model in which particle scattering are superimposed on the quiet time spiral field have shown that the semi-diurnal component of the cosmic ray variation arising as a result of a particle density gradient perpendicular to ecliptic plane. Galactic particles arriving over the solar poles experience easy access, since they diffuse along almost straight field lines, but those entering in the solar equatorial plane are constrained to follow many spiral loops. Thus the cosmic ray density should rise each side of the solar equatorial plane. The cosmic ray density distribution in interplanetary space has been described by them as,

$$N_e = N_s \exp \left\{ - \frac{2.4}{P} \sin^2 \theta \right\} \quad (33)$$

where N_e and N_s are respectively the density at earth and at the boundary of modulation region and P is rigidity.

Using a Taylor expansion of equation (33), the peak to peak amplitude of the semi-diurnal variation has been shown as

$$r_2 = \frac{1}{2} R^2 \frac{1}{N_e} \left(\frac{\partial^2 N}{\partial Z^2} \right)_{\theta=\pi/2} \cong 0.005 \text{ P\%} \quad (34)$$

The expression shows the rigidity dependence of the semi-diurnal component.

Hence both the theories predict that the semi-diurnal anisotropy (1) has a positive exponent of the spectrum of variation, (2) varies as $\cos^2 \lambda$ where λ is the mean asymptotic latitude of response and (3) has a maximum flux in a direction perpendicular to the interplanetary magnetic field.

1.7 A study of the cosmic ray daily variation

The daily variation of meson intensity at Ahmedabad measured with east and west pointing telescopes inclined to zenith at 45° has been studied by the author during the period 1963-1965. An experimental set up of the inclined telescopes has been described in Chapter 2. Data from these detectors are used to study the influence of the angle of opening of telescopes on the nature of the daily variation. The yearly mean daily variations during 1963-1965 are compared with Nerurkar's (1955) and Rao's (1960) results to examine the long term changes of anisotropy.

Studies of the daily variation in cosmic ray intensity have interpreted the daily variation in terms of an anisotropy in the intensity of the primary radiation. Using the data of the high counting rate MIT meson detector and the Deep River neutron monitor, Rao and Sarabhai (1964) have shown that even though the time of maximum observed at MIT and Deep River is very well correlated, the ratio of

the amplitudes has a wide dispersion. This can be interpreted on the basis of the day-to-day changes of the energy spectrum of the anisotropy. Sarabhai and Subramanian (1966) have shown that if a day-to-day analysis is made and if the fractional variational spectrum is of the form $\frac{\delta D(E)}{D(E)} = AE^X$, then during the period 1958-1963, some 37% of the days had $X = -1$, 11% gave $X = 0$, 23% fitted $X = +1$, and the remainder(30%) were not resolved. It should be noted that the data were obtained using IGY monitors which have low statistical accuracy for diurnal analyses made on a day-to-day basis.

The installation of a substantial number of super neutron monitors of very high counting rate ($> 5 \times 10^5$ counts/hr) enables one to study the daily variation more precisely than previously, since statistical uncertainty in an hour's counting rate is as small as $\sim 0.1\%$. Using the data recorded by a world-wide net work of super neutron monitors, the characteristics of the anisotropy of galactic cosmic ray intensity on individual days have been derived by the author. The characteristics considered are the strength, the directions of maximum and minimum of intensity and the energy spectrum of anisotropy. In Chapter 3, the experimental results are compared with the predictions of the characteristics arising from different processes which appear capable of contributing to an anisotropy of galactic cosmic rays in interplanetary space.

C H A P T E R - II

DIRECTIONAL MEASUREMENTS OF THE COSMIC RAY DAILY VARIATION AT AHMEDABAD

2.1 Introduction

Measurements of the meson and nucleonic components are being carried out on a world-wide scale, the nucleonic component at sea level and mountain level by means of neutron monitors and the meson component incident vertically and at different inclined angles to zenith, by means of GM counter or scintillation counter telescopes. The meson component is also being recorded at many places by shielded ion chamber. The importance of the study of time variations of cosmic ray intensity, measured with the telescopes inclined to the zenith towards the east, west, north and south azimuths, has been demonstrated by Kolhorster (1941), Malmfors (1949), Elliot and Dolbear (1951), Sarabhai and Nerurkar (1956), Sandstrom et al (1955), Elliot and Rothwell (1956), Rao and Sarabhai (1961), Ahluwalia et al (1965) and Peacock et al (1968). It has been concluded that the daily variation of cosmic ray intensity is consistent with its being produced by an anisotropy of primary cosmic radiation.

The cosmic ray time variation at low latitudes measured with Geiger counter directional telescopes has been studied during 1954-55 by Nerurkar (1954) and during 1957-58 by Rao (1960) at Ahmedabad (23°N , 72.61°E). Escobar et al

(1959) and Ahluwalia et al (1965) have studied the daily variations recorded by halogen counter directional telescopes at Chacaltaya (-16.31, -68.15) while Hasim et al (1968) have studied the daily variation using the large scintillation telescopes pointed in the east and west directions at an equatorial station Makerere (.33, 32.50). The author has operated during 1963-1965, triple coincidence Geiger counter telescopes inclined to zenith at 45° towards east and west directions at Ahmedabad.

Fig.2.1 shows the asymptotic directions of approach of particles of various rigidities (McCracken et al, 1965) for east, west and vertical telescopes at Ahmedabad. It can be seen that the east, west and vertical telescopes, scan the same part of the celestial sphere successively as the earth spins on its axis.

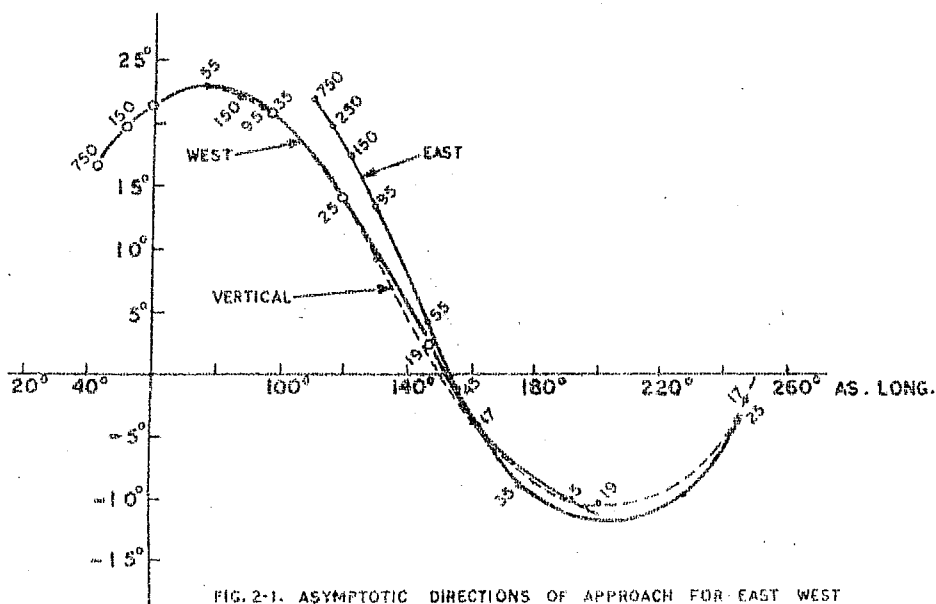


FIG. 2-1. ASYMPTOTIC DIRECTIONS OF APPROACH FOR EAST WEST & VERTICAL TELESCOPES AT AHMEDABAD. THE POINTS REFER TO DIFFERENT RIGIDITIES.

2.2 The Apparatus

The apparatus consisted of two counter sets, inclined to the zenith in east and west directions at 45° . Each set consists of three trays of eight counters. Counters of length 96 cm and diameter 4.2 cm are used. The distance between the extreme trays was 96 cm. An absorber of 10 cm of iron plates was interposed between the middle and the bottom trays. Fig.2.2 shows the arrangement of the apparatus. The counter sets were mounted in boxes on a frame.

Telescopes having different angles of opening in the east-west plane were provided. In each tray, pairs of adjoining counters were connected together to separate electronic quenching units Q_1, Q_2, Q_3, Q_4 and so on. By mixing the outputs of various quenching units, triple coincidence rates were measured from two independent telescopes ($10^\circ T$) with semi angles of 10° and from one telescope ($20^\circ T$) having semi angle of 20° in the east-west plane. The mean primary energies of response of east and west pointing telescopes, derived by using coupling coefficients are given below:

Direction	Cut-off energy BeV	Mean energy Response BeV
$45^\circ E$	27.5*	52.5
$45^\circ W$	12.4*	32.5

* calculated by Daniel and Stephans (1966a)

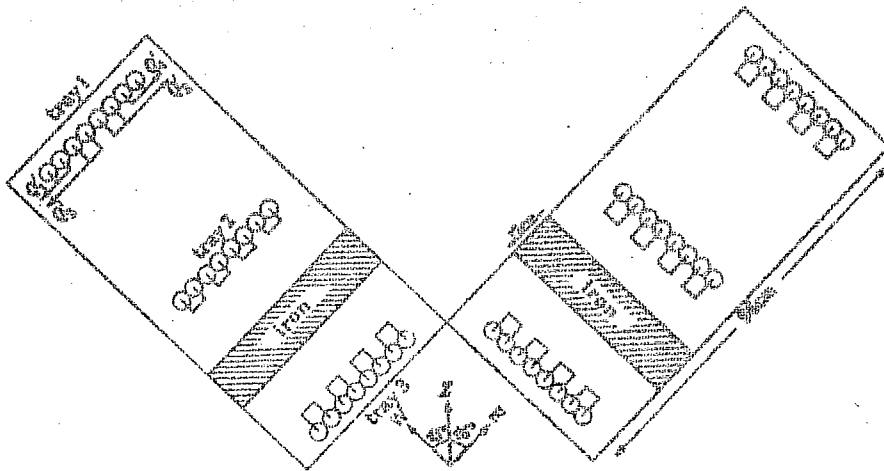


Fig.2.2 Arrangement of the Unit.

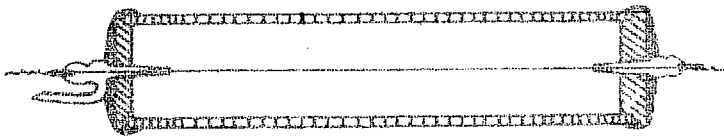


Fig.2.3 Geiger counter.

2.3 The Geiger Muller Counter

The Geiger counter because of its simplicity and reliability has been used extensively in the past for cosmic ray studies. A typical counter is shown in Fig.2.3.

In the early stages of operation the Geiger counter behaves as a proportional counter but when the electron avalanche approaches the counter wire considerable electron multiplication takes place in the very high field there. This multiplication is accompanied by the emission of large numbers of photons, which in turn, are responsible for the rapid propagation of the avalanche along the wire. The photons generate further electrons at greater distances from the wire but these are unable to produce avalanches on arriving near the wire on account of the reduction of the field by the dense cloud of positive ions. The discharge then ceases but the positive ions liberate^e electrons which together with photo-electrons can produce a further discharge.

This succession of discharges is obviously undesirable and in practice it is arranged that the secondary discharges are suppressed or 'quenched'. Two procedures can be adopted. In one of these (external quenching) it is arranged that by the time the positive ion sheath reaches the cathode, the field has been reduced to such a level that a further discharge cannot occur. The reduction in field

is usually produced by a subsidiary electronic quenching unit, which is 'triggered' by the primary discharge and which applies a negative pulse to the anode. In other procedure (internal quenching) a polyatomic vapour is added to the filling gas to reduce the probability of secondary discharges. By the vapour, many of the photons will be absorbed before they can reach the cathode.

In practice the usual procedure is to reduce the number of spurious pulses to a minimum by using both internal and external quenching. For the present work, we have used self-quenching type Geiger-Muller counters, filled with argon and ethyl acetate in the proportion of 9:1 respectively to a total pressure of 10 cms of mercury. These counters have an operating potential of ~ 1000 V, plateau of ~ 200 V, efficiency of 99.9% and dead-time of ~ 100 micro sec. In addition to the self-quenching of the counters, an external electronic device is used.

2.4 Electronic Units

Continuous recording of cosmic rays intensity was carried out by vacuum tube units in the laboratory up to 1963. The transistorized units which are operated by battery have been fabricated for the operation of east-west unit to record the meson intensity. P.N.P.alloy junction transistors of the type 2N396 have been used for quenching,

coincidence, and scaler circuits where fast switching action is required. The audio and general switching type transistors are incorporated in recording circuits. The electronic units used in our experiment are briefly described in the following section:

(a) Quenching unit

It is a monostable multivibrator which is triggered by the negative counter pulses. The transistorized monostable multivibrator cannot supply a quenching pulse of the order of 200 volts, since the available transistors have collector voltage limited to 100 volts at the most. Therefore an additional vacuum tube circuit was incorporated. The complete circuit is shown in Fig.2.4.

A positive pulse of 12 to 15 volts from the monostable multivibrator is fed to the grid of the vacuum tube which is normally cut-off. The positive pulse drives it into conduction thereby causing a voltage drop at the plate and hence on the central wire of the counter. The quenching pulse height and width are of the order of 200 volts and 1000 μ sec. respectively.

(b) Emitter follower

The aim of the emitter follower is to furnish a positive pulse across a low impedance in order to feed it to a number of channels. The circuit is shown in Fig.2.5.

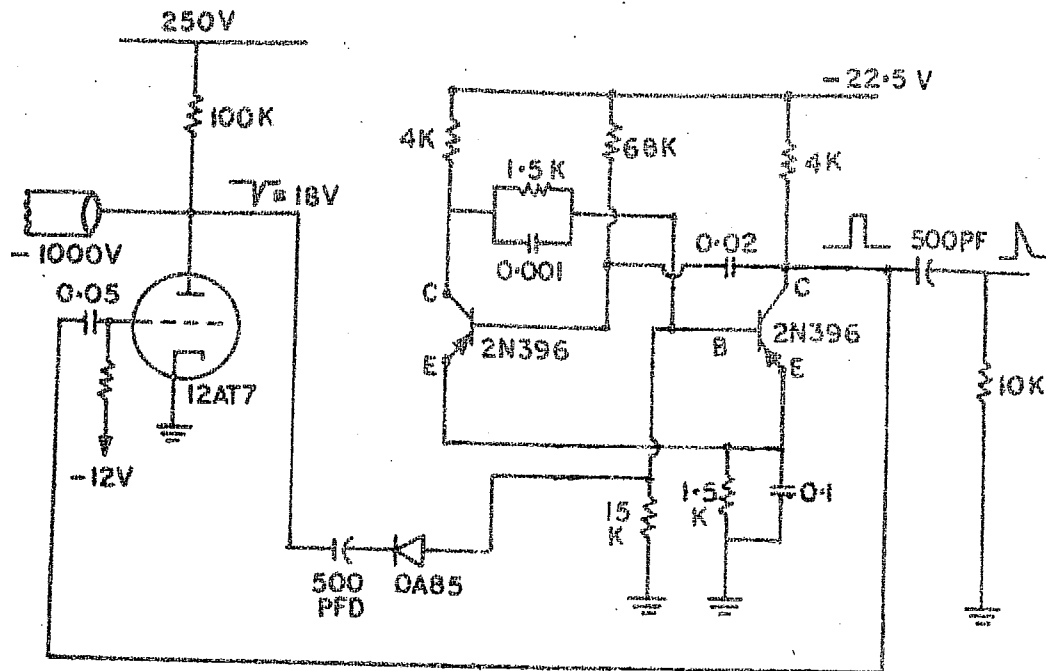


FIG. 2.4 HYBRID QUENCHING CIRCUIT

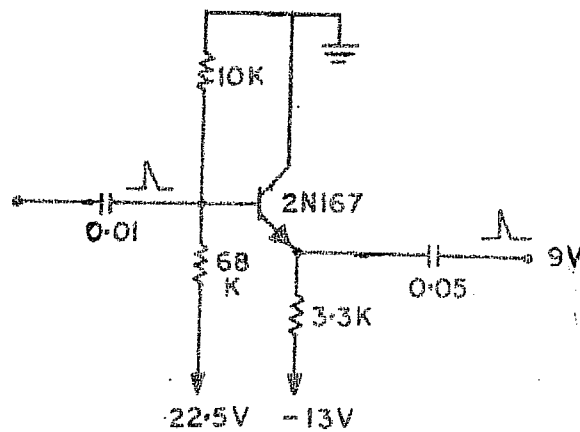


FIG. 2.5 EMITTER FOLLOWER

The transistor NPN is normally kept non conducting by the -ve bias voltage at the base w.r.t.emitter. It will go into full conduction when the positive pulse from the mixer circuit arrives at the base, giving rise to positive output pulse at the emitter with a voltage amplification less than unity.

(c) Coincidence circuit

The sharp positive pulse from the Emitter follower is then fed to the coincidence circuit, shown in Fig.2.6. When there is no input to the base, all transistors are in the on state. When all the positive inputs are simultaneously applied, it gives a negative output.

(d) Scaler

The coincidence pulse is then fed to the binary scaling circuit. The basic binary shown in Fig.2.7, is Eccles-Jordan type of bistable multivibrator.

If T_1 is cut-off and T_2 is conducting then a negative trigger pulse applied at the base of T_1 causes T_1 to conduct. The collector voltage will decrease. The change in voltage is coupled to the base of T_2 and reduces its forward bias. Conduction in T_2 begins to decrease. The collector current of T_2 decreases and the collector voltage changes from zero to a negative value (approaching to the value of supply

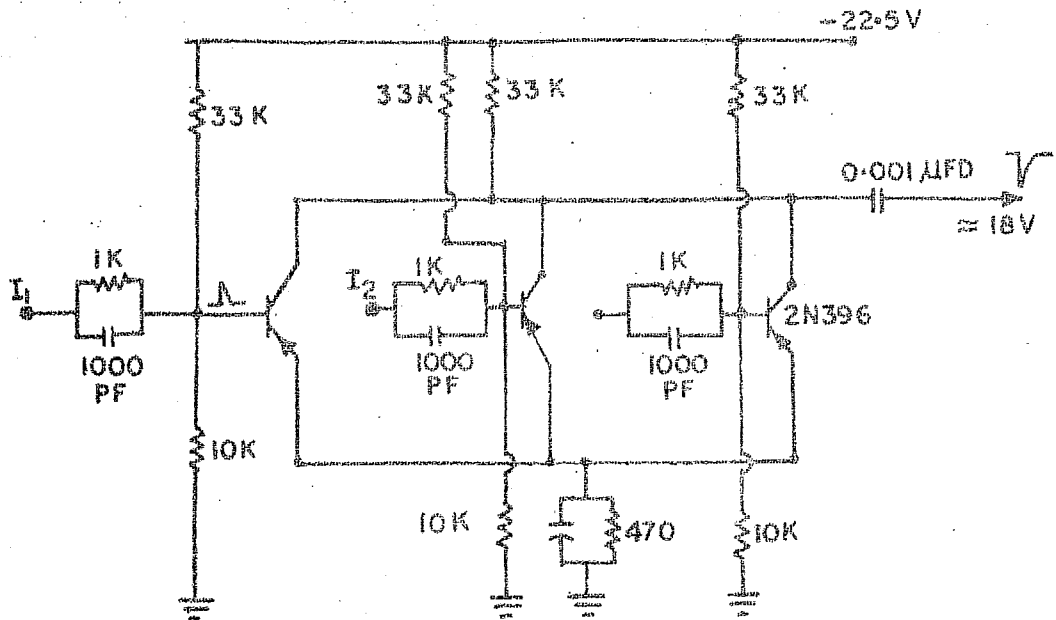


FIG.2-6. ROSSI COINCIDENCE CIRCUIT

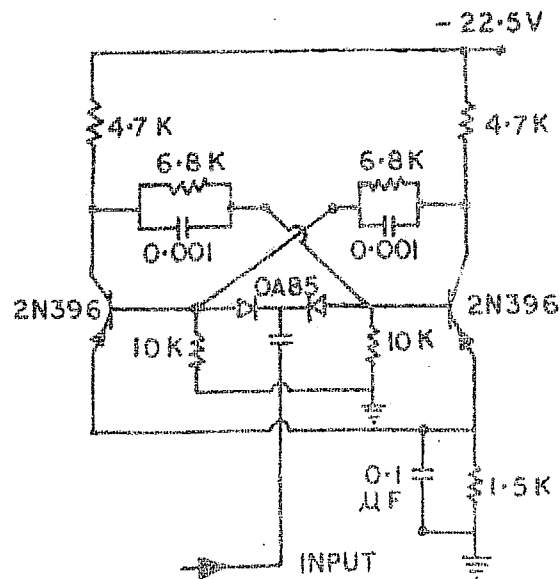


FIG.2-7. SCALER

voltage). The action is cumulative and finally T_1 goes to saturation and T_2 is cut-off. The next pulse will restore the circuit to the normal position since the input pulse can now pass through the diode connected to the base of T_2 . The triggering sensitivity lies between 2V to 10V, negative pulse and the resolution obtained is $\sim 20 \mu$ sec. The reliability of triggering and negative operation is achieved by diode interstage coupling.

(e) Recording unit

The final recording of the data is done on electro-mechanical telephone type recorder. The recorder operates reliably at a current of 20-25 ma. To drive them, low power P.N.P. transistors are used in a monostable multi-vibrator circuit, as shown in Fig.2.8. The mechanical recorder is connected in the collector circuit of one transistor which is made to conduct for a time defined by the discharge of the capacitor C.

During the quiescent state T_1 is in saturation and its collector voltage is near earth. The base of T_2 is near earth and therefore T_2 is cut-off. Its collector voltage will be approximately equal to that of the supply voltage. C provides rapid application of the regenerative signal from the collector of T_2 to the base of T_1 and it is charged to supply voltage.

A positive pulse applied to the base of T_1 decreases forward bias of T_1 . Base and collector current of T_1 begins to decrease. Collector voltage of T_1 which is coupled to the base of T_2 increases negatively. It drives T_2 into saturation and T_1 into cut-off. The current flows through the recorder. C discharges through R. Base of T_1 becomes less positive and when it goes slightly negative T_1 again conducts and T_2 cut-off. This stable condition is maintained until another pulse triggers the circuit. The duration of the pulse on the recorder is determined by the time taken for the T_1 base to fall below earth i.e., by the value of C and R.

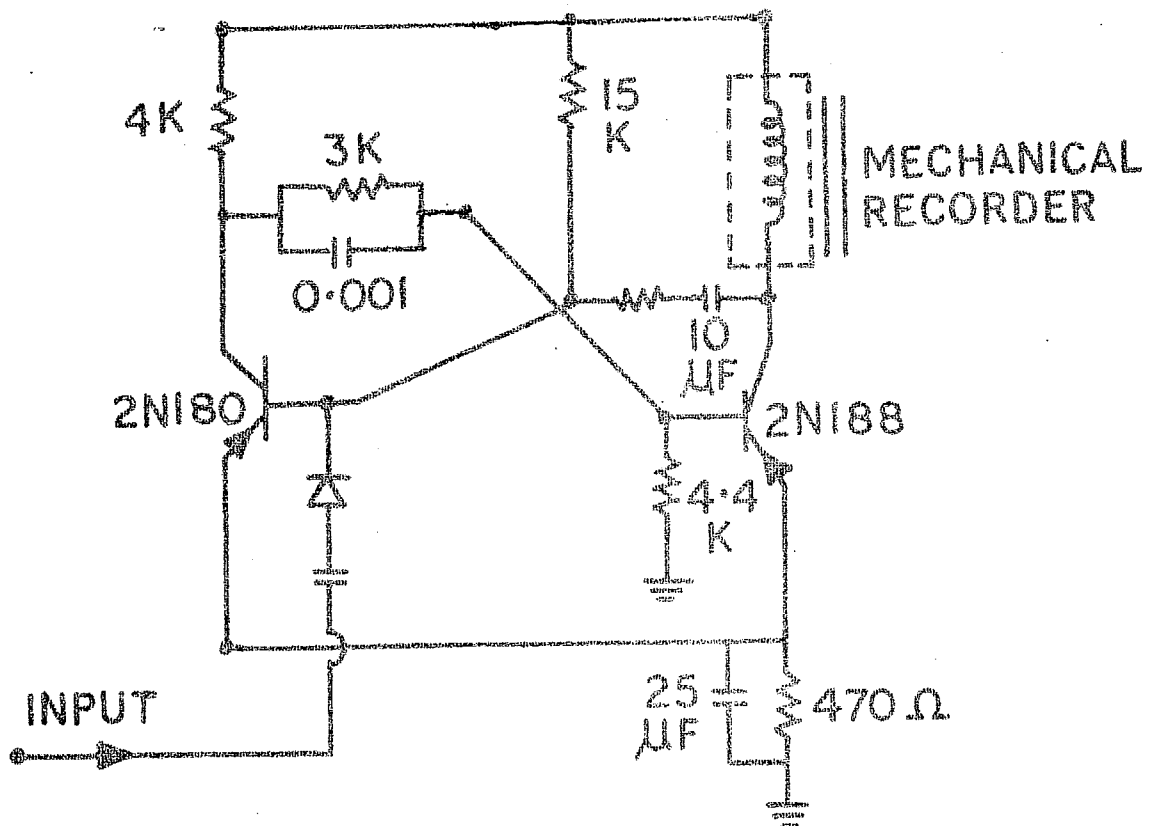


FIG. 2.8. RECORDER

(f) Photographic Unit

Hourly cosmic ray records have been photographed by an automatic photographic device. A clock and the mechanical recorders are mounted at one end of a light tight box, a detachable open shutter type camera is fitted at the other end of the box as shown in Fig.2.9.

Electric bulbs E_1 and E_2 flash to illuminate the panel, by an electrical contact of the minute hand of the clock at hourly intervals. The spool S_2 in the camera is geared to the shaft of a low speed motor to roll the film after each exposure.

The automatic sequence control unit, shown in Fig. 2.10, consisting of two thyratrons, gets automatically reset after 30 seconds of each exposure. The first thyatron controls the flashing of the bulbs and the second operates the motor. When the minute hand makes the hourly contact, a positive pulse of 200 volts is fed to the grid of the highly biased thyatron T_1 which makes it conducting. The current passing through T_1 closes the relay R_1 resulting in a momentary flash of the bulbs. At the same instance the plate circuit of T_1 becomes open, resetting it to its original non-conducting condition which opens the relay R_1 and switches off the lamp circuit. The positive pulse from the plate of T_1 is fed to the grid of the second thyatron

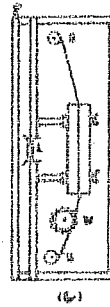
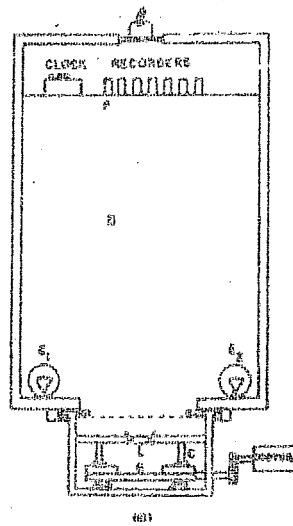


Fig.2.9 The camera unit.

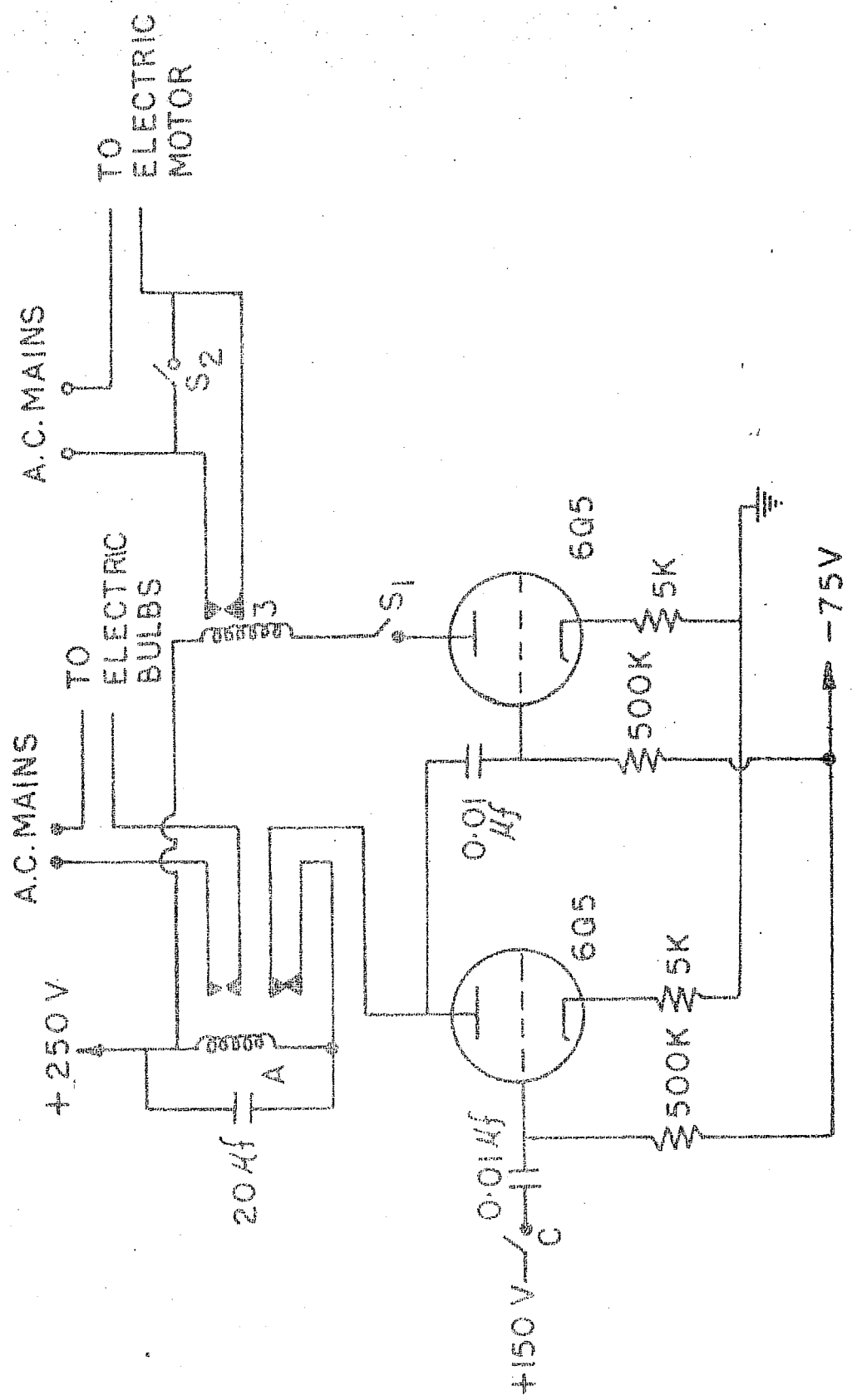


Fig: 2.10 Automatic sequence control circuit.

T_2 which starts conducting and operates the relay R_2 . The motor gets the mains voltage as its circuit is complete and the main shaft starts rotating. The gearing is so adjusted as to move the film by one frame when the shaft completes half revolution.

(g) Power supplies

To achieve reliability in the working of electronic circuits, stabilisation of voltage against line voltage fluctuations and load variations becomes necessary. A constant voltage transformer giving a stabilised output of 230 volts A.C. within $\pm 1\%$ for an input variation from 180 to 250 volts was used to stabilise mains voltage. To get stabilised D.C. voltage a regulating circuit shown in Fig.2.11 is used.

It gives a close control over the output voltage, a high stabilising ratio and a low internal impedance. The circuit consists of a half wave rectifier with low pass filter feeding about 2500 volts to the degenerative regulating net work. The regulation obtained by this circuit is of the order of ± 2 volts at 1300 volts for an input variation from 180 to 240 volts. The power supply is adjusted to give voltages from 800 volts to 1300 volts in steps of 50 volts by using a bleeder.

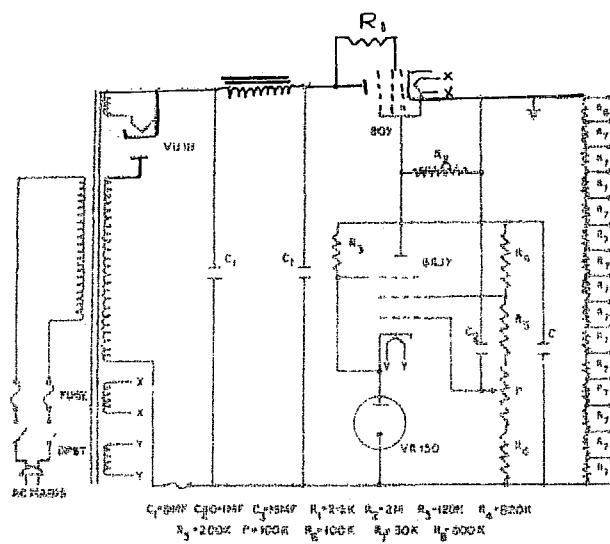


Fig. 2-11 H. T. POWER SUPPLY.

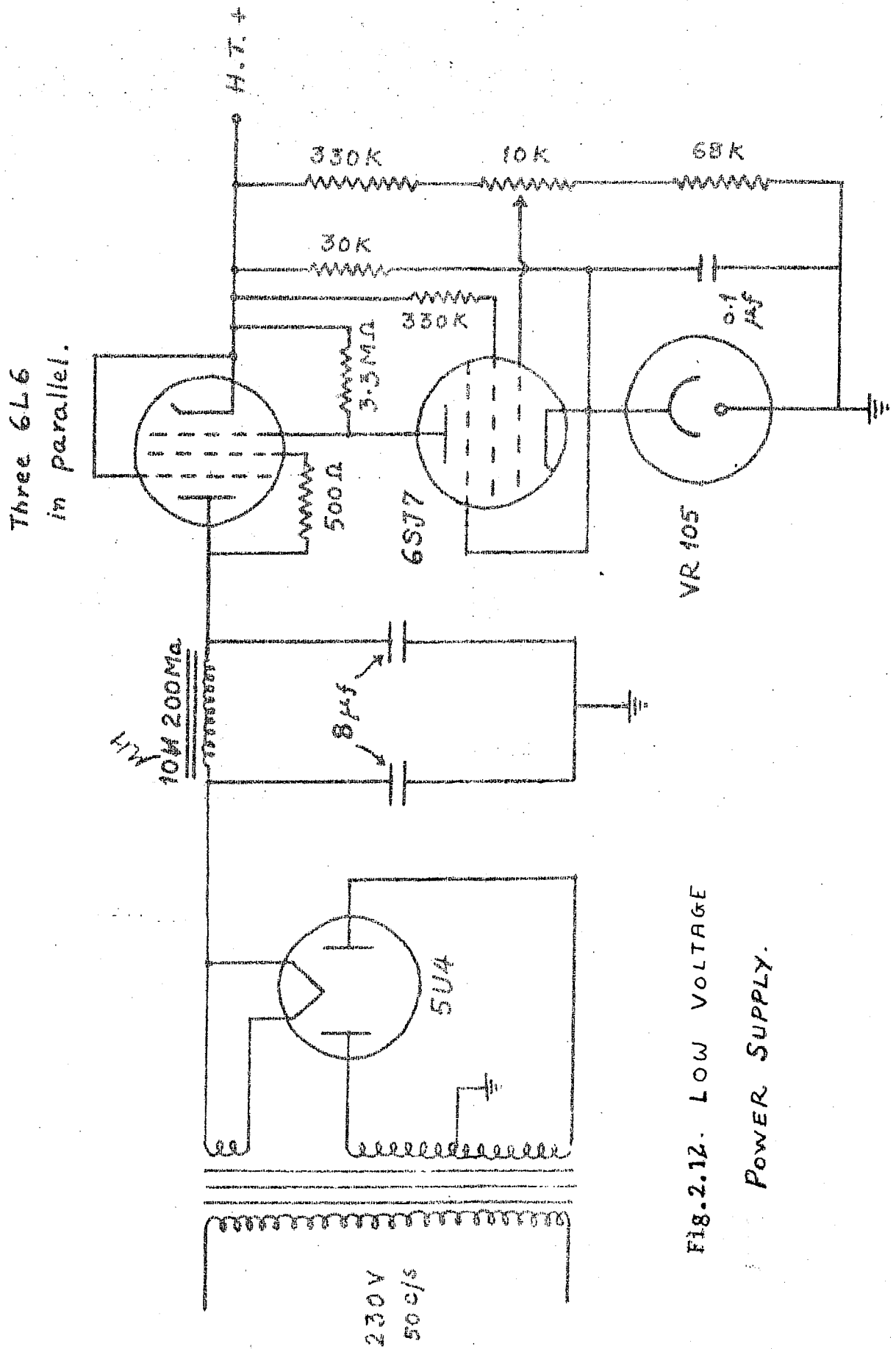


Fig. 2.12. LOW VOLTAGE
POWER SUPPLY.

(h) Low Voltage Power Supply

A conventional low voltage power supply with a degenerative regulation has been used. The circuit shown in Fig.2.12 consists of a full-wave rectifier which gives about 450 volts D.C. to a regulating section. Regulating section uses three 6L6 power pentodes in parallel to supply sufficient current. VR-105 tube has been used for the reference voltage. Error voltage amplified by 6SJ7 is given to the grid of the series tube 6L6 which corrects the output voltage.

2.5(a) Processing of data

The photographic records of the mechanical recorders corresponding to odd hours, are noted down such that the basic data of cosmic ray intensity are given as time series in terms of bihourly counting rates centered at 0 hours, 2 hours, etc. in local time. Where more than one telescope of identical dimension exist, the deviations of the bihourly counting rate from their respective daily means are examined to check whether they are similar within the limits of statistical errors. The data can also be tested for self-consistency in the following way. Let C_1, C_2, \dots, C_n

and D_1, D_2, \dots, D_n be the two series denoting the bihourly readings of two independent telescopes. A third series $E_1 = C_1 - D_1, E_2 = C_2 - D_2, \dots, E_n = C_n - D_n$ is found by subtraction of the respective terms of the two series.

This new series E_1, E_2, \dots, E_n should have a mean value zero and a variance twice that of the individual series. However, due to the differences in the geometrical set up and circuitry, there will exist a mean value, say 'd', which will be different from zero for the third series. The variance σ_1^2 and σ_2^2 of the two series may not be the same and the variance σ^2 of the individual series. Assuming a normal distribution for the third series, the probability that a third series exceeds $d \pm 2\sigma_3$ on either side is 4.6%. Consequently, if there are greater number of deviations in third series than the expected 4.6%, the data are considered not to be self-consistent and the individual series are further checked for any systematic error.

2.5(b) Method of moving averages

To separate out the daily variation from changes which have periods of more than a day, a method of moving averages is followed. Average values of cosmic ray intensity are found as

$$C_{6.5} = \frac{1}{12} \sum_{i=1}^{12} C_i$$

where C_i 's are the bihourly values and the bar denotes the average which is centered at 6.5 in bihourly hours.

Similarly

$$\bar{C}_{7.5} = \frac{1}{12} \sum_{i=1}^{13} C_i$$

which is centered at 7.5th bihourly hours and the mean of these two averages is centered at 7th bihourly. This series therefore represents the long term trend of cosmic ray intensity. This trend is removed in the difference series ($C_7 - \bar{C}_7$) which therefore contains only variation of short term with the period of a day and less.

2.5(c) Harmonic analysis

Any observed time dependent function can be expressed in terms of a Fourier series of the type

$$F(t) = a_0 + \sum_{n=1} (a_n \cos nt + b_n \sin nt)$$

Where a_n and b_n are the coefficients of the n th harmonic and are independent of t , and $F(t)$ is a function defined at 'r' equidistant points in the interval $t = 0$, to $t = 2\pi$ in to a series of harmonic components (Chapman and Bartels, 1940).

In the case of bihourly measurements the value of 'r' is 12 and the maximum number of harmonics coefficients

From the theory of probability it is found that the distributions of a_n and b_n are Gaussian if the bihourly values have also the same distribution. The standard error of the various harmonic components are

$$\sigma_{an} = \sigma_{bn} = \sqrt{\frac{\sigma_i^2}{6}}$$

where σ_i is the standard deviation of bihourly values.

$$\sigma_{rn} = \sigma_{an}$$

$$\sigma_{\phi n} = \frac{\sigma_{rn}}{r_n}$$

2.6 Cosmic ray intensity variations recorded by the inclined telescopes at Ahmedabad

In the present study the characteristics of the daily variation, recorded at Ahmedabad during 1963-1965 by the telescopes inclined at an angle of 45° to the verticle and pointing in the east and west directions, have been examined. By appropriately mixing the outputs of various quenching units, triple coincidences were measured from the two independent telescopes, having a semi-angle of opening of 10° and from the telescope, having a semi-angle of opening of 20° in the east west plane. The triple coincidence counting rates of the different telescopes pointing towards east and west are shown in Table 2.1,

Table 2.1

Types of telescopes	No. of telescopes	Approximate total bihourly rate of telescopes.
West pointing telescopes		
(1) $10^{\circ} \times 45^{\circ}$	2	6000
(2) $20^{\circ} \times 45^{\circ}$	1	12000
East pointing telescopes		
(1) $10^{\circ} \times 45^{\circ}$	2	5200
(2) $20^{\circ} \times 45^{\circ}$	1	10400

For the barometric pressure effects on the cosmic ray intensity it has been found that there were no significant differences between the pressure coefficients obtained for the vertical telescopes and those for the inclined telescopes (Elliot and Dolbear, 1951; Bachlet and Conforto, 1956; Peacock et al. 1968). We have therefore corrected the cosmic ray intensities in east and west directions for variations of pressure using the same barometric coefficient of -0.22% per MM of Hg. However, we are unable to correct the cosmic ray μ meson intensity for the variation of the atmospheric temperature because of the non-availability of upper air temperature data on a large number of days per month.

The average daily variation of the meson intensity from east and west directions, measured by the different angles of opening in the east west plane, during 1963-65 is shown in Fig.2.13. The amplitude of the daily variation measured by telescopes having a semi-angle of opening of 10° and 20° in the east-west plane is about the same.

In Fig.2.14, we show the histograms of diurnal and semi-diurnal amplitudes for east and west telescopes on individual days. It can be seen that the peaks of the amplitudes of diurnal and semi-diurnal components of east and west telescopes occur round about the same value. This can be also observed in Fig.2.13 where the average daily variation of intensities for the east and west directions during 1963-65 are shown. The average diurnal amplitudes for east and west 10° T, are $0.20 \pm .04$ percent and $0.26 \pm .04$ percent respectively. No difference between the amplitudes of the variations measured by 10° and 20° telescopes can be established at a level of statistical significance.

Razdan (1960) has reported that the amplitude of the 12 month mean daily variation of vertical intensity measured by narrow angle telescopes during 1957-58 was not larger than the amplitude measured with a wide angle telescope. Rao and Sarabhai (1961) have also made similar observations for the study conducted by them.

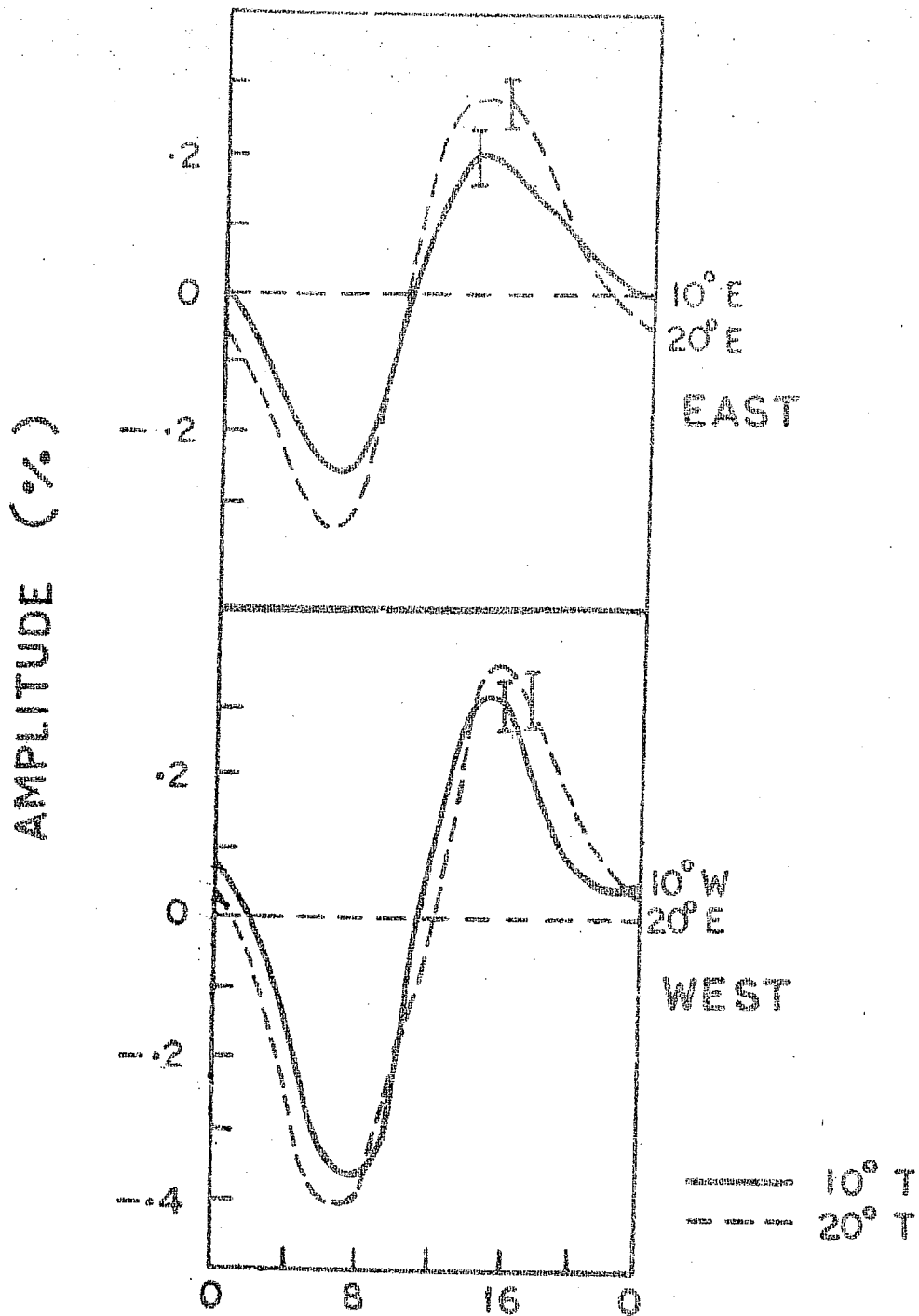


FIG.2-13. AVERAGE DAILY VARIATION DURING 63-65 FOR THE EAST-AND WEST POINTING TELESCOPES AT AHMEDABAD

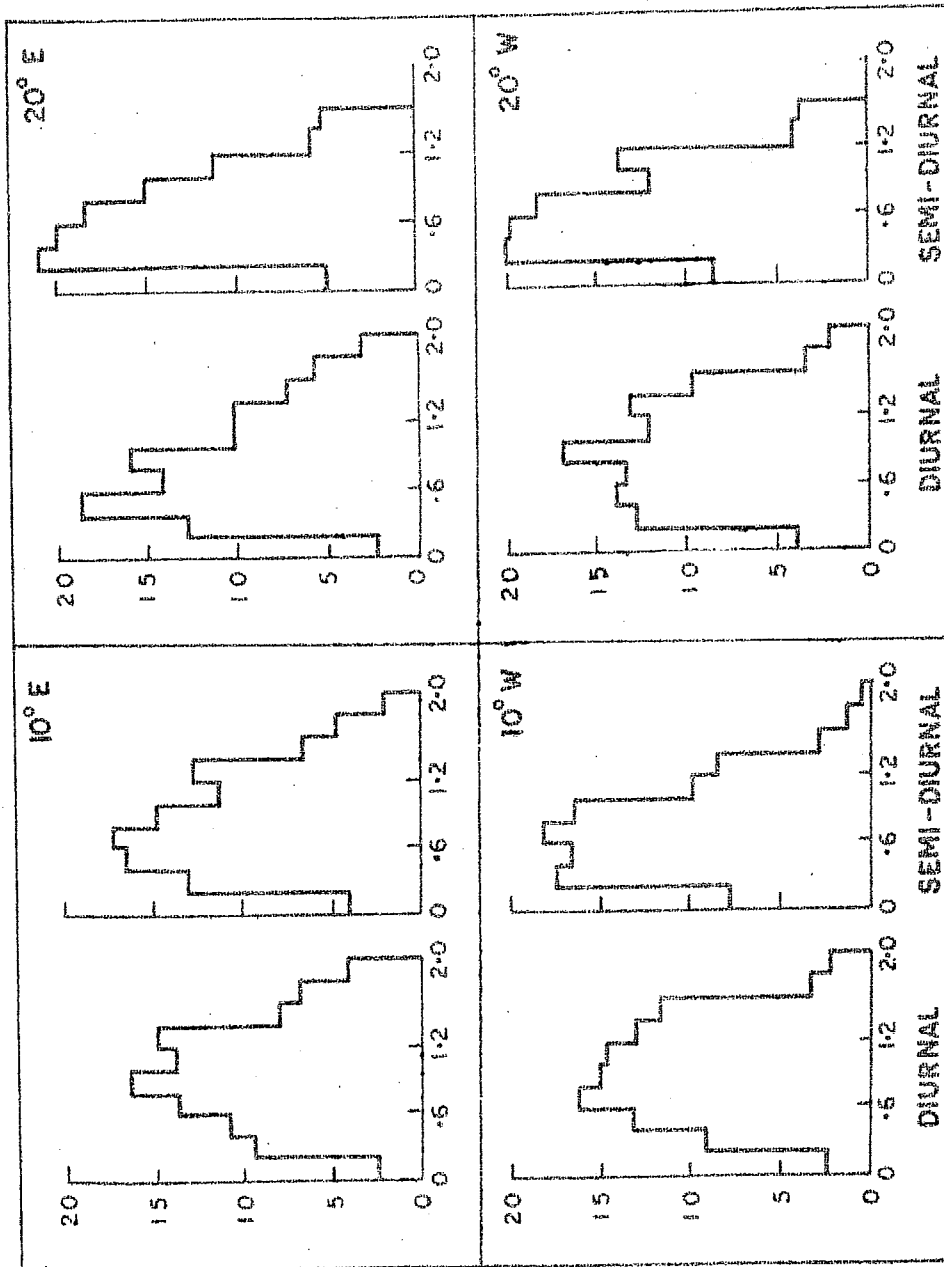


FIG.2.14 FREQUENCY DISTRIBUTION OF AMPLITUDES IN EAST & WEST DIRECTIONS DURING 63-65

AMPLITUDE (%)

2.7 Daily variation of cosmic ray intensity for east and west during solar maximum and solar minimum

Fig.2.15 shows the daily variation of cosmic ray intensity for the periods 54-55 and 57-58 observed by means of inclined telescopes at Ahmedabad by Nerurkar (1956) and Rao (1961) respectively. The average daily variation during 63-65 is also shown in the same figure. The amplitude and time of maximum are given in Table 2.2.

Table 2.2

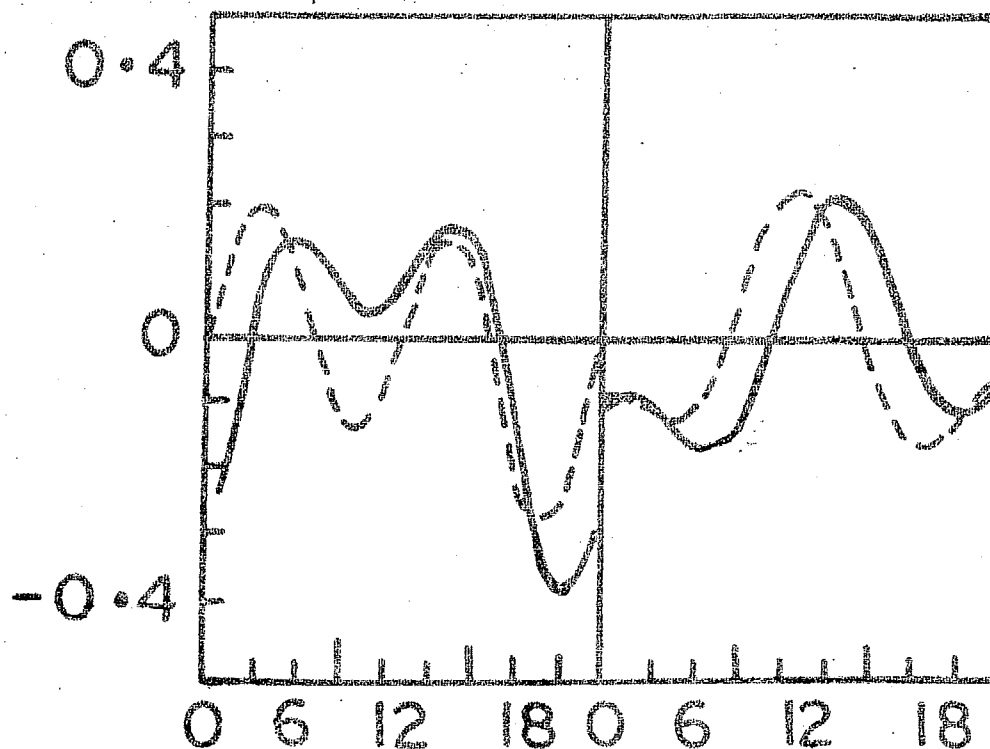
	Year	r_1 %	ϕ_1	r_2 %	ϕ_2
EAST	54-55	$.07 \pm .04$	107°	$.10 \pm .04$	78°
	57-58	$.16 \pm .02$	173°	$.10 \pm .02$	0°
	63-65	$.20 \pm .04$	252°	$.06 \pm .04$	27°
WEST	54-55	$.20 \pm .04$	154°	$.16 \pm .04$	117°
	57-58	$.16 \pm .02$	225°	$.08 \pm .02$	69°
	63-65	$.26 \pm .04$	267°	$.15 \pm .04$	59°

Examination of the daily variation reveals a phase shift of the diurnal variation during the period 1954-65. The daily variation which exhibits in 1954-55, two maxima, one in the early morning and one at about noon, shows only one maximum during 57-58 and in 63-65. While the difference between the times of diurnal maximum of the east and west

MAY. 54
TO APR. 55

JUN. 57
TO DEC. 58

- 83 -



63-65

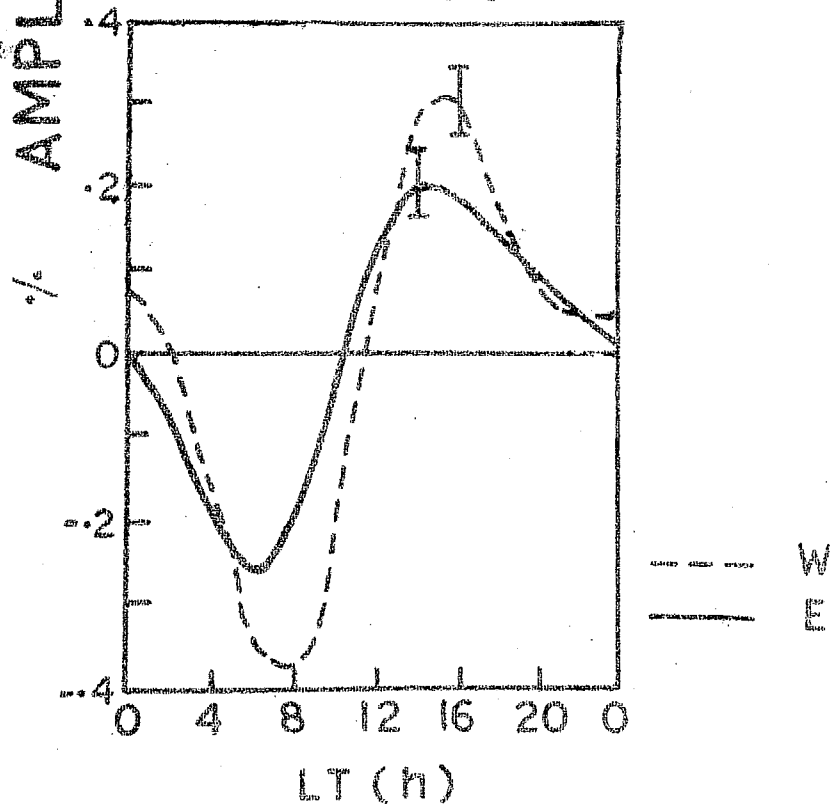


Fig.2.15

The average daily variation observed by inclined telescopes during different periods of solar cycle at Ahmedabad.

pointing telescopes is about ~ 3 hours in 54-55 and 57-58, there is no appreciable phase difference between the east and west directions during 63-65. This is in agreement with the result from measurements made at the equatorial station Makerere by Hasim et al.(1968) during 1965. They have shown that the diurnal variation in the east and west telescopes had an amplitude of about $0.2 \pm 0.02\%$ and difference between the time of maximum in two directions was $0.3 \pm .3$ hr.

The phase of the diurnal components during above periods are shown on harmonic dial in Fig.2.16. It can be seen that the phase of the diurnal variation is changing during 1954 to 1965. Similar long term phase shifts of the diurnal variation have been observed by Sandstrom et al.(1967), using the data of the inclined teelscopes in the east and west directions at Uppsala, as shown in Fig.2.16. From a study comprising most of the records of the diurnal variation, Elliot and Thambyampillai (1953) and Sarabhai et al.(1955) have found that the phase varies with the sunspot number. The minimum value of the time of maximum intensity coincides with sunspot minimum, the period being 22 years. Further studies have shown that the phase shift of the nucleon component displays a much smaller magnitude than the phase shift of the meson component. The phase of the first harmonic attained a minimum in 1953-54.

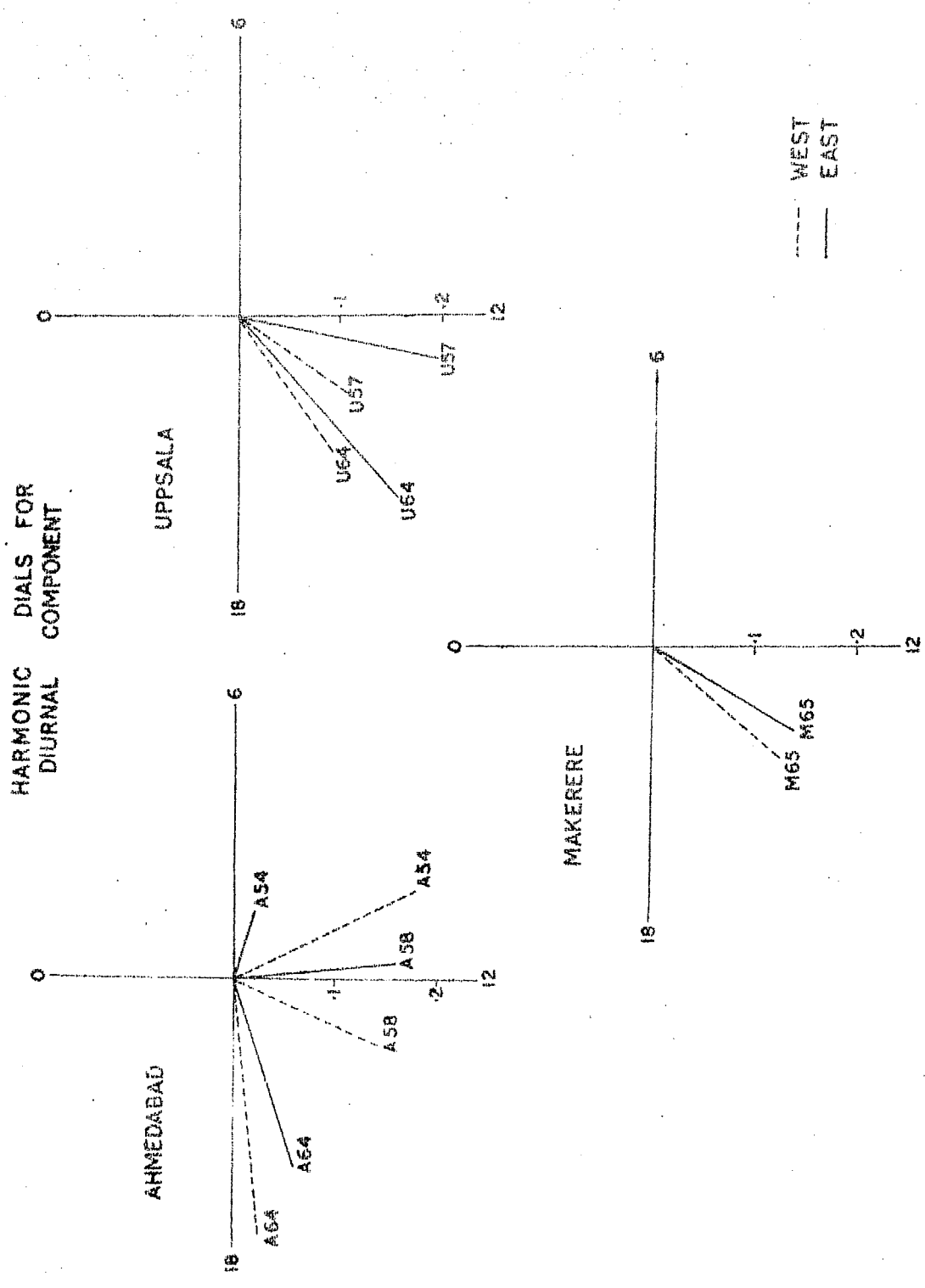


Fig. 2/6 The phase of diurnal component during 1954, 1958 & 1964, 1965.

In conclusion the results of the study of the daily variation measured by the inclined telescopes at Ahmedabad during 1963-65 can be summarised as follows -

- (a) The amplitudes of the average daily variation measured by the two telescopes having semi-angles of opening of 10° and 20° in the east-west plane, are about the same within the statistical accuracy.
- (b) The expected phase difference (~ 6 hrs.) between the times of diurnal maximum of the east and west telescopes is found to be almost zero.
- (c) The phase of the diurnal time of maximum shifts to later hours from 1954 to 1965.

The significance of the present study has been limited due to the low counting rate of the instrument. A study of the energy dependence of the anisotropy and large rapid changes in intensity, needs reliable measurement of intensity with high counting rate instruments. To resolve the difficulty, the cosmic ray group at Physical Research Laboratory, Ahmedabad, undertook the construction of large area scintillation telescopes in vertical and inclined directions. These have started functioning since May 1968. The total counting rates for vertical and inclined directions telescopes are $\sim 10^6$ counts/hr. and $\sim 1.8 \times 10^5$ counts/hr.

respectively (Kargathra, 1968). Meanwhile the author has done a detailed analysis of the data from world-wide super neutron monitors to study the Characteristics of the anisotropy of the galactic cosmic rays on a day-to-day basis. The results of the above analysis are described in Chapter-3.

C H A P T E R - III

CHARACTERISTICS OF THE ANISOTROPIES OF GALACTIC COSMIC RAYS

3.1 Introduction

It is well known that the characteristics of the anisotropy of galactic cosmic rays vary from day-to-day. In the present work anisotropies of galactic cosmic rays are studied through the diurnal component, the semi-diurnal component and the deficiency, which often appears along the direction of the interplanetary magnetic field, in intensity measured by monitors on the spinning earth. The characteristics of the anisotropies and level of the isotropic intensity collectively provide a finger print, for identifying modulating processes and the electromagnetic state of interplanetary space in the neighbourhood of the earth.

The following characteristics of the anisotropy of the cosmic ray intensity measured on the earth, have been derived.

- (1) An energy spectrum of variation of the anisotropy defined by the exponent X , and limiting energies E_{\min} and E_{\max} in the equation (Dorman, 1957).

$$\begin{aligned}\frac{\delta D(E)}{D(E)} &= a E^X \quad \text{for } E_{\min} \leq E \leq E_{\max} \\ &= 0 \quad \text{for } E < E_{\min} \text{ and } E > E_{\max}.\end{aligned}$$

where $D(E)$ is the differential energy spectrum of primary cosmic ray particles of energy, E and $\delta D(E)$ is the energy spectrum of the variational part.

- (2) The direction in space of maximum intensity T_{\max} and of minimum intensity T_{\min} .
- (3) The magnitude of the anisotropy in space defined in terms of a percent change in the 24 hourly mean intensity of galactic cosmic rays.

In section 3.2, we describe the method of variational coefficients, defined by McCracken et al, (1962), to relate the variation measured by a detector to the strength of the anisotropy from a solid angle Ω_i beyond the geomagnetic field. McCracken et al, (1965) have evaluated the cosmic ray variational coefficients for several stations for ten values of β , the exponent of the spectrum of variation. It ranges from +.6 to -1.5. The energy limits extend from near the cut off rigidity to 500 BV. In order to make a detailed study of the anisotropy of galactic cosmic rays it is necessary to make additional calculations using more values of the exponent β and E_{\min} . We have, therefore, evaluated variational coefficients for different stations used in analysis for twelve values of β ranging from +1.0 to -1.2 and for different limits of lower rigidities (E_{\min}), keeping the upper limit of rigidity constant to 250 BV. The method

of analysis of the anisotropies and their characteristics during 1964-65 are described in section 3.3. The characteristics of the daily variation which must be expected from different processes that appear of contributing to produce an anisotropy have been described in sections 3.5 and 3.6.

3.2 Variational coefficients

For any arbitrary anisotropic flux of cosmic radiation, the differential counting rate of any detector can be calculated as

$$\dot{n}_i = J_i(P) \cdot S(P) \cdot Z(\theta, \phi) d\Omega \cdot dp \quad (3.1)$$

where $J_i(P)$ is the differential rigidity spectrum due to all asymptotic directions within a solid angle Ω_i , $S(P)$ expresses the secondary component as a function of primary rigidity and $Z(\theta, \phi)$, the influence of the atmosphere as a function of the position θ, ϕ , of the centre of the source element. $d\Omega$ is the solid angle subtended by the particle flux at the top of the atmosphere. Expressing the influence of the atmosphere by a separable function of rigidity and direction and integrating over all directions θ, ϕ , the counting rate due to radiation arriving from asymptotic directions within Ω_i is given by

$$dn_i = J_i(P) \cdot S(P) \cdot Y(\Omega_i, P) dP \quad (3.2)$$

where $Y(\Omega_i, P)$ is the integral of $Z(\theta, \phi)$ over all directions of θ, ϕ that are accessible to the detector from Ω_i , for rigidity P .

For the isotropic radiation equation (3.2) can be expressed as,

$$dN = J_0(P) \cdot S(P) \cdot Y(4\pi, P) dP \quad (3.3)$$

where N is the total counting rate and $J_0(P)$ the differential rigidity spectrum of primaries from all asymptotic directions. Dorman's coupling constant $W(P)$, defined in section 1.5, gives

$$S(P) = \frac{N W(P)}{J_0(P) Y(4\pi, P)}$$

substituting in equation (3.2) we obtain

$$dn_i = NW(P) \frac{J_i(P)}{J_0(P)} \cdot \frac{Y(\Omega_i, P)}{Y(4\pi, P)} \cdot dP \quad (3.4)$$

The differential rigidity spectrum, due to the source element Ω_i can be expressed as

$$J_i(P) = J_0(P) + \Delta J_i(P)$$

and by substitution in equation (3.4) and integrating over P it becomes

$$n_i = N \int W(P) \left[1 + \frac{\Delta J_i(P)}{\Delta J_0(P)} \right] \cdot \frac{Y(\Omega_i, P)}{Y(4\pi, P)} \cdot dP \quad (3.5)$$

If Δn_i is the part of the counting rate corresponding to the radiation $\Delta J_i(P)$ from the source element Ω_i , we have

$$\frac{\Delta n_i}{N} = \int W(P) \frac{\Delta J_i(P)}{J_0(P)} \cdot \frac{Y(\Omega_i, P)}{Y(4\pi, P)} \cdot dP \quad (3.6)$$

Assuming $\frac{\Delta J_i(P)}{J_0(P)} = A_i P^\beta$ where A_i is a function of asymptotic direction, equation (3.6) reduces to,

$$\frac{\Delta n_i}{N} = A_i V(\Omega_i, \beta) \quad (3.7)$$

$$\text{where } V(\Omega_i, \beta) = \int W(P) \cdot P^\beta \cdot \frac{Y(\Omega_i, P)}{Y(4\pi, P)} \cdot dP \quad (3.8)$$

$V(\Omega_i, \beta)$ is called the variational coefficient of the detector corresponding to the solid angle Ω_i .

For an evaluation of the variational coefficients, the ratio $\frac{Y(\Omega_i, P)}{Y(4\pi, P)}$ should be computed as a function of rigidity. Rao et al; (1963) have adopted a method of approximation founded upon a division of the celestial hemisphere in a number of regions. They have divided the celestial hemisphere into nine regions centred around the vertical and geomagnetic north, south, east and west with zenith angles 16° and 32° . For every rigidity region the ratio between the number of asymptotic directions comprised within each Ω_i , and the corresponding number for the whole celestial sphere, has been used as a measure of $\frac{Y(\Omega_i, P)}{Y(4\pi, P)}$.

Application to the Daily Variation

Consider an anisotropy that is an arbitrary function of η , the angle measured eastward from the meridional plane (Fig.3.01), and is expanded as a Fourier series

$$f(\eta) = J_0(P) \sum_{m=1}^{\infty} \alpha_m \cos m(\eta - C_m) \quad (3.9)$$

where α_m and C_m are arbitrary amplitude and phase constants.
From Fig.3.01

$$\eta = \psi + 15T - 180^\circ$$

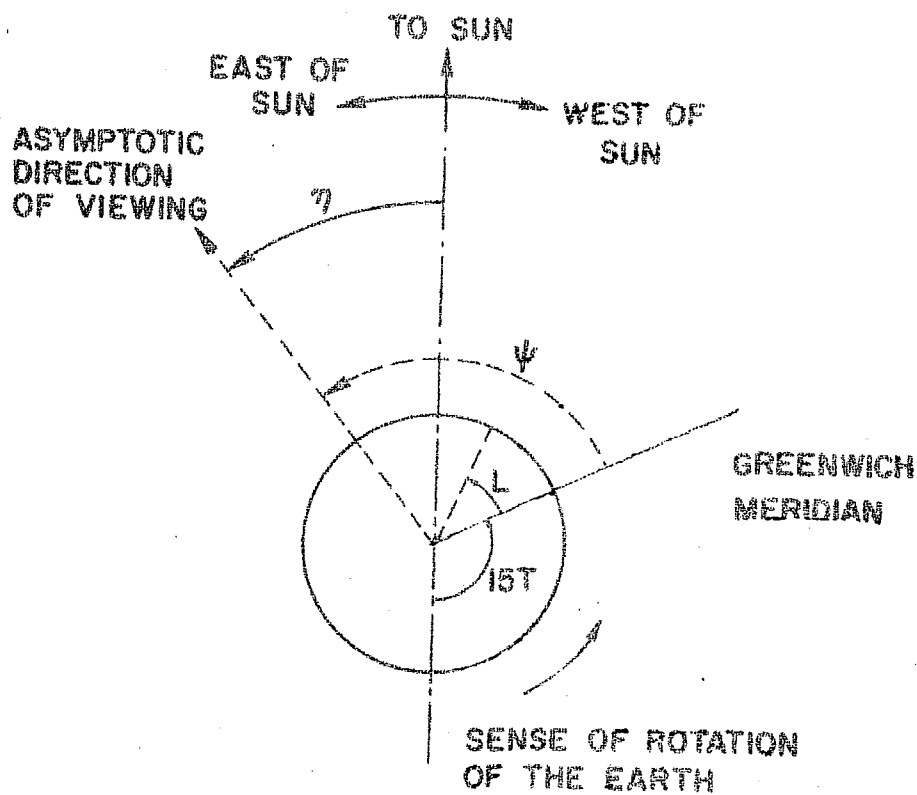


Fig.3.01 Asymptotic direction of viewing of an arbitrary station.

Substituting in equation 3.9, we may write the intensity from asymptotic longitude ψ , as

$$f(\psi) = J_0(P) \left[\sum_{m=1}^{\infty} \alpha_m \cos m(\psi + 15T - 180^\circ - C_m) \right] \quad (3.10)$$

where $\psi = (5i + 2.5)$; the mean longitude of all the particles arriving from the solid angles lying between $\psi = 5i$ and $\psi = 5(i + 1)$. Summing over i , the change in the total counting rate, as given by equation (3.7) will be

$$\begin{aligned} \frac{\Delta n_i}{N} &= f(\psi_j) \cdot V(\psi_j, \beta) \\ &= \sum_{i=0}^{71} V(\psi_j, \beta) \sum_{m=1}^{\infty} \alpha_m \cos m(\psi + 15T - 180^\circ - C_m) \\ &= \sum_{m=1}^{\infty} \alpha_m B_m \cos [m(15T - (m-180^\circ) + \varphi_m)] \quad (3.11) \end{aligned}$$

where

$$\begin{aligned} B_m^2 &= \left\{ \sum_{i=0}^{71} V(\psi_j, \beta) \sin m(5i + 2.5) \right\}^2 \\ &\quad + \left\{ \sum_{i=0}^{71} V(\psi_j, \beta) \cos m(5i + 2.5) \right\}^2 \end{aligned}$$

$$\text{and } \tan \varphi = \frac{\sum_{i=0}^{71} V(\psi_j, \beta) \sin m(5i + 2.5)}{\sum_{i=0}^{71} V(\psi_j, \beta) \cos m(5i + 2.5)}$$

In equation 3.11, $\alpha_m B_m$ and $(-m C_m + \varphi_m)$ represent the amplitude and phase constant of the m^{th} harmonic.

The universal time at which the maximum intensity is observed is given by

$$T_m = \frac{180 m + m C_m - \gamma_m}{15 m} \text{ hours}$$

and the local time of maximum intensity is given by

$$t_m = \frac{180 m + C_m - (\gamma_m - mL)}{15 m} \text{ hours}$$

where L is the geographic longitude of the station. The term $(\gamma_m - mL)$ is called the "geomagnetic bending" of the cosmic ray flux.

3.3 Methods of Analysis

Data from neutron monitors which are indicated in Table 3.1 are used for our analysis. Possible range of threshold rigidities has been used. The asymptotic direction of viewing of each neutron monitor is itself dependent on the energy spectrum of variation of the anisotropy. Moreover all the stations scan interplanetary space in the range of latitudes $\pm 30^\circ$.

Bi-hourly cosmic ray data corrected for variations of barometric pressure have been harmonically analysed to derive the amplitudes (r_1 and r_2) and the phase angles ϕ_1 , and ϕ_2 of the diurnal and the semi-diurnal components as well as the peak to peak amplitude (A), T_{\max} and T_{\min} , the direction of maximum and minimum of the intensity, for the composite variation produced by the superposition of the two components.

Table 3.1

CHARACTERISTICS OF COSMIC RAY STATIONS (1964-65)

STATION	HOURLY COUNTING RATE $\times 10^3$	STANDARD ERROR ⁺ (%)	CUT OFF RIGIDITY ⁺⁺ (G.V)	ASYMPTOTIC LATITUDE (DEGREES ⁺⁺) FOR		MEAN DEFLECTION IN LONGITUDE FOR DIURNAL COMPONENT (IN HOURS)			SOURCE OF DATA
				10 EV	25 EV	CASE I ⁿ	CASE II ⁿ	CASE III ⁿ	
CHURCHILL	7.74	.032	.21	33.0	45.7	1.03	1.25	1.41	D.C. ROSE
DEEP RIVER	6.26	.038	1.04	5.4	28.7	1.64	2.33	3.06	J.F. STELJES & H. CARMICHAEL
SULPHUR MOUNTAIN	8.80	.031	1.15	5.6	26.1	1.26	1.73	2.51	B.G. WILSON
CLIMAX	4.21	.043	3.06	-24.0	9.1	1.93	3.24	5.34	J.A. SIMPSON
DALLAS	7.86	.032	4.30	-31.4	2.6	2.08	3.47	5.39	R.G. McCracken
HERMANUS	.10	.069	4.90	32.5	-6.8	1.88	3.55	6.12	A.M. VAN WIJCK

+ STANDARD ERROR IN HARMONIC COEFFICIENT (EACH DAY)

++ IGSY INSTRUCTION MANUAL NO.10 (1963)

n CASE I - EXPONENT $X = +.6$, $E_{MIN} = 2$ GEVCASE II - EXPONENT $X = 0$, $E_{MIN} = 2$ GEVCASE III - EXPONENT $X = -1.0$, $E_{MIN} = 2$ GEV

DIFFERENT ENERGY SPECTRA OF VARIATION K

$\begin{matrix} X \\ E_{MIN} \text{ IN GEV} \end{matrix}$	+1.0	+.8	+.6	+.4	+.2	0	-.2	-.4	-.6	-.8	-1.0	-1.2
2	1	2	3	4	5	6	7	8	9	10	11	12
4	13	14	15	16	17	18	19	20	21	22	23	24
8	25	26	27	28	29	30	31	32	33	34	35	36



GROUP I → GROUP III → GROUP II → GROUP IX → 

Fig. 3.02 Different energy spectra of variation K

In determining the energy spectrum, 36 combinations of X and E_{\min} , designated by the serial numbers $K = 1$ to 36, as shown in Fig.3.02 have been considered to describe the energy dependence of the anisotropy. The exponents X , range from -1.2 to +1.0, while E_{\min} ranges from atmospheric cut off to 8 GeV. For each combination of X and E_{\min} the effect of an anisotropy on the amplitudes and phase of the diurnal and semi-diurnal components as would be observed by different detectors (Rao et al, 1965) is calculated by the method of variation coefficient, as described in Section 3.2. The multiplicity values are taken from Quenby and Webber (1959). E_{\max} in all the cases is taken as 250 GeV. For each combination of X and E_{\min} , the attenuation factor α_{jik} by which the amplitude of the j th harmonic is reduced with respect to its free space value and the effective bending angle τ_{ijk} in the geomagnetic field, are calculated for a station i . For the observed diurnal and semi-diurnal components (a_j, b_j), the free space values (denoted by $*$) are calculated as follows (Subramanian, 1964; Sarabhai and Subramanian, 1966).

$$\begin{aligned} X_{jik} &= \alpha_{jik} \cos \tau_{jik} \\ Y_{jik} &= \alpha_{jik} \sin \tau_{jik} \\ Q_{jik}^* &= \frac{a_{ji} \cdot X_{jik} - b_{ji} \cdot Y_{jik}}{\alpha_{jik}^2} \quad (3.12) \end{aligned}$$

$$b^*_{jik} = \frac{a_{ji} \cdot Y_{jik} + b_{ij} \cdot X_{jik}}{\alpha^2_{jik}}$$

For each assumed spectrum of variation K, we compute a parameter S_K^2 to provide a measure of the scatter of derived $\gamma_1, \phi_1, \gamma_2, \phi_2$ in space, corresponding to the observed variation at each station. It is given by:

$$S_K^2 = \sum_{i=1}^n \sum_{j=1}^z \frac{(a^*_{jik} - \overline{a^*_{jk}})^2 + (b^*_{jik} - \overline{b^*_{jk}})^2}{\sigma^2_{jik}} \quad (3.13)$$

where the bar denotes values averaged over all stations.

The denominator represents the variance of the corresponding term in the numerator and is given by

$$\sigma^2_{jik} = \frac{(N^2 - 2N) \alpha^2_{jik} \sigma^2_{ji} + \sum_{i=1}^N \alpha^2_{jik} \sigma^2_{ji}}{N^2} \quad (3.14)$$

the minimum value of S_K^2 indicates the best fit of the experimentally measured daily variation at each station with the variation that can be expected on the basis of the assumed spectrum. The determination of the spectrum is done separately for the diurnal and the semi-diurnal components of the variation.

Even though 36 different spectra have been considered by us, the inherent resolution that is possible in discriminating between spectra has to be taken into account. The criterion that is applied is $\chi^2(N)$ which is the standard

error of S_{\min}^2 . It depends on the number of stations N . If one has a group of spectra for which S^2 values differ from S_{\min}^2 by more than $\chi^2(N)$, then the value of K for which the minimum occurs, is deemed to be the spectrum of choice. Moreover, other values of K which differ by less than $\chi^2(N)$ from S_{\min}^2 , are also considered possible alternative choices, within the resolution of the method. If on the other hand the range of S^2 for the different spectra on a particular day does not exceed $\chi^2(N)$ the determination of the energy spectrum is impossible. The procedure is best understood by the examination of Fig.3.03, which indicates the values of S^2 corresponding to three different days. Fig.3.03A corresponds to a day when conditions are particularly favourable and only 6 equally acceptable spectra, i.e., $K = 4$ to 8 and 17, emerge as possible candidates. On a different day conditions are as shown in Fig.3.03b. The spectrum $K = 6$, can be chosen, since it corresponds to S_{\min}^2 . However 18 other spectra are equally acceptable. Fig.3.03c illustrates conditions on a day for which determination of the spectrum is not possible.

The days on which S_{\min}^2 was very high, (≥ 400 in arbitrary unit) were rejected for the further analysis. Almost all days on which major Forbush decreases have occurred or when data from one or more of the stations is erratic get rejected according to this criterion. Also some of the days

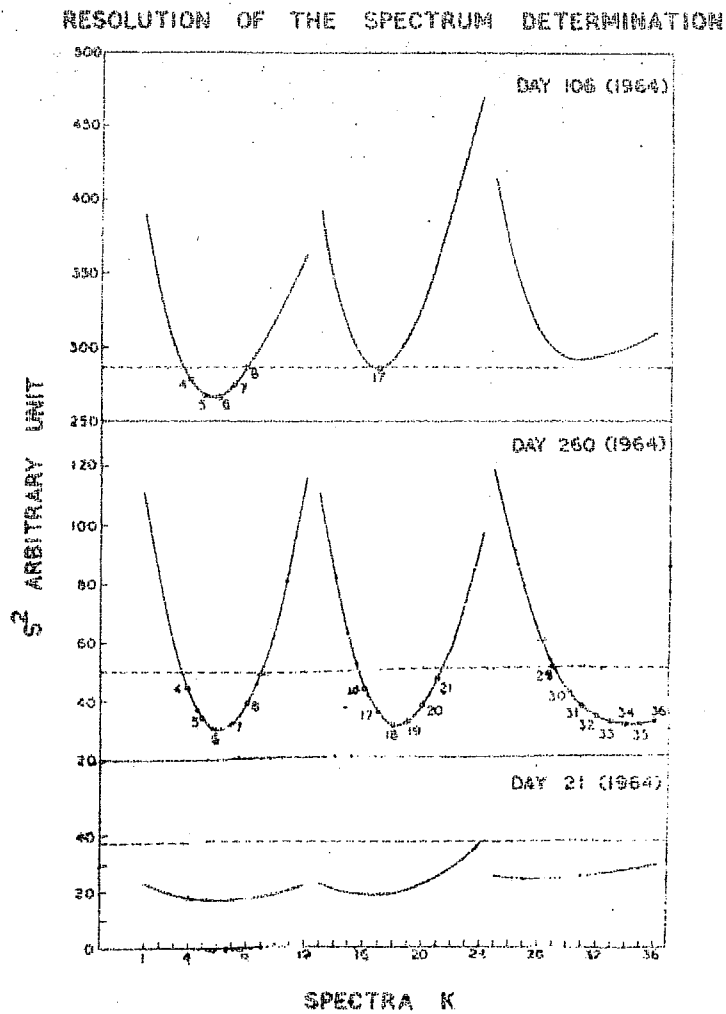


Fig.3.03 S^2 values for three typical days are plotted for different spectra designated by 1 to 36 as indicated in Fig.3.02. The broken line indicates the χ^2 limit which determines the resolution between spectra.

were rejected on account of lack of resolution between various spectra where determination was not possible. For each remaining day, a spectrum corresponding to S_{\min}^2 and one or more equivalent spectra are identified.

3.4 Day-to-day changes of the Anisotropies

The frequency of occurrence of spectra determined from the diurnal and semi-diurnal components, during 1964-1965 are shown in Fig.3.04. Primary as well as equivalent spectra have been included. The following observations can be made:

- (a) The diurnal variation has principally a spectrum with a zero exponent and $E_{\min} = 2$ or 4 GeV. The spectra of choice are therefore $K = 6$ and 18.
- (b) The semi-diurnal variation has principally a spectrum with a positive exponent (+0.6 to +1.0) and $E_{\min} = 2, 4$ or 8 GeV ($K = 1$ to 3, 13 to 15, and 25 to 27).
- (c) For $E_{\min} = 8$ GeV, negative exponents occur in both diurnal and semi-diurnal components.
However, since in the grid of stations, there is no detector with a cut off rigidity greater than 4.2 GV, good resolution is not achieved ($K = 31$ to 36).

FREQUENCY OF OCCURRENCE OF SPECTRA

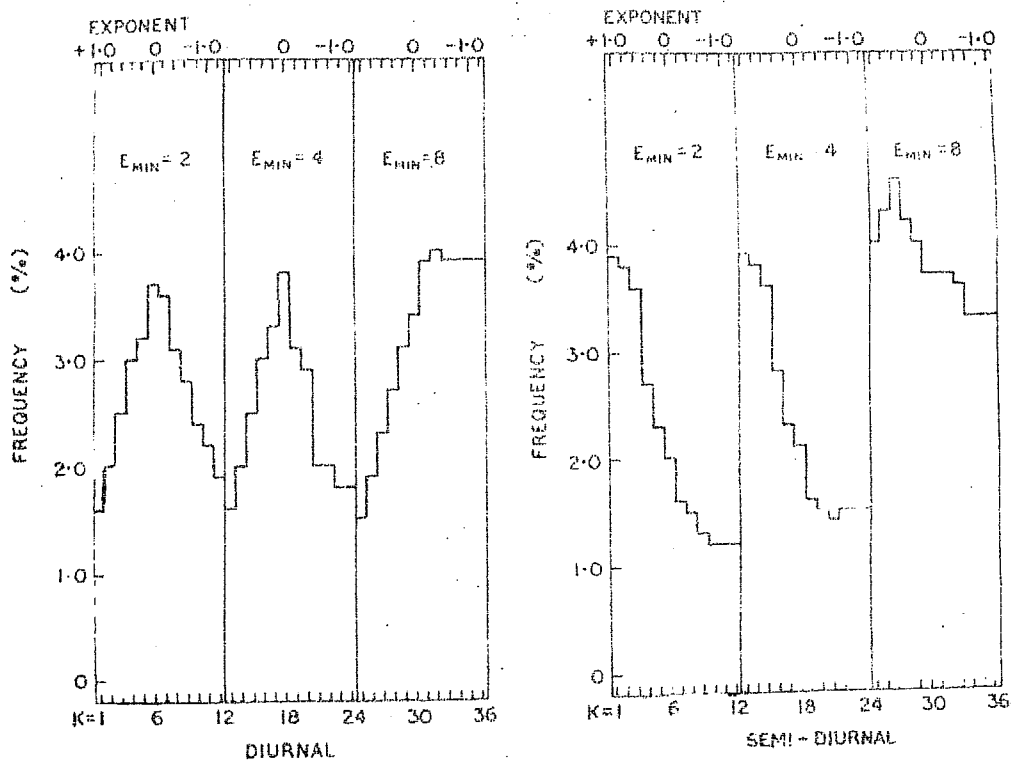


Fig.3.04 The frequency distribution of occurrence of the energy spectra of variation for diurnal and semi-diurnal components during 1964-1965.

We therefore conclude from a day-to-day ^{analysis} of anisotropies that the predominant spectra of variation of the diurnal and semi-diurnal components are characteristically different. This is confirmed through the comparison in Fig.3.05 of the diurnal and semi-diurnal amplitudes of the average daily variation during 1964-1965, measured at a set of stations with geomagnetic cut off rigidities, ranging from 2-13 GV. Allowance has been made for the attenuation of the diurnal and semi-diurnal components due to the width of the asymptotic cones of acceptance of the detectors (McCracken and Rao, 1965). Note that while the diurnal component has a spectrum of variation which is essentially independent of rigidity and has an exponent $X \sim 0$, the semi-diurnal component has a spectrum which has a positive exponent.

The three prominent types of spectra which are identified from Fig.3.04, have been further investigated to separately ascertain for each of them the extent to which other spectra are equally acceptable. For this purpose a frequency distribution is drawn of occurrence of spectra which are equally acceptable as the spectrum of choice. Fig.3.06 shows the distribution when spectra 6 and 18 with an exponent $X = 0$, and $E_{\min} = 2$ or 4 GeV respectively are selected on the criterion of being associated with S_{\min}^2 . Spectra with $K = 4$ to 8 and 17 occur with the same frequency

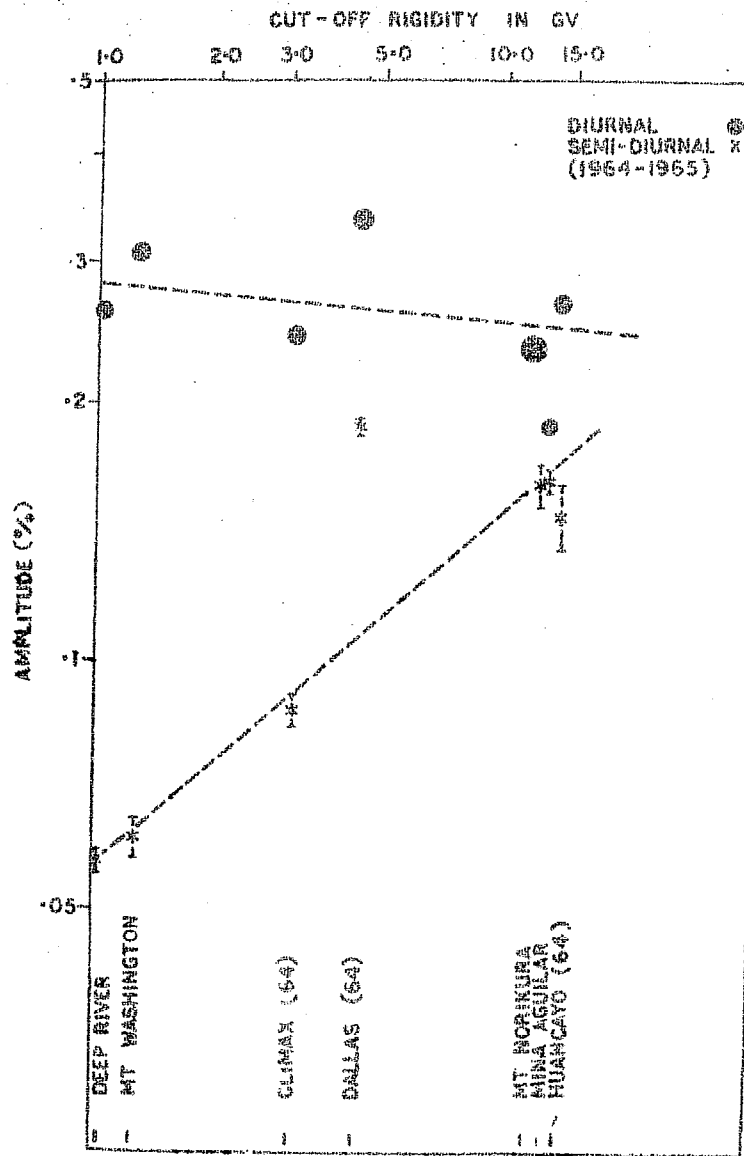


Fig.3.05 The dependence of amplitude of the annual average diurnal and semi-diurnal components on cut-off rigidity from 1 to 15 Gv.

as the spectra of choice $K = 6$, and 18 , and are grouped as equivalent spectra. Thus the resolution with available data is such as to make it necessary to group together days on which the exponent is $+ .4$ to $- .4$ with $E_{\min} = 2$ GeV and those on which the exponent is $+ .2$ with $E_{\min} = 4$ GeV. The procedure is repeated for the spectra with an exponent $X = +1$ and $E_{\min} = 2, 4$ and 8 GeV for the second group and with an exponent $X = -1$ and $E_{\min} = 8$ GeV for the third group. Additionally we also identify a fourth group of spectra which are equivalent to the spectrum with an exponent $X = -1.0$ and $E_{\min} = 2$ or 4 GeV.

Clusters of equally acceptable spectra associated with each of the four types are indicated in Fig.3.02. The percent frequency of occurrence of each of the four clusters of spectra in diurnal anisotropy and in the semi-diurnal anisotropy are shown in table 3.2. Only days on which it was possible to determine spectra of variation for diurnal as well as semi-diurnal anisotropies are considered for this analysis. Note that the semi-diurnal variation predominantly appears with a positive exponent of spectrum. Negative exponent can also occur, but rarely zero exponent. On the other hand the diurnal variation can occur with anisotropies having spectra with negative, zero, and positive exponents. It is because of this mix of spectra, that the average diurnal

FREQUENCY DISTRIBUTION OF OCCURRENCE OF EQUALLY ACCEPTABLE SPECTRA

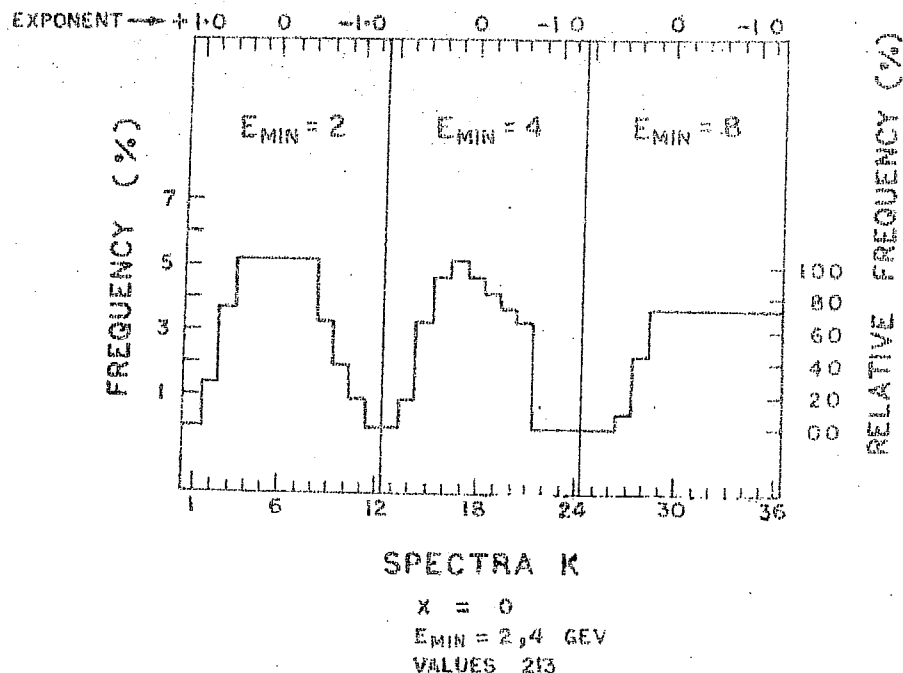


Fig.3.06 The frequency distribution of equivalent spectra associated with spectra K = 6 & 15.

Table 3.2

PERCENTAGE FREQUENCY OF VARIATION SPECTRA
FOR DIURNAL AND SEMI-DIURNAL COMPONENTS
DURING 1964-65

ANISOTROPY	GROUP I X = 0 E _{MIN} = 2.4 GEV %	GROUP II X = +1 E _{MIN} = 2.4, 6 GEV %	GROUP III X = -1 E _{MIN} = 8 GEV %	GROUP IV X = -1 E _{MIN} = 2.4 GEV %
DIURNAL	16.2	23.7	26.0	23.5
SEMI-DIURNAL	2.0	51.1	24.6	12.8

TOTAL NO OF DAYS : 358

and semi-diurnal variations show different characteristics which we observed Fig.3.05.

3.5 Characteristics of processes producing anisotropics in interplanetary space

At least four processes appear to contribute to produce an anisotropy. All need not necessarily be active on the same day to the same extent. They are (a) azimuthal streaming (Parker, 1964; Axford, 1965; Krymskiy, 1964); (b) streaming due to non-uniform diffusion in a longitudinal sector structure of interplanetary magnetic fields (Parker, 1964); (c) scattering at irregularities along the interplanetary magnetic field short-circuiting latitudinal gradients (Sarabhai and Subramanian, 1966) and (d) latitudinal gradients in a relatively smooth magnetic field (Subramanian and Sarabhai, 1967; Lietti and Quenby, 1968). Due to the first two processes, omnidirectional intensity in interplanetary space would remain unchanged, the third and fourth processes would be perceived through virtual sources or sinks, generating semi-diurnal and diurnal components as well as a variation of omnidirectional intensity. In the following section we will describe the mechanism of each process and the characteristics of the daily variation which must be expected from each process.

(a) Azimuthal streaming

For the process to occur it is necessary that in interplanetary space $\epsilon = \frac{K_{\perp}}{K_{\parallel}}$ should be less than 1, K_{\parallel} and K_{\perp} are the coefficients for cosmic ray diffusing parallel and perpendicular to the direction of the interplanetary magnetic field respectively. ϵ depends on the density and scale length of the field irregularities and on the gyro-radius of the cosmic ray particles. The finger-print of the process giving rise to azimuthal streaming is that in the range of energies for which the process is effective the spectrum of variation should correspond to co-rotation of cosmic rays with the sun. In consequence an excess of cosmic rays should appear to arrive from the 1800 direction giving rise to a time of maximum in the daily variation corresponding to this direction.

(b) Streaming in longitudinal sector structure

When the solar wind velocity, or the density of irregularities change with heliolongitude, additional streaming of cosmic rays would occur as discussed by Parker (1964). The resulting anisotropy should generally be diurnal with an exponent $X = 0$. T_{\max} and T_{\min} will not be alog 1800 and 0600 hours respectively and the amplitude could be larger than .6%. The other considerations discussed in the earlier section related to azimuthal streaming would generally apply to this process.

(c) Scattering at magnetic field irregularities

Scattering at magnetic field irregularities along smooth field lines short circuits the latitudinal gradients. If the cosmic ray intensity decreases with increasing helio-latitudes as could be the case in a region $\pm 15^\circ$, lower cosmic ray density will be observed along the direction of interplanetary magnetic field (Sarabhai, Pai and Wada, 1965; Sarabhai and Subramanian, 1966). If the efficiency of scattering due to irregularities along the field line, excluding the domain of interplanetary space in the neighbourhood of the earth, is the same for all cosmic ray particles up to an energy $E_{\text{max}} = 80 - 100$ GeV, the exponent of the spectrum of the anisotropy will be the same as that of the 11 year variation of cosmic ray intensity. The ratio of the relative amplitudes of the diurnal and semi-diurnal components generated by this process, provides an indication of the pitch angle distribution of the scattered particles as they approach the earth. When the distribution is broad the semi-diurnal component will relatively be less important. A consequence of this is that when the scattering centre is at some distance from the earth, the pitch angle distribution would be narrower and hence a sharper deficiency would be observed along the garden hose direction. This process is particularly relevant in observing the travel outward of magnetic field irregularities generated close to the sun as

during the occurrence of blast waves associated with flares and type IV bursts which ultimately produce Forbush decreases in the cosmic ray intensity measured at the earth. The finger print of this process involves a spectrum with an exponent which is generally negative, a deficiency along the direction of magnetic field, usually in the direction of the sun. The diurnal component involved in this anisotropy would be superposed on the diurnal component due to azimuthal streaming. In consequence T_{\max} would normally be shifted from the 1800 direction.

(d) Latitudinal gradients of cosmic ray intensity

The existence of latitudinal gradients of cosmic ray intensity in a domain of relatively smooth interplanetary magnetic field gives rise to semi-diurnal and diurnal components (Subramanian and Sarabhai, 1967). A semi-diurnal variation is also explained by Lietti and Quenby (1968) who have considered the gradient due to the decreasing tightness of the interplanetary magnetic field with increasing heliolatitude. The direction of maximum of the semi-diurnal anisotropy will generally be perpendicular to the interplanetary magnetic field and also in the sense of the N-S asymmetry of cosmic ray density, N and S of the equatorial plane. The exponent of the energy spectrum of variation of the resulting anisotropies will depend on the form of distribution of the

cosmic ray intensity with heliolatitude and on the phase of the solar cycle of activity. Note that the diurnal component is related to a N-S asymmetry of the latitudinal gradient. The energy spectrum of variation of the diurnal component has an exponent $1 - \beta$, while the semi-diurnal component has an exponent $2 - \beta$ (Subramanian and Sarabhai 1967). β , determines the rigidity dependence of the latitudinal variation of cosmic ray density. As a first approximation it has been assumed that β is the same as for the spectrum of galactic intensity in the plane of the ecliptic and is independent of heliolatitude. However β ranges from 2 during minimum sunspot activity to 0.5 during maximum solar activity (Webber, 1965). During most periods of the solar cycle β is less than 2. Hence it is expected that the semi-diurnal variation will have a positive exponent and the diurnal will have either positive or negative in contrast to zero exponent for the azimuthal drift. The diurnal and semi-diurnal components should be about .3% and .2% respectively for a transverse gradient of 6% per A.U. for particles of energy $E > 2$ GeV and a N-S asymmetry of 14% arising from an asymmetrical distribution of cosmic ray density about the equatorial plane (Subramanian and Sarabhai, 1967). The north-south asymmetry is defined as

$$A = \frac{2(\rho_N - \rho_S)}{(\rho_N + \rho_S)} \times 100\%$$

where \mathcal{P}_N is the average cosmic ray density for heliolatitudes 0° to $+30^\circ$ and \mathcal{P}_S is the average cosmic ray density for heliolatitudes 0° to -30° at 1 A.U. Note that asymmetry for the coronal 5303A $^\circ$ intensity was about 60% and 86% during the year 1964 and 1965 respectively for heliolatitudes $\pm 30^\circ$. Models considered by Lietti and Quenby (1968) give a positive exponent for the energy spectrum of variation of the semi-diurnal component in the 1 to 15 GeV range with an amplitude of about 0.05% at 10 GeV. The existence of a semi-diurnal component is a necessary condition for the occurrence of this process.

All four processes producing anisotropies have one thing in common, which is that when the interplanetary magnetic field in the immediate neighbourhood of the earth is disturbed as during the passage of a radially travelling blast wave or a corotating shock front causing Forbush decreases, the amplitude of anisotropies would be temporarily reduced.

3.6 Identification of Anisotropies

The characteristics of the basic processes described in section 3.5 are summarised in Table 3.3. After following the procedure for unambiguous determination of spectrum of variation described in section 3.4, we try to identify the extent to which the various processes are operative on any

particular day and show that T_{\max} and T_{\min} and the amplitudes of the daily variation are consistent with what each process demands.

Table 3.3

CHARACTERISTICS OF ANISOTROPY ASSOCIATED WITH
DIFFERENT PROCESSES

	CHARACTERISTICS	PROCESS			
		1	2	3	4
		AZIMUTHAL STREAMING	STREAMING IN LONGITUDINAL SECTION STRUCTURE	SCATTERING AT IRREGULARITIES	LATITUDINAL GRADIENT
1	NATURE OF THE ANISOTROPY ARISING FROM THE PROCESS	DIURNAL	DIURNAL	DEFICIENCY ALONG THE FIELD LINE DIURNAL AND SEMI-DIURNAL	DIURNAL AND SEMI-DIURNAL
2	EXPONENT OF THE SPECTRUM OF VARIATION				
	(a) DIURNAL	0	0	GENERALLY NEGATIVE	POSITIVE OR NEGATIVE
	(b) SEMI-DIURNAL	—	—	—	POSITIVE
3	T_{\max} HOURS	1800	VARIABLE	2100	1500 OR 0300
4	T_{\min} HOURS	0600	VARIABLE	0900	0900 OR 2100
5	$T_{\max} - T_{\min}$ HOURS	1200	—	1100	0600
6	DIURNAL AMPLITUDE I_1	·4 %	·4 %	·4 %	·3 %
7	SEMI-DIURNAL AMPLITUDE I_2	—	—	·2 %	·2 %

The process corresponding to azimuthal drift is identified by picking up all days on which the exponent is zero for the diurnal component. A further restriction

imposed is the requirement that the semi-diurnal component should not have a positive exponent X , and this allows the exclusion of the process corresponding to latitudinal gradient. Days on which this occurs are classified as Group A. The process of scattering at irregularities, is identified by selecting all days on which the exponent X is negative for diurnal component while the exponent is not positive for the semi-diurnal component. Days on which this occurs are classified as Group B. The process of latitudinal gradient is identified by selecting days on which the exponent of the semi-diurnal component is positive, but the exponent for the diurnal component is not zero. Days on which this occurs are classified as Group C. The days belonging to these three groups during 1964-1965, account for 58.1% of the total days.

3.7 Orientation of the diurnal and semi-diurnal components with respect to the interplanetary magnetic field

The frequency distributions of the direction of maximum (T_{\max}) and the direction of minimum (T_{\min}) of the anisotropy for the three groups during 1964-1965, are shown in Fig.3.07. In group A the most probable value of T_{\max} is 1800 hours. The diurnal character of the anisotropy on these days is brought out by a separation of about 12 hour between the probable values of T_{\max} and T_{\min} . The characteristics of anisotropy for days in this group are, therefore consistent with azimuthal streaming being the principal process.

In group B, the most probable value of T_{\min} is 0800 hours, i.e., along the garden hose direction and of T_{\max} along 1800 hours. T_{\min} is consistent with the operation of scattering, a process which does not interfere with azimuthal streaming except through E_{\min} .

In group C, the most probable value of T_{\max} is about 15 hours and the most probable value of T_{\min} is 0800 hours, along the interplanetary magnetic field. The difference between T_{\max} and T_{\min} is about 0700 hours which indicates that the semi-diurnal component is predominant. The direction of maximum is along the perpendicular to the interplanetary magnetic field for this group. This is consistent with the anisotropy on these days being caused by the existence of latitudinal gradient in a smooth magnetic field.

The frequency distributions of T_{\max} and T_{\min} of daily variation at Deep River and Huancayo neutron monitors during 1964 are shown in Fig.3.08 for the days in group C, after correcting for geomagnetic bending. T_{\min} as measured by huancayo neutron monitor, which has a higher mean energy of response (~ 30 GeV) than Deep River neutron monitor (12 GeV) flips over from garden hose direction to anti-garden hose direction, while for Deep River, it is essentially along the garden hose direction. This phenomenon is in agreement with an earlier study by Sarabhai, Pai and Wada (1965) and Sarabhai

ANISOTROPY IN SPACE (1964-1965)

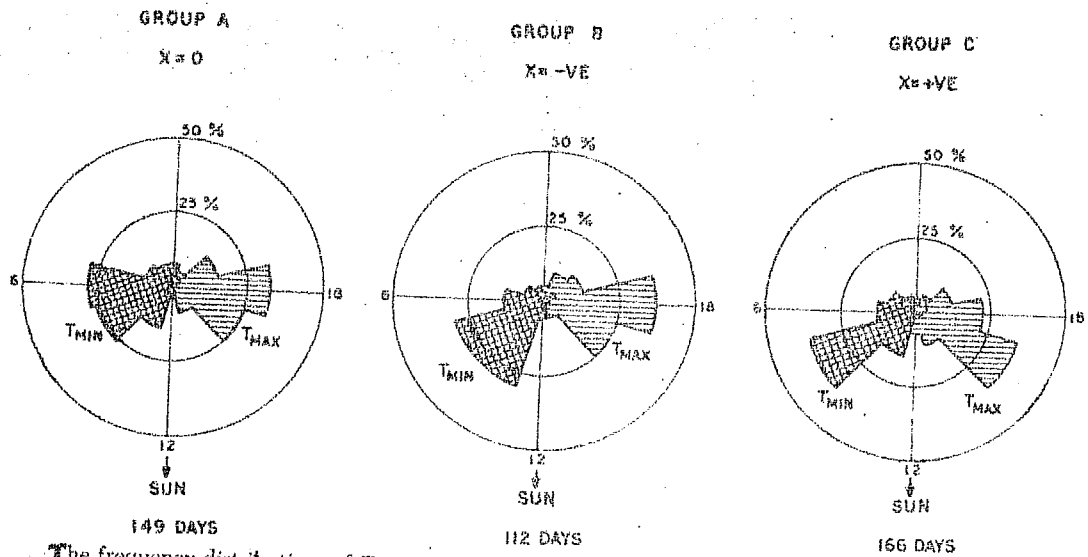


Fig.3.07.

ANISOTROPY (SPACE) 1964

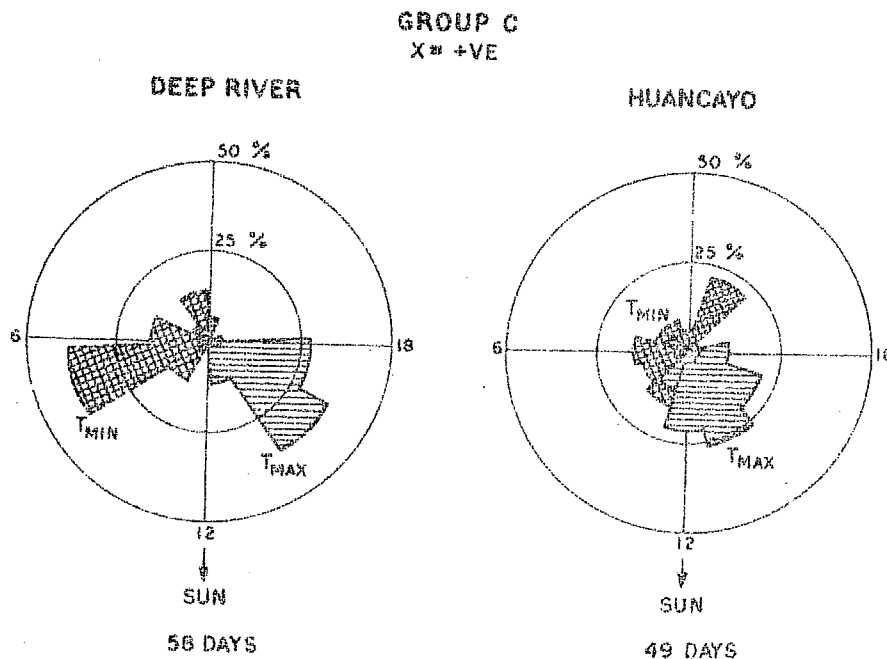


Fig.3.08 The frequency distributions of T_{max} and T_{min} for days in Group C for Deep River and Huancayo neutron monitors.

and Subramanian (1966) using daily variation of cosmic ray intensity obtained from neutron and meson detectors at Deep River.

3.8 Amplitudes in space for the different processes of the modulation

Fig.3.09 shows the frequency distributions of the normalised amplitudes of the diurnal and semi-diurnal amplitudes in space. The most probable values of the diurnal amplitude is $\sim .4\%$ for the days in group A, which is consistent with the Parker-Axford's theory of streaming. The diurnal amplitude is significantly higher in group A as compared to group C.

The amplitude of the semi-diurnal anisotropy is of the order of about $0.1 \sim .4\%$ on individual days (Sarabhai et al, 1965; Ables et al, 1965). In group C, the semi-diurnal component is $\sim .2$ to $\sim .3\%$ and is significantly higher compared to group A.

3.9 Variation in anisotropy associated with the sector structure of the interplanetary field

The diurnal variation of cosmic ray intensity for each day of solar rotations during the period August 27, 1962 to December 25, 1963 has been analysed by Mori et al, (1964) using the meson monitor at Tokyo. They have observed

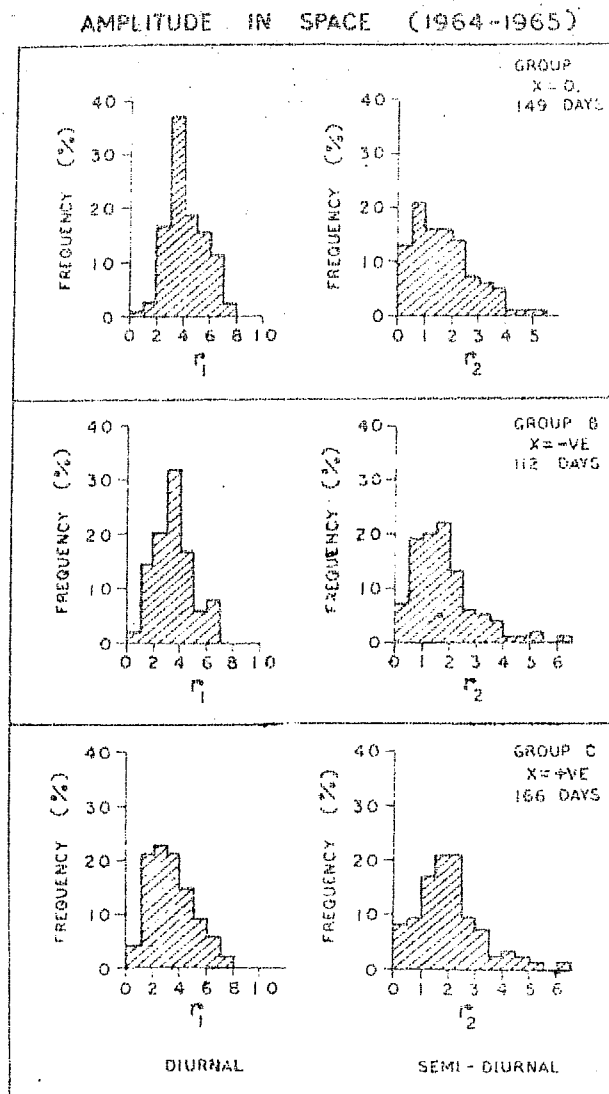


Fig.3.09 The frequency distribution of the normalised amplitude of diurnal and semi-diurnal components in space for different energy spectra of variation.

additional anisotropic flows of cosmic ray diurnal variation in a sector structure that is similar to the IMP-1, magnetic-sector structure. The boundaries agree to within about one day.

Ryder and Hatton (1968) have linked the diurnal cosmic ray anisotropy to the sector structure observed by IMP-1, using a wide band filter applied to the pressure corrected intensity recorded by the Deep River neutron monitor. A super imposed epoch analysis of the filtered time series shows that there is a systematic change in the observed anisotropy through the sectors. The amplitude is smaller when the field is negative than when the field is positive.

The four sectors, A, B, C and D, per solar rotation have been identified during IMP-1, period according to the interplanetary field direction. Out of the four sectors, the field was directed away from the sun (+) during A and C and towards the sun (-) in sectors B and D. Using a set of neutron monitors we have computed the average diurnal variation for positive and negative sectors during the period of IMP-1. The sector D, being only of short duration was not used in the analysis. The remaining sectors are of approximately 8 days duration.

Table 3.4 shows the average diurnal variation when the field is directed away from the sun and the field is directed towards the sun. The amplitude is higher during

the positive sector than during negative sector. One of the predictions arising out of the process of latitudinal gradient (Subramanian and Sarabhai, 1967) is that the diurnal component arising out of the latitudinal gradients should reverse with reversal of either magnetic field or the gradient. When the gradient is such that the solar activity north of the equatorial plane is greater than the south, the latitudinal gradient should give rise to a diurnal anisotropy with its direction of maximum on the average along 1500 hours when the field is directed away from the sun (+) and along 0300 hours when the field is directed towards the sun(-). Such an asymmetry will increase the amplitude of the diurnal component due to azimuthal streaming when the field is away from the sun.

Table 3.4

Mean diurnal component during Nov.29, 1963
to Feb.19, 1964.

	Station	Positive	Negative
		sector	sector
		<u>.7.</u>	<u>.7.</u>
1	DEEP RIVER	.33 ± .01	.27 ± .01
2	SULPHUR MT.	.28 ± .01	.24 ± .01
3	CLIMAX	.31 ± .01	.22 ± .01
4	MT.WASHINGTON	.38 ± .01	.18 ± .02
5	MAWSON	.19 ± .02	.09 ± .03
6	WILKES	.28 ± .02	.12 ± .01
7	MINA AGUILAR	.21 ± .01	.12 ± .01
8	HAUNCAYO	.20 ± .01	.16 ± .01
9	MT.NORIKURA	.15 ± .01	.09 ± .02

3.10 Estimation of the limiting energies E_{\max} and E_{\min} for the process of azimuthal streaming

Theories of modulation of galactic cosmic rays

(Ahluwalia and Dessler, 1962; Parker, 1964; Axford, 1965) have indicated that charged particles approaching the Earth's orbit with gyro-radii greater than about 1 a.u. would be too energetic to take part in the cosmic ray anisotropy which appears to be responsible for the observed daily variation at the earth. Consequently it has been predicted that at the high energy end there would be a cut off for the modulating process which depends in Axford's derivation on the gyro radius of co-rotating cosmic ray particles within a domain of field lines determined by the extent of the sector structure.

Fig.3.11 illustrates the relationship of E_{\max} with the width of the sector structure for three assumed values of the interplanetary magnetic field. During the last period of minimum solar activity, sectors corresponding to 6-8 days have been observed. These would imply an E_{\max} between 100 to 200 GeV, depending upon the strength of the interplanetary magnetic field. With increase of solar activity if the width of each sector diminishes one would expect E_{\max} also to diminish provided the strength of the interplanetary magnetic field does not also alter with solar cycle. Note however that an increase in the value of the interplanetary magnetic field with increased solar activity may compensate partially or

totally the effect of reduced width of the sector.

We have estimated the nature of the daily variation that would be observed by the neutron monitors at Deep River and at the equatorial station, of Hauncayo due to azimuthal streaming, assuming a range of values of E_{\min} and E_{\max} . Instead of the maximum amplitude due to azimuthal streaming which would be .6% for the diurnal variation, the expected amplitude is smaller and can be expressed as

$$\gamma_1 = .6\alpha_1$$

where α_1 is calculated using variational coefficients by the method outlines by McCracken, Rao and Shea (1962). In the present case, in considering the effects of azimuthal streaming we choose coefficients for a spectrum with exponent $X=0$. α_1 is shown in Fig.3.12 for Hauncayo and for Deep River as a function of E_{\min} for several values of E_{\max} . At an equatorial station α_1 does not change with E_{\min} in the range 2-15 GeV but decreases for $E_{\min} > 15$ GeV. The decrease is rapid when E_{\max} is low. On the other hand, for a neutron monitor situated at a high latitude α_1 starts decreasing rapidly for $E_{\min} > 4$ GeV. α_1 is altogether less sensitive to change of E_{\max} than it is to changes of E_{\min} for a neutron monitor at middle or high latitudes.

Fig.3.13 shows the ratio of α_1 at the Huancayo to that at Deep River as a function of E_{\min} for various values

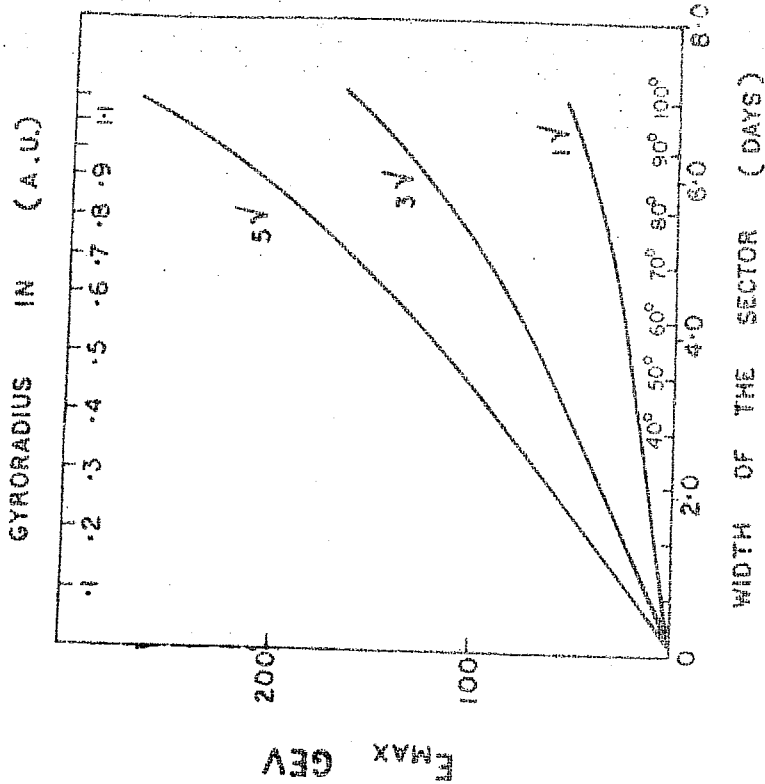


Fig.3.11 The relationship of E_{max} with the width of the sector structure for three values of the interplanetary magnetic field.

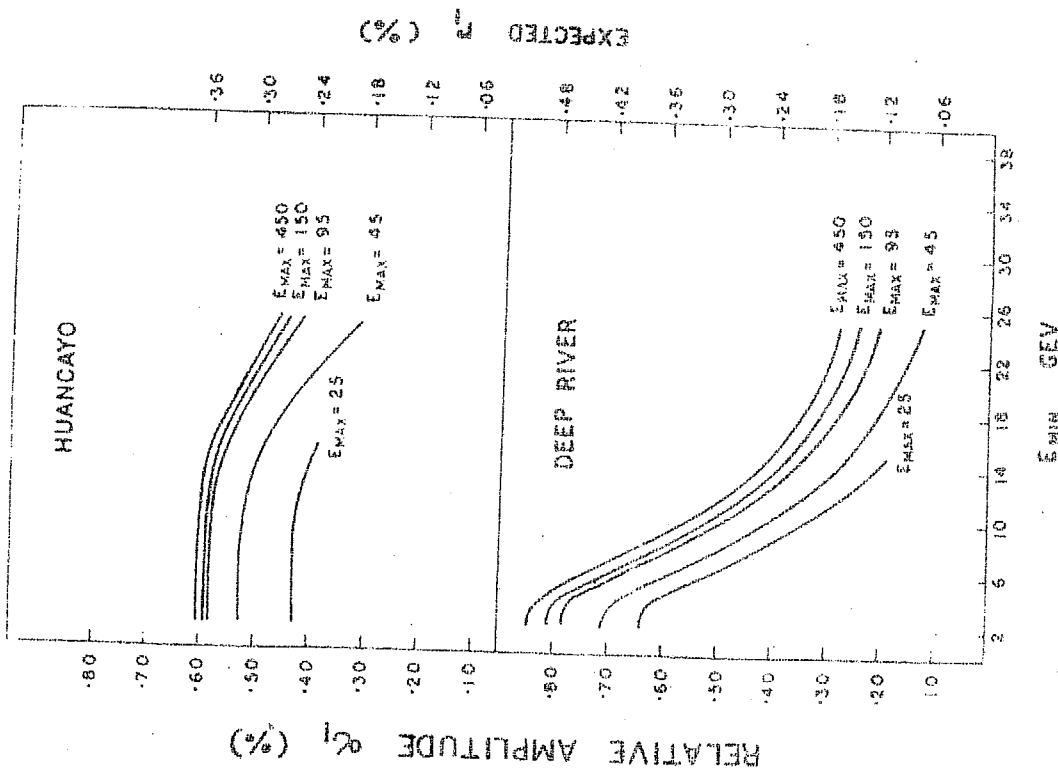


Fig.3.12 The relative diurnal amplitude for a zero spectrum as a function of E_{min} for different values of E_{max} .

of E_{\max} . The ratio increases with E_{\min} , only for $E_{\min} > 4$ GeV. As long as one uses neutron monitors situated on the surface of the earth at latitudes where geomagnetic cut off energy is not greater than 4 GeV, we cannot derive significant information concerning E_{\min} involved in the azimuthal streaming process. Similarly, unless the daily variation with meson detectors is studied it is difficult to draw conclusions concerning changes of E_{\max} . Only if the ratio of amplitude of diurnal variation at Huancayo to Deep River lies in the range .65 to 2.0, the spectrum can be represented by a zero exponent using combinations of E_{\min} from 4 to 15 GeV and E_{\max} from 25 to 45 GeV. Thus a ratio in this range is a necessary condition for attributing the variation to azimuthal streaming.

In the study of cosmic ray anisotropy several authors have suggested that positive and negative exponents occur in the expression for the spectrum of variation (Rao and Sarabhai (1964), Rao et al. (1963), Sarabhai and Subramanian (1966), Nagashima et al. (1961)). The conclusion is based on an analysis of the characteristics of the daily variation simultaneously measured by detectors situated at locations with different cut off rigidities or by meson and neutron detectors. An important characteristic is the ratio of the amplitude of the diurnal variation measured by the neutron monitor at Huancayo and Deep River. For $E_{\min} = 2$ GeV, corresponding to

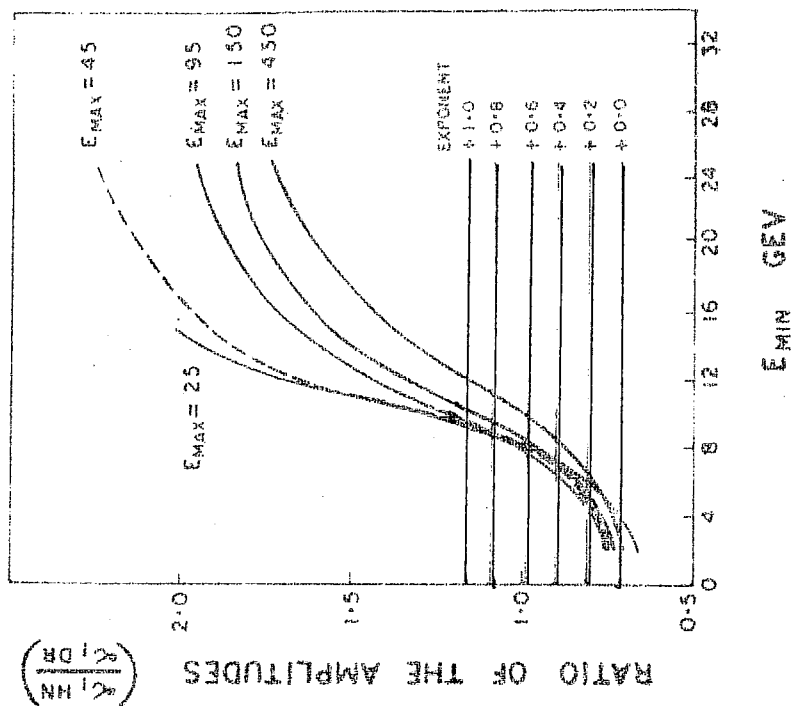


Fig: 3.13.

The ratio of the amplitude at Huancayo to that at Deep River as a function of E_{min} for several values of E_{max} .

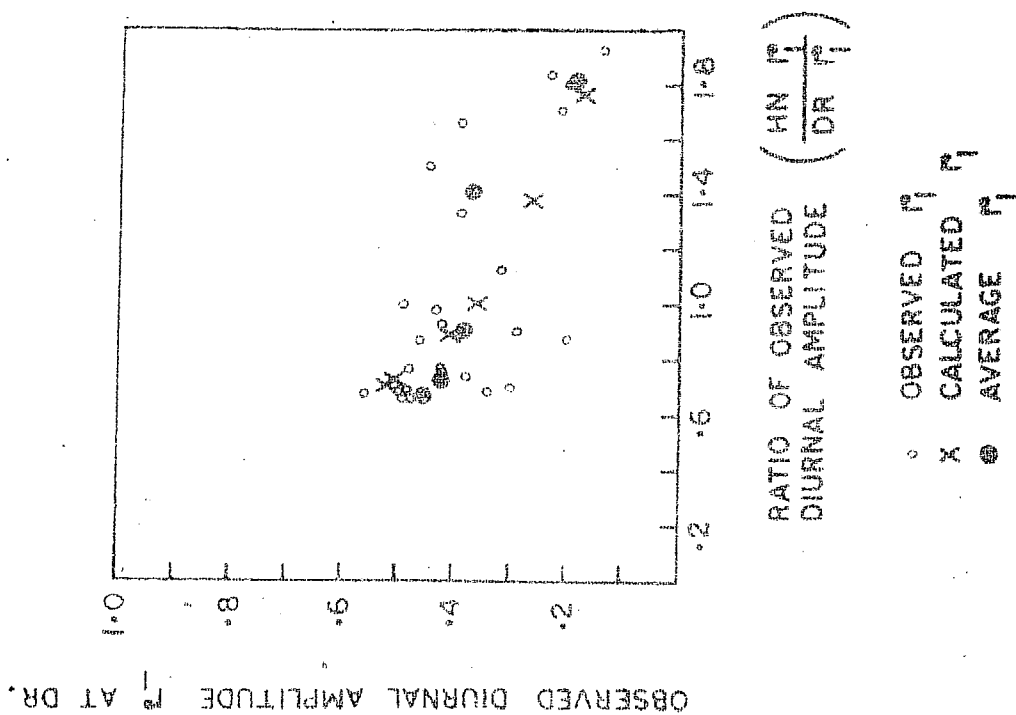


Fig.3.14 The observed diurnal amplitude at Deep River as a function of the ratio of the observed diurnal amplitude at Huancayo to that at Deep River for days corresponding to $X = 0$.

atmospheric cut off and $E_{\max} = 250$ GeV one can calculate the ratio $(\frac{\alpha_1 \text{ HN}}{\alpha_1 \text{ DR}})$ for various values of the exponents in the range -1.2 to 1.0. The ratio is less than .62 for negative exponents. This implies that when a negative exponent occurs, we must look to a process other than azimuthal streaming. However for positive exponents the situation is more complex. We have indicated in Fig.3.13 by horizontal lines the ratio corresponding to exponents $X = 0, +.2, +.4, +.6, +.8$ and $+1.0$ when $E_{\min} = 2$ GeV and $E_{\max} = 250$ GeV. Each horizontal line intersects the family of curves drawn in the same figure, indicating the E_{\min} and E_{\max} with a zero exponent which would produce same ratio as a spectrum with the particular positive exponent. The alternative spectrum with zero exponent would then be consistent with azimuthal streaming provided two further conditions are satisfied. First, that the amplitude of the variation as shown in Fig.3.12 is consistent with the process of azimuthal streaming and values of E_{\max} and E_{\min} as may be chosen, and second, the direction of maximum is close to 1800 hours. Thus not all days on which the spectrum has a positive exponent can be regarded as arising out of a process other than azimuthal streaming. On the other hand several days for which exponent is positive can be associated with azimuthal streaming. Large negative exponents derived from data of neutron monitors alone would not be consistent with azimuthal streaming occurring by itself. Fig.3.14 shows the

observed diurnal amplitude r_1 at Deep River as a function of the ratio of the observed amplitude of diurnal variation at Huancayo (HN r_1) and at Deep River (DR r_1) in the range .65 to 2.0 during 1964 for days when the process of azimuthal streaming is operative, i.e., $X = 0$. 26% of total days in group A having a ratio less than .65 which is the minimum required for azimuthal streaming, have been eliminated in the diagram. While the scatter of observed r_1 for different ratios is quite large, an unmistakable trend can be seen in the value of the vector average of r_1 for days during which the ratio lies in discrete intervals. The diurnal amplitude decreases as the ratio increases, which is what one should expect for this processes (See Fig.3.11 and Fig.3.12). An interesting consequence of this analysis is the possibility of estimating the limiting energy E_{\min} below which the modulating process is inoperative on any particular day. E_{\min} is interpreted as arising from the scale length of irregularities in the interplanetary magnetic field for which essentially isotropic diffusion of cosmic rays occurs.

3.11 Anisotropy of Galactic Cosmic Rays during the solar cycle

Applying the method of best fit to the daily variation of cosmic ray intensity observed by the neutron monitors at Huancayo, Churchill, Mawson and Mt.Norikura and Cubical Meson

telescope at Mawson and Churchill, we have determined for each day from 1958 to 1963 the amplitude, the directions in space of maximum and minimum intensity and the energy spectrum of variation of the anisotropy of galactic cosmic rays, as described in section 3.3. In the present analysis, E_{\min} ranges from 2 to 15 GeV in an order of 2, 10 and 15 GeV, while E_{\max} has a constant value of 250 GeV (Fig.3.02).

Following the procedure described in section 3.4, we identify four different groups of spectra, which include primary as well as equally acceptable spectra. Table 3.5 shows the frequency of occurrence of each of the four groups during solar maximum (58-60) and during the period of declining solar activity (61-63) for diurnal and semi-diurnal anisotropies.

Table 3.5

Group	Exponent	E_{\min} in BeV	Anisotropy	
			Diurnal Frequency in %	Semi-diurnal Frequency in %
I	$X \sim 0$	2,6,15 a	24.6	11.1
		b	25.9	8.5
II	$X \sim +Ve$	2,6,15 a	32.1	47.8
		b	20.5	35.7
III	$X \sim -Ve$	15 a	21.9	12.3
		b	23.8	15.8
IV	$X \sim -Ve$	2,6 a	21.5	28.8
		b	29.7	40.0

a - during 58-60;

b - during 61-63.

The changes with the declining activity are:

- (1) For the diurnal anisotropy the frequency of occurrence of Group II, ($X \sim +Ve$) decreases from 32.1% to 20.5% during solar maximum to solar minimum period, while for Group IV ($X \sim -Ve$) the frequency of occurrence increases from 21.5% to 29.7%.
- (2) For the semi-diurnal anisotropy, the frequency of occurrence of Group II ($X \sim +Ve$) decreases from 47.8% to 35.7% during solar maximum to minimum period and for Group IV ($X \sim -Ve$) it increases from 28.8% to 40.0%.
- (3) The frequency of occurrence of the semi-diurnal anisotropy is lowest in Group I ($X \sim 0$) during both the periods.

The decrease in the percentage frequency of Group II, and increase of Group IV, with declining solar activity gives revealing information concerning the change of electromagnetic conditions of interplanetary space. The changes in the frequency could be interpreted in terms of decrease of E_{\max} and E_{\min} , (Jacklyn and Humble, 1965) or because of the appropriate decrease in the relative gradient of the cosmic rays with the solar activity. The changes might be associated with a decrease of strength and the scale length of the irregularities of the interplanetary field in sectors of the interplanetary space.

Eliminating Forbush decrease days, a yearly average of diurnal amplitude and semi-diurnal amplitude is obtained for a set of stations used in analysis during 1958-63 and 1964 to 1966. For each year a spectrum, the time of maximum and minimum for diurnal and semi-diurnal anisotropies and the amplitudes in space have been obtained. Fig.3.15 shows the energy spectrum of the diurnal and semi-diurnal amplitudes of the average daily variation during 1964-65. It confirms that the diurnal component has a spectrum of variation which is essentially independent of rigidity and has an exponent $X \sim 0$, whereas the semi-diurnal component has a spectrum which has a positive exponent $X \sim +.6$. Table 3.6 shows the energy spectrum of variation during 1958-1966 for the diurnal and semi-diurnal anisotropies.

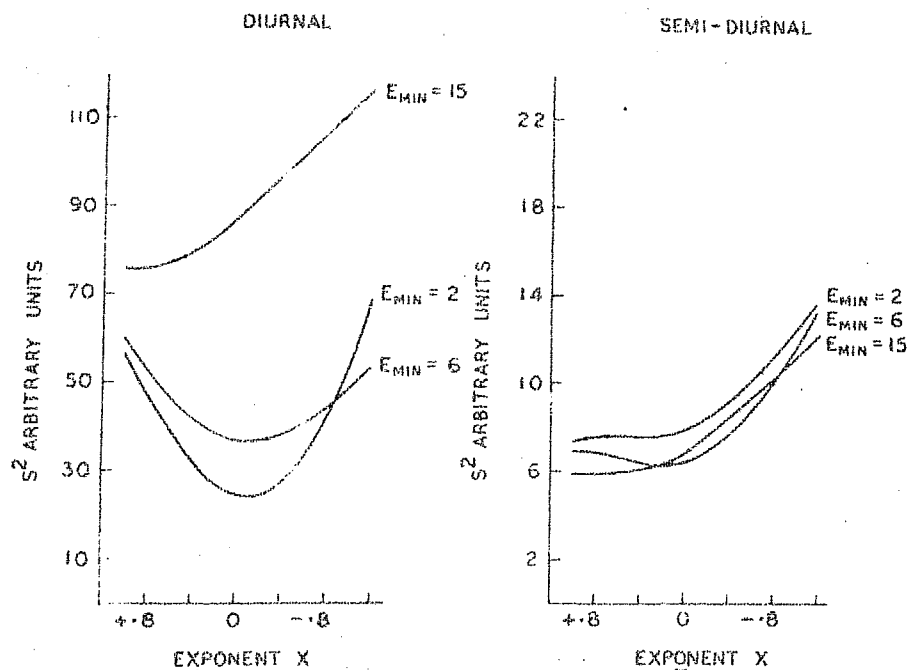


Fig.3.15 S^2 values for different exponents of the energy spectrum during 64-65.

Table 3.6

Year	Exponent X	
	Diurnal anisotropy	Semidiurnal anisotropy
1958	X = 0	X = +1
1959	X = 0	Poor resolution
1960	X = +.2	Poor resolution
1961	X = 0	X = +1
1962	X = -.2	X = +1
1963	X = +.2	X = +1
1964-65	X = 0	X = +.6
1966	X = 0	X = +.6

The result presented in table 3.6 supports the studies by Fallier and Marsden (1966), McCracken and Rao (1966), Willets et al.(1969), who have reached to essentially identical conclusion that the average diurnal anisotropy is independent of energy. Moreover semi-diurnal anisotropy shows a power law spectrum with a positive exponent. The diurnal and semi-diurnal amplitudes are of the order of 0.3% to .4% and 0.1% respectively. The diurnal time of maximum is 1800 hours and the semi-diurnal time of maximum is ~ 03 hours.

3.12 Variations in upper atmospheric temperature estimated from the daily variation of cosmic rays

Atmospheric temperature effects on the diurnal variation of cosmic ray meson intensity have been studied by many authors and the results arrived at are of great variety. The usual method is to use the meteorological data of the upper atmosphere obtained by a sounding balloon. This does not give enough information on diurnal variation since a balloon is launched only twice a day. The diurnal variation of the meson intensity due to the temperature change has been calculated by using a proper temperature coefficient for the meson intensity (Dorman, 1957; Wada and Kudo, 1962).

The other method is to compare the diurnal variation of the meson and neutron components with each other. Since the temperature effect on neutron component is negligibly small the observed diurnal variation can be considered to be due to cosmic ray anisotropy in interplanetary space. Two kinds of analysis have been reported, one is characterised by a comparison of two components at one station at a high latitude (Bercovitch et al., 1963) and the other is taking difference between diurnal vectors of meson and neutron components at Huancayo (Quenby and Thambyahpillai, 1960).

In the present analysis we have derived the temperature effect on M meson intensity by comparing the observed daily

variation in inclined directions with the expected variation due to the primary anisotropy and pressure changes. The magnitude and the direction of the cosmic ray anisotropy in interplanetary space as well as its energy spectrum on individual days have been obtained from a world wide net work of super neutron monitors as described in previous sections, 3.3 and 3.4.

Days on which the energy spectrum of the anisotropy has a zero exponent during 1966 have been considered to calculate the expected diurnal variation of the meson intensity, due to the cosmic ray anisotropy, in the inclined directions at Bologna (44.50, 11.33). Then the difference between the observed variation and the expected one can be attributed to the atmospheric diurnal effect on the meson intensity.

Fig.3.16 shows the temperature curve for the east and west directions at Bologna. The mean vector has an amplitude of .13% for the east direction and .24% for the west direction. However the phase of the temperature curve is ~ 18 hours L.T. The result is in fair agreement with the result of Quenby and Thambyahpillai (1960). They have estimated the phase from the difference between diurnal vectors of meson and neutron components at Huancayo. Moreover the resultant phase of temperature variation is consistent with the diurnal component analysed by Harris (1959) from data of tropospheric temperatures

at Washington D.C. However Wada and Kudo (1962) as well as Dorman (1957) have reported the phase vector of temperature around ~ 13 hours.

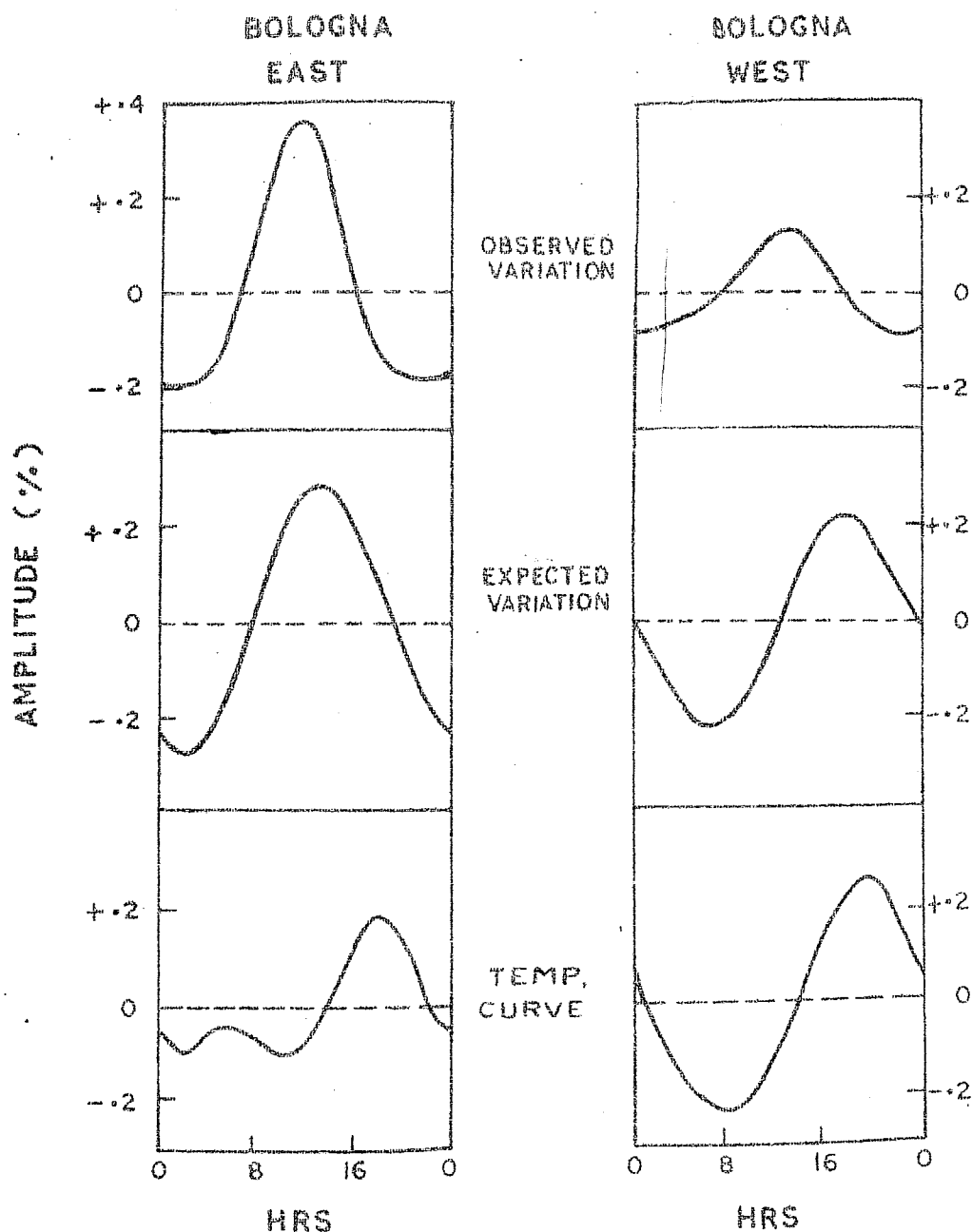


Fig.3.16 Temperature curves for the east and west directions at Bologna during the year 1966.

C H A P T E R - I V

SUMMARY AND CONCLUSIONS OF THE WORLDWIDE STUDY OF DAILY VARIATION

4.1 Study of anisotropies of galactic cosmic rays

It is well known that the spectrum of variation observed for the 11-year modulation varies from period to period and for Forbush decreases from event to event. Rao and Sarabhai (1964) pointed out that this occurs also for the anisotropy on a day-to-day basis. Sarabhai and Subramanian (1966) have reported the changes in the energy spectrum of the anisotropy with an exponent varying between -1 and +1 over limited energy ranges. In the present work we have studied the anisotropy of the galactic cosmic rays using data recorded by a worldwide net work of super neutron monitors during 64-66. Characteristics of the anisotropy on days with zero, negative and positive exponent of the spectrum of variation are identified and compared with what one may expect from one or other of four processes for the anisotropy in inter-planetary space.

The predictions from theory regarding the directions of maximum and of minimum, the nature of the anisotropy and its energy spectrum of variation are shown in table 3.3. The essentially different energy spectra of variation of the diurnal and semi-diurnal components as predicted are

experimentally observed for the anisotropy on day-to-day basis (Fig.3.04) and for the annual average daily variation observed with a worldwide net work of eight neutron monitors (Fig.3.05). The diurnal component has a spectrum with an exponent $X = 0$ while the semi-diurnal component has an exponent $X \sim +.6$. On a day-to-day basis, the semi-diurnal component is significantly larger when the spectrum has a positive exponent than when it has a negative or zero exponent (Table 3.2). The predictions, concerning the three processes are substantiated in fig.3.07, where the directions of maximum and minimum for the anisotropy in three groups distinguished from their spectra of variation are indicated. For days with positive exponent of the spectrum, T_{\min} the direction of minimum intensity is along the interplanetary magnetic field and T_{\max} , the direction of maximum intensity is almost perpendicular to the field, significantly inclined to the 1800^{Hr.} direction, characteristic of azimuthal streaming. Moreover $T_{\max} - T_{\min} \sim 7$ hours for the positive exponent may be contrasted with T_{\max} along 1800 hours and T_{\min} along 0600 hours when the exponent is zero. T_{\min} is clearly observed along 0900 hours when the exponent is -1. For days with positive exponent of the spectrum, high energy primaries show the direction of minimum intensity T_{\min} either along the garden hose direction or along the anti-garden hose direction, while the low energy primaries show T_{\min} only along the garden hose direction. (Fig.3.08).

The diurnal amplitude in space is significantly higher for the days when the exponent of the spectrum is zero as compared to the days when the exponent of the spectrum is positive, while it is otherwise for the semi-diurnal component (Fig.3.09). The observational implications of the azimuthal drift process on the low energy end through E_{\min} and the high energy end through E_{\max} lead to estimate the limiting energy E_{\min} below which the modulating process is inoperative on any particular day.

Days with the positive exponent of the variation of the spectrum for the diurnal and the semi-diurnal anisotropies decrease from solar maximum to solar minimum, while the days with the negative exponent of the variation of the spectrum increase from solar maximum to minimum. The frequency of occurrence of the days with zero exponent of the variation of the spectrum for the semi-diurnal anisotropy is lower during solar cycle (Table 3.5). However there has been no significant change in the exponents of the spectrum of variation derived from a yearly average of the diurnal and semi-diurnal components during 1958-1966

If indeed the evidence that has been presented here is to be taken as supporting the postulated latitudinal gradients of cosmic ray intensity in the solar system, there should be confirmative evidence from two other directions. First the level of the isotropic intensity of cosmic rays should change as heliolatitude of the earth alters with seasons. Dorman et al. (1967) have found the gradient of the

cosmic ray intensity in the direction perpendicular to the ecliptic plane to be $1\% / \text{a.u.}$ for 1960.

Second, the diurnal anisotropy caused by the latitudinal gradients should reverse as the magnetic field or the gradient reverses. When the gradient is such that solar activity north of the equatorial plane is greater than south, the latitudinal gradient should give rise to a diurnal anisotropy with its direction of maximum on the average along 1500 hours when the field is directed away from the sun (+) and along 0300 hours when the field is directed towards the sun (-). Such an asymmetry will increase the amplitude of the diurnal component due to azimuthal streaming when the field is away from the sun. This is verified using a set of neutron monitors during IMF-1 period (Wilcox and Ness, 1964) when interplanetary magnetic field direction in different sectors has been identified. In table 3.4 are shown the mean diurnal components when the field is directed away from the sun, and when the field is directed towards the sun.

4.2 Estimation of the atmospheric temperature effect

Knowing the exponent of the variation of the spectrum on a day-to-day basis, the temperature variation curve has been obtained for the μ meson component, by comparing the solar daily variation observed by crossed telescopes at Bologna during 1966, with the expected variation due to

primary anisotropy. The first harmonic of the temperature curve has its phase along ~ 18 hrs and the amplitude is about .1% (Fig.3.16). A similar result has been obtained by Harris (1959) and Quenby and Thambyahpillai (1960).

4.3 Conclusions

It is demonstrated that the diurnal and the semi-diurnal components of the anisotropy have characteristically different energy spectra of variation. There has been no significant change in the exponents of the spectrum of variation of the annual diurnal and semi-diurnal anisotropies during the solar cycle (58-65). However the frequency of occurrence of days of different groups shows significant variation.

From a comparison between the observational evidences with the theoretica predictions, we deduce that, in addition to azimuthal streaming giving rise to diurnal component with a maximum in 1800 Hr. direction, there is indeed evidence which indicates that processes of scattering at magnetic field irregularities and latitudinal gradients, do in fact occur and produce anisotropies oriented with respect to the interplanetary magnetic field. The predominant process responsible for the diurnal component is the azimuthal streaming while the semi-diurnal component appears to be due to scattering at magnetic field irregularities and latitudinal gradients.

The results of the study support the postulate of a gradient of galactic cosmic rays in the solar system perpendicular to the plane of the ecliptic. With a clear quantitative understanding of the implications of the various processes by which cosmic ray anisotropy and modulation occur in the solar system, coupled with increasingly accurate data from a worldwide net work of cosmic ray super neutron monitors and meson detectors, we should be able to gain insight of the state of interplanetary magnetic field and plasma from variations of cosmic ray intensity and geomagnetic field on the surface of the earth.

REFERENCES

- Ables, J.G., 1966 Proc. 9th Int.Conf., London
McCracken, K.G. and 1, 208.
Rao, U.R.
- Abraham, P.R., 1966 Phys. Rev., 150, 1088.
Brunstein, K. and
Cline, T.
- Agrinier, B., Koechlin, 1964 Proc. 8th Int.Conf. on
Y., Parlio, B.,
Boella, G., cosmic rays (Jaipur), 3, 167
Degli Antoni, G.,
Dilworth, C., Scarsi, L.
and Sironi, G.
- Ahluwalia, H.S., and 1962 Planet. Space Sci. 9, 195.
Dessler, A.J.
- Ahluwalia, H.S., 1965 Proc. Int.Conf.on cosmic rays,
Escobar, V.I.,
Zubieta, M., Anda, R., London, 1, 190.
Schreir, M., and
Troncoso, O.
- Axford, W.I., 1963 Ap. J. 137, 1268.
Dessler, A.J. and
Gottlieb, B.
- Axford, W.I. 1965 Planet. Space Sci. 13, 115.
- Babcock, H.W. 1953 Astrophys. J. 118, 387.
- Babcock, H.D. 1959 Ap. J., 130, 364.
- Bachelet, F., and 1956 Nuovo Cim. 4, 1479.
Conforto, A.M.
- Bachelet, F., 1965 Nuovo Cim. 70, 2469.
Balata, P., Dyring, E.,
and Iucci, N.
- Bachelet, F., 1967 Nuovo Cim. 52B, 106.
Dyring, E., Iucci, N.,
and Villoresi, G.

- Balasubramanyan, V.K. 1967 Bull. A.P.S., 12, 582.
- Bartley, W.C.,
Bukata, R.P.,
McCracken, K.G., and
Rao, U.R. 1966 J. Geophys. Res. 71, 3297.
- Bercovitch, M. 1963 J. Geophys. Res. 68, 4366.
- Bercovitch, M.,
Steijes, J.P., and
Carmichael, H. 1963 Proc. 8th cosmic Ray Conf.
Jaipur, 2, 327.
- Bercovitch, M., and
Robertson, B. 1966 Proc. Int. Conf. Cosmic Rays,
London, 1, 489.
- Biermann, L. 1951 Z. Astrophys., 29, 274.
- Birkeland, Kr. 1908 The Norwegian Aurora Polaris
Expedition Vol. 1.
- Birkeland, Kr. 1913 Ibid Vol. 1.
- Biswas, S.,
Ramadurai, S., and
Sreenivasan, N. 1966 Phys. Rev., 149, 1037.
- Bland, C.J.
Boella, G.,
Degli Antoni, G.,
Dilworth, C.,
Scarsi, L., Sironi, C.,
Agrinier, B.,
Koechlin, Y.,
Parlier, B., and
Vasseur, J. 1966 Phys. Rev. Letters 17, 813.
- Bridge, H., Egidi, A.,
Lazarus, A., Lyon, E.,
and Jacobson, L. 1965 Space Res., 5, 969.
- Brunberg, E.A. 1953 Tellus, 2, 135.
- Brunberg, E.A., and
Dattner, A. 1953 Tellus, 3, 269.

- Bumba, V., and Howard, R. 1965 Astrophys. J. 141, 1502.
- Cain, J.C., Daniels, W.E., and Hendricks, S.J. 1965 J. Geophys. Res. 70, 3469.
- Callender, R.H., Manzano, J.R., and Winckler, J.R. 1965 J. Geophys. Res. 70, 1965.
- Carmichael, H., Bercovitch, M., Steljes, J., and Magidin, M. 1966 Proc. Int. Conf. Cosmic Rays (London) 1, 553.
- Carmichael, H., Bercovitch, M., and Steljes, J.F. 1967 Tellus, 19, 143.
- Chapman, S., and Bartels, J. 1940 Geomagnetism Vol, 2, Oxford University Press.
- Clay 1927 Proc. Acad.Sci.Amsterdam, 30, 1115.
- Cocconi, G. 1960 Astrophys. J. Suppl. 4, 417.
- Coleman, P.J.Jr., Davis, L., and Sonett, C.P. 1960 Phys. Rev.Letters, 5, 43.
- Coleman, Jr., P.J., Sonett, C.P. and Davis, Jr.L. 1961 J. Geophys. Res. Letters, 5, 43.
- Coleman, P.J.Jr. 1966 J. Geophys. Res. 71, 5509.
- Coleman, P.J.Jr., Davis, L., Jr., Smith, E.J., and Jones O.E. 1966 J. Geophys. Res., 71 2831.
- Coleman, P.J.Jr., Smith, E.J., Davis, L., Jr., and Jones D.E. 1966a Space Res., 6, 907

- Compton, A.H., and
Gettling, I.A. 1935 Phys. Rev. 47, 817.
- Daniel, R.R., and
Stephens, S.A. 1966 Phys. Rev. Letters, 17, 935.
- Daniel, R.R., and
Stephens S.A. 1966a Proc. Ind. Aca. Sci. A,
63, 276.
- Dattner, A., and
Venkatesan, D. 1958 Tellus, 11, 239.
- Davis, L. Jr.,
Smith, E.J.,
Coleman, P.J.Jr., and
Sonett, C.P. 1966 Interplanetary magnetic
Measurements in the solar
wind. pp. 35, Pergamon Press,
New York.
- Dessler, A.J. and
Fejer, J.A. 1963 Planet. Space Sci. 11, 505.
- Dorman, I.V., and
Dorman, L.V. 1965 Geomagn. and Aeronomy, 5, 666.
- Dorman, I.V., and
Dorman, L.I. 1967 J. Geophys. Res. 72, 1513.
- Dorman, L.I., and
Feinberg, E.L. 1955 Memoria del V congreso Int.
de Radiation cosmica
(Guanajuato), 393.
- Dorman, L.I. 1957 Cosmic ray variations
(Moscow state Pub.House).
- Dorman, L.I. 1963 Progress in elementary particle
and Cosmic Ray Physics.Vol.VII,
North Holland Pub.Co.,
Amsterdam.
- Duggal, S.P.,
Forbush, S.E., and
Pomerantz, M.A. 1967 Nature, 21W, 154.
- Earl, J.A. 1961 Phys. Rev. Letters, 6, 125.
- Ehmert, A. 1960 Proc. 6th Int.Cosmic Ray Conf.
Moscow, 3, 142.

- Elliot, H. and
Dolbear, D.W.N. 1951 J. Atmos.Terr. Phys. 1, 215.
- Elliot, H., and
Rothwell, P. 1956 Phil. Mag. 1, 699.
- Elliot, H. 1960 Phil. Mag. 5, 601.
- Escobar, V.I.,
Uria, C., and
Weil, R. 1959 Int.Conf.on cosmic rays,
Moscow.
- Faller, A.M., and
Marsden, P.L. 1966 Proc. 9th Int. Conf.(London)
1, 231.
- Fah, C.Y.,
Meyer, P., and
Simpson, J.A. 1961 Phys. Rev. Letters, 5, 269.
- Fanselow, J.L.,
Hartman, R.C.,
Hildebrad, R.H., and
Meyer, P. 1969 EFI Preprint.
- Fichtel, C.E. 1961 Nuovo Cim., 19, 1100.
- Fichtel, C.E., and
Reames, D.V. 1966 Phys. Rev., 149, 995.
- Finch, H.P., and
Leaton, B.R. 1957 Monthly Notices
Roy. Astron.Soc., Geophys.
Suppl. 7, 314.
- Fonger, W. 1953 Phys. Rev., 91, 351.
- Forbush, S.E. 1954 J. Geophys. Res. 59, 525.
- Forbush, S.E. 1958 J. Geophys. Res. 63, 651.
- Forbush, S.E. 1967 J. Geophys. Res. 72, 4937.
- Forman, M.A. 1968 Canad. J.Phys. 46, 1087.
- Freier, P.S., and
Waddington, C.J. 1965 Space. Sci. Rev. 4, 313.
- Freon, A., and
McCracken, K.G. 1965 J. Geophys. Res. 70, 4117.

- Gall, R.,
Jimenez, J., and
Camacho, L. 1968 J. Geophys. Res. 73, 1593.
- Ginzburg, V.L., and
Syrovatskii, S.I. 1964 "The origin of Cosmic Rays",
MacMillan Co., New York.
- Gleeson, L.J., and
Axford, W.I. 1968 AP. J., 154, 1011.
- Gleeson, L.J., and
Axford, W.I. 1968a Astrophysics and Space
Sci. 2, 431.
- Gloeckler, G. 1965 J. Geophys. Res. 70, 5333.
- Gloeckler, G., and
Jokipii, J.R. 1966 Phys. Rev. Letters, 17, 203.
- Greenstadt, E.W. 1965 TRW Report. 9890 - 6001 -
R 4000.
- Griffiths, W.K.,
Hatton, C.J.,
Ryder, P., and
Harman, C.V. 1966 J. Geophys. Res. 71, 1895.
- Harman, C.V., and
Hatton, C.J. 1968 Canad. J. Phys. 46, 1052.
- Harris, M.F. 1959 J. Geophys. Res. 64, 983.
- Hartman, R.C.,
Meyer, P., and
Hildebrand, R.H. 1965 J. Geophys. Res. 70, 2713.
- Hartman, R.C. 1967 AP. J., 150, 371.
- Hasim, A.,
Thambyahpillai, T.,
Thomson, D.M., and
Mathews, T. 1968 Canad. J. Phys. 46, S801.
- Hasim, A.,
Peacock, D.S.,
Quenby, J.J., and
Thambyapillai, T. 1969 Planet. Space Sci. 17, 1749.
- Hatton, C.J., and
Carswell, J.A. 1963 Report No. CRGP - 1165, Atomic
energy of Canada Ltd.

- Hatton, C.J.,
Marsden, P.L., and
Willetts, A.C. 1968 Canadian J. Phys. 46, 915.
- Hendricks., and
Cain, J.C. 1966 J. Geophys. Res. 71, 346.
- Hurwitz, L.,
Knapp, D.G.,
Nelson, J.H. and
Watson, D.E. 1966 J. Geophys. Res. 71, 2373.
- Jacklyn, R.M., and
Humble, J.E. 1965 Australian J. Phys. 18, 451.
- Janossy, L.Z. 1937 Z. Physik, 104, 430.
- Jensen, J.C., and
Whitker, W.A. 1960 J. Geophys. Res. 65, 2500.
- Jensen, D.C., and
Cain, J.C. 1962 J. Geophys. Res. 67, 3568.
- Jokipii, J.R. 1966 Astrophys. J. 146, 480.
- Jokipii, J.R., and
Parker, E.N. 1967 Planet Space Sci., 15, 1375.
- Jokipii, J.R. 1967 AP. J. 150, 675.
- Jokipii, J.R. 1968 Canad. J. Phys. 46, 950.
- Jokipii, J.R., and
Coleman, P.J., Jr. 1968 J. Geophys. Res., 73, 5495.
- Jokipii, J.R. 1969 AP. J. 156, 1107.
- Jokipii, J.R., and
Davis, L. 1969 AP. J. 156, 1101.
- Jokipii, J.R., and
Parker, E.N. 1969 AP. J. 155, 777.
- Jory, F.S. 1956 Phys. Rev., 103, 1068
- Kaminer, N.S.,
Ilgach, S.F., and
Khadakhanova, T.S. 1966 Proc. Int. Conf. Cosmic Rays
(London), 1, 486.
- Kargathra, L.V. 1968 Proc. 10th Symposium on cosmic
rays, Elem. Particle Physics and
Astrophysics, Aligarh, (India).
Page. 159.

- | | | |
|---|------|---|
| Katzman, J., and Venkatesan, D. | 1960 | Canad. J. Phys. <u>38</u> , 1011. |
| Katzman, J., and Rose, D.C. | 1962 | Canad. J. Phys. <u>46</u> , 1319. |
| Kodama, and Miyazaki | 1957 | Rept. Iono Space Res. Japan, <u>11</u> , 99. |
| Kodama | 1964 | Deep River Laboratory, Atomic Energy of Canada Ltd. |
| Kohlhorster, W. | 1941 | Phys. Z <u>42</u> , 55. |
| Krimsky, G.F., Krivoschapkin, P.A., and Skripin, G.V. | 1966 | Proc. Int. Conf. Cosmic Rays, London, <u>1</u> , 503. |
| Krymskiy, G.F. | 1964 | Geomagn. and Aeronomy <u>4</u> , 763. |
| LaPointe, S.M., and Rose, D.C. | 1962 | Canad. J. Phys. <u>40</u> , 687. |
| Laster, H., Lencheck, A.M., and Singer, S.F. | 1962 | J. Geophys. Res. <u>67</u> , 2639. |
| Lindgren, S., and Lindholm, F. | 1961 | Tellus, <u>13</u> , 280. |
| Lockwood, J.A., and Razdan, H. | 1963 | J. Geophys. Res. <u>68</u> , 1581. |
| Lockwood, J.A., and Kaplan, J. | 1967 | J. Geophys. Res. <u>72</u> , 431. |
| Lust, R., and Simpson, J.A. | 1957 | A.D.I. Auxil. Pubs. Project Doc. 5356. Library of Congress, Washington. |
| Maeda, K., and Wada, M. | 1954 | J. Sci. Res. Inst. <u>48</u> , 71. |
| Maeda, K. | 1960 | J. Atm. Terr. Phys. <u>12</u> , 184 |
| Malmfors, K.G. | 1945 | Arkiv. Mat. Astron. Fysik., 32A, No. 8. |
| Malmfors, K.G. | 1949 | Tellus, <u>1</u> , 55. |

- | | | |
|---|------|---|
| Marsden, P.L. | 1968 | J.G. Emming (ed.)
Electromagnetic Radiation in
Space. |
| Mathew, P.M. | 1959 | Canad. J. Phys. <u>37</u> , 85 |
| Mathew, T.,
Venkatesan, D., and
Wilson, B.G. | 1969 | J. Geophys. Res. <u>74</u> , 1218. |
| McCracken, K.G. | 1958 | Ph.D. Thesis, University of
Tasmania. |
| McCracken, K.G., and
Parsons, N.R. | 1958 | Phys. Rev., <u>112</u> , 1798. |
| McCracken, K.G., and
Johns, D.H. | 1959 | Nuovo. Cim. <u>13</u> , 96. |
| McCracken, K.G. | 1962 | J. Geophys. Res. <u>67</u> , 423. |
| McCracken, K.G.,
Rao, U.R. and
Shea, M.A. | 1962 | Technical Report No.77. MIT. |
| McCracken, K.G., and
Rao, U.R. | 1965 | Proc. 9th Int.Conf.Cosmic Rays,
London, <u>1</u> , 213. |
| McCracken, K.G.,
Rao, U.R.,
Fowler, B.C., and
Shea, M.A. | 1965 | IQSY, Instruction Manual No.10,
London. |
| McCracken, K.G., and
Ness, N.F. | 1966 | J. Geophys. Res. <u>71</u> , 3315. |
| McCracken, K.G.,
Rao, U.R., and
Bukata, R.P. | 1966 | Phys.Rev.Letters, <u>17</u> , 928. |
| McDoland, F.B.,
and Webber, W.R. | 1959 | Phys. Rev., <u>115</u> , 194. |
| Meyer, P., and
Vogt, R. | 1961 | Phys. Rev. Letters, <u>6</u> , 193. |
| Mori, S., Veno, H.,
Nagashima, K., and
Sagisaka, S. | 1964 | Rept.Ionosphere and Space Res.
Japan, <u>18</u> , 275. |
| Nagashima, K. | 1953 | J. Geomagnet.Geoelec. <u>5</u> , 141. |

- Nagashima, K.,
Potnis, V.R., and
* Pomerantz, M.A. 1961 Nuovo. Cim. 19, 292.
- Neher, H.V., and
Anderson, H.R. 1965 Proc. Int. Conf. Cosmic Rays
London, 1, 153.
- Nerurkar, N.W. 1956 Ph.D. Thesis, University of
Gujarat.
- Ness, N.F.,
Scearce, C.S., and
Seek, J.B. 1964 J. Geophys. Res., 69, 3531.
- Ness, N.F., and
Wilcox, J.M. 1964 Phys. Rev. Letters, 13, 461.
- Ness, N.F., and
Wilcox, J.M. 1965 J. Geophys. Res. 71, 322.
- Ness, N.F. 1966 J. Geophys. Res. 71, 3319.
- Neugebauer, M., and
Snyder, C.W. 1963 Science 138, 1095.
- Neugebauer, M., and
Snyder, C.W. 1965 J. Geophys. Res. 70, 1587.
- O'Gallagher, J.J. 1967 Astrophys. J. 150, 675.
- O'Gallagher, J.J.,
and Simpson, J.A. 1967 Astrophys. J. 147, 819.
- Ormes, J.F., and
Webber, W.R. 1968 J. Geophys. Res., 73, 4231.
- Pal, Y., and
Peters, B. 1963 Proc. Int. Conf. Cosmic Rays,
Jaipur.
- Parker, E.N. 1958 AP. J. 128, 664.
- Parker, E.N. 1958a Phys. Rev., 110, 1445-
- Parker, E.N. 1963 Interplanetary Dynamical
Processes, Interscience Publishers,
New York.
- Parker, E.N. 1964 Planet. Space Sci. 12, 735.
- Parker, E.N. 1965 Planet. Space Sci. 13, 9.

- Parker, E.N. 1966 Planet. Space Sci., 14, 1966.
- Parker, E.N. 1967 Planet. Space Sci., 15, 1723.
- Patel, D.,
Sarabhai, V., and
Subramanian, G. 1968 Planet. Space Sci., 16, 1131.
- Pathak, P.N., and
Sarabhai, V. 1970 Planet. Space Sci., 18, 81.
- Peacock, D.S.,
Dutt, J.C., and
Thambyahpillai, T. 1968 Canad. J. Phys. 46, S788.
- Quenby, J.J., and
Webber, W.R. 1959 Phil. Mag., 4, 90.
- Quenby, J.J., and
Webber, W.R. 1959a Phil. Mag., 4, 654.
- Quenby, J.J., and
Thambyahpillai, T. 1960 Phil. Mag., 5, 585.
- Quenby, J.J., and
Lietti, B. 1968 Planet. Space Sci., 16, 1209.
- Ramaty, R., and
Lingenfelter, R.E. 1969 AP. J. 155, 587.
- Rao, U.R. 1960 Ph.D. Thesis, University of
Gujarat.
- Rao, U.R., and
Sarabhai, V. 1961 Proc. Roy. Soc. 263, 101.
- Rao, U.R.,
McCracken, K.G., and
Venkatesan, D. 1963 J. Geophys. Res., 68, 345.
- Rao, U.R., and
Sarabhai, V. 1964 Planet. Space Sci., 12, 1055.
- Rao, U.R., and
Agarwal, S.P. 1970 J. Geophys. Res., 75, 2391.
- Razdan, H. 1960 Ph.D. Thesis, University of
Gujarat.
- Ryder, P., and
Hatton, C.J. 1968 Canad. J. Phys. 46, S999.

- Sandstrom, A.E.,
Dyring, E., and
Lindgren, S. 1962 J. Physical Soc. of Japan,
17, 471.
- Sarabhai, V., and
Kane, R.P. 1953 Phys. Rev., 92, 415.
- Sarabhai, V.,
Desai, U.D., and
Venkatesan, D. 1955 Phys. Rev., 99, 1490
- Sarabhai, V., and
Nerurkar, N.W. 1956 Annual Review of Nuclear
Science, 6.
- Sarabhai, V., and
Bhavsar, P.D. 1958 Nuovo Cim. 8, 299.
- Sarabhai, V. 1963 J. Geophys. Res., 68, 1555.
- Sarabhai, V.,
Pai, G.L., and
Wada, M. 1965 Nature, 206, 703.
- Sarabhai, V., and
Subramanian, G. 1966 Proc. 9th Int. Conf. Cosmic
Rays, London, 1, 204.
- Sarabhai, V., and
Subramanian, G. 1966a AP. J. 145, 206.
- Sari, J.W., and
Ness, N.F. 1969 Solar Physics, 8, 155.
- Schmidt 1935 NASA TT-F - 8888(1964).
- Shea, M.A.,
Smart, D.F., and
McCracken, K.G. 1965 J. Geophys. Res., 70, 4117.
- Shea, M.A., and
Smart, D.F. 1967 J. Geophys. Res., 72, 2021.
- Shea, M.A.,
Smart, D.F.,
McCracken, K.G., and
Rao, U.R. 1968 IQSY Instruction Manual
No.10.
- Shklovsky, I.S.,
Moroz, V.I., and
Kurt, V.G. 1961 Soviet Astron. AJ, 4, 871.
- Silberberg, R. 1966 Phys. Rev., 148, 1247.

- Simpson, J.A., Babcock, H.W., and Babcock, H.D. 1955 Phys. Rev., 98, 1402.
- Simpson, J.A. 1963 Proc.Int.Conf.Cosmic Rays, (Jaipur), 2, 155.
- Simpson, J.A., and Wang, R.A. 1967 Astrophys. J. 149, L73.
- Snyder, C.W., Neugebauer, M., and Rao, U.R. 1963 J. Geophys. Res. 68, 6361.
- Stern, D. 1964 Planet. Space. Sci., 12, 973.
- Stormer, S. 1930 Z. Phys. 61, 237.
- Stormer, S. 1931 Z. Astrophys. 3, 31.
- Stormer, S. 1955 The Polar Aurora
Oxford University Press,
London.
- Subramanian, G. 1964 Ph.D. Thesis, University
of Gujarat.
- Subramanian, G., and Sarabhai, V. 1967 AP. J. 149, 417.
- Thambyahpillai, ^T and Elliot, H. 1953 Nature, Lond. 171, 918.
- Trieman, S.B. 1952 Phys. Rev., 86, 917.
- Wada, M. 1961 Sci.Papers Inst. Phys. Chem.
Res., Tokyo, 55, 7.
- Wada, M., and Kudo, S. 1962 Rep.Ionos.Space.Res. 16, 57.
- Wada, M., and Kudo, S. 1968 Canad. J. Phys. 46, 5934.
- Webber, W.R. 1965 Physics of Interplanetary
Medium.
Argentine National Commission
on Space Research.

- Willets, A.C., 1969 Pre-print, University of
Griffiths, W.K., Leeds, England.
Hatton, C.J., and
Marsden, P.L.
- Wolfe, J.H., 1966 J. Geophys. Res., 71, 1319.
Silva, R.W., and
Myers, M.A.
-
- * Nagashima, K., 1966 Planet. Space Sci., 14, 177.
Duggal, S.P., and
Pomerantz, M.A.